OCEAN QUAHOG FIGURES

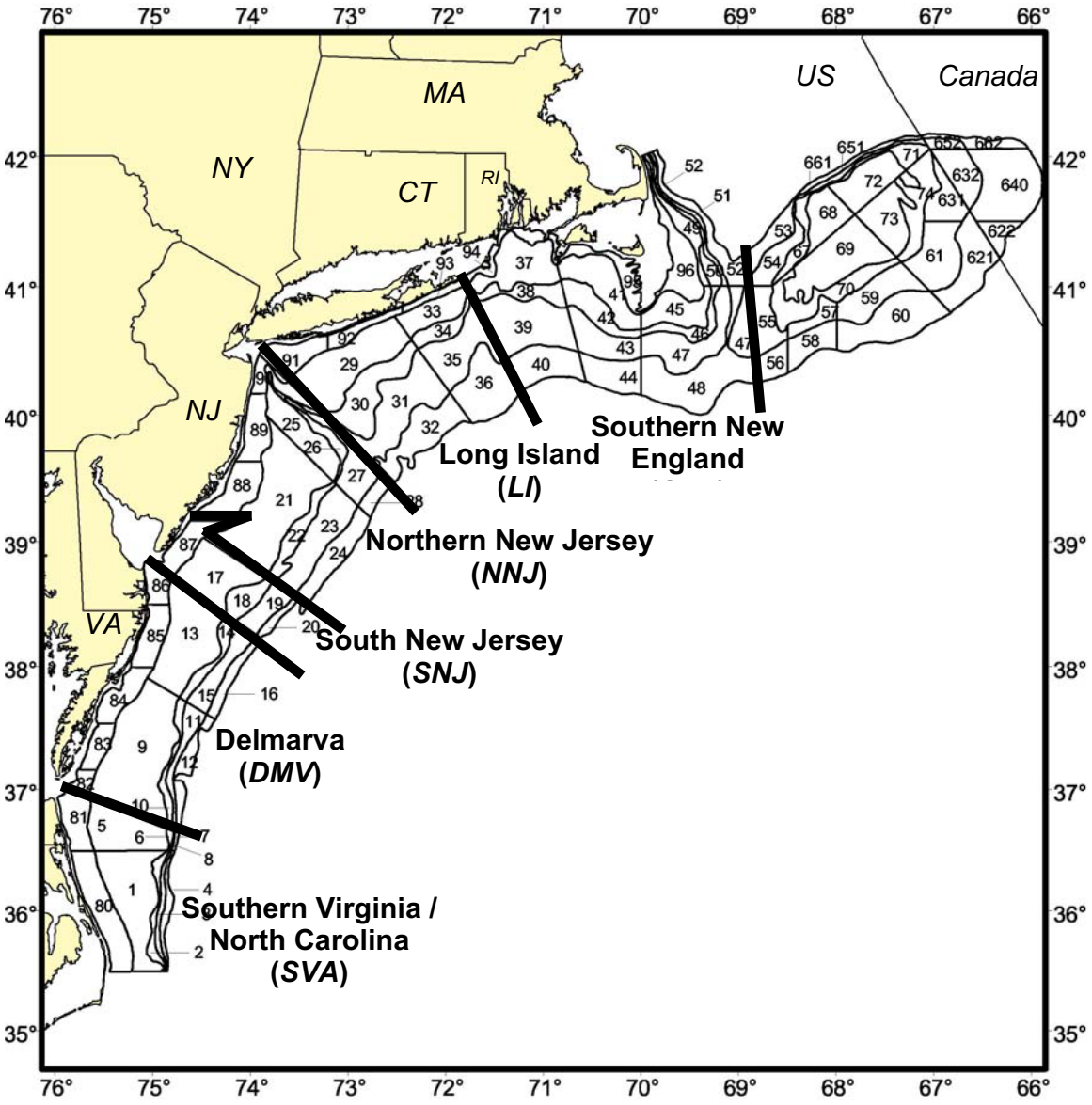

Figure A1. Stock assessment regions for ocean quahog in the US EEZ, with NEFSC shellfish survey strata numbers and boundaries.

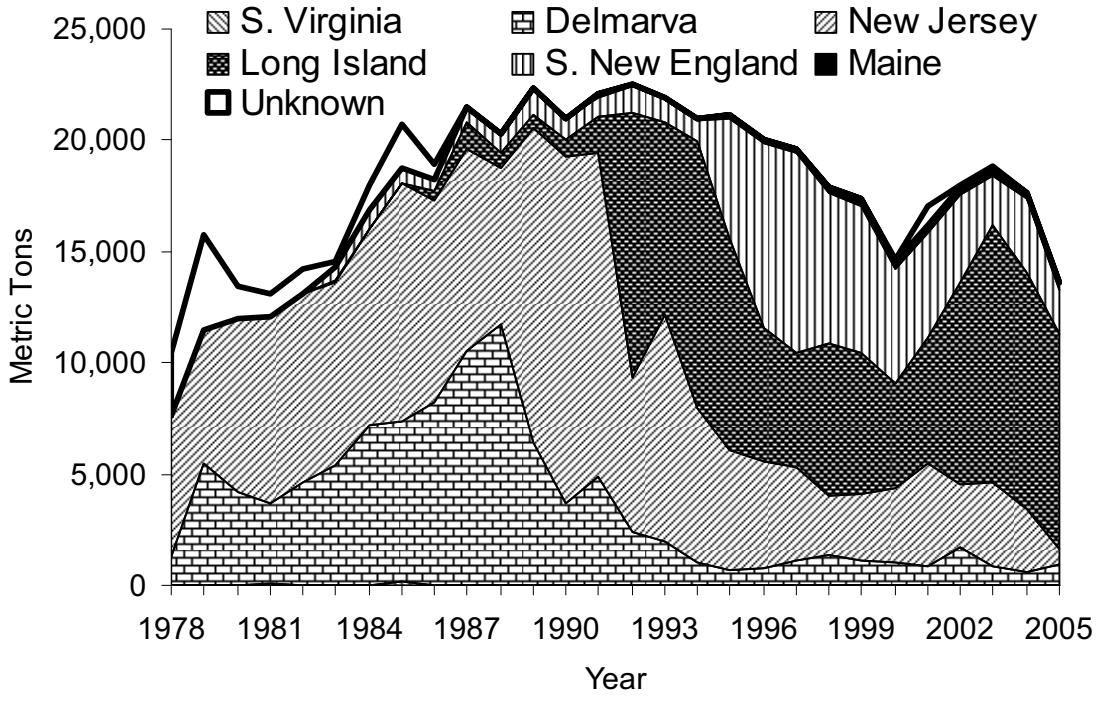

Figure A2. Ocean quahog commercial landings (meat weights) from the US EEZ during 1978-2005. Data for 2005 are preliminary and may be incomplete.

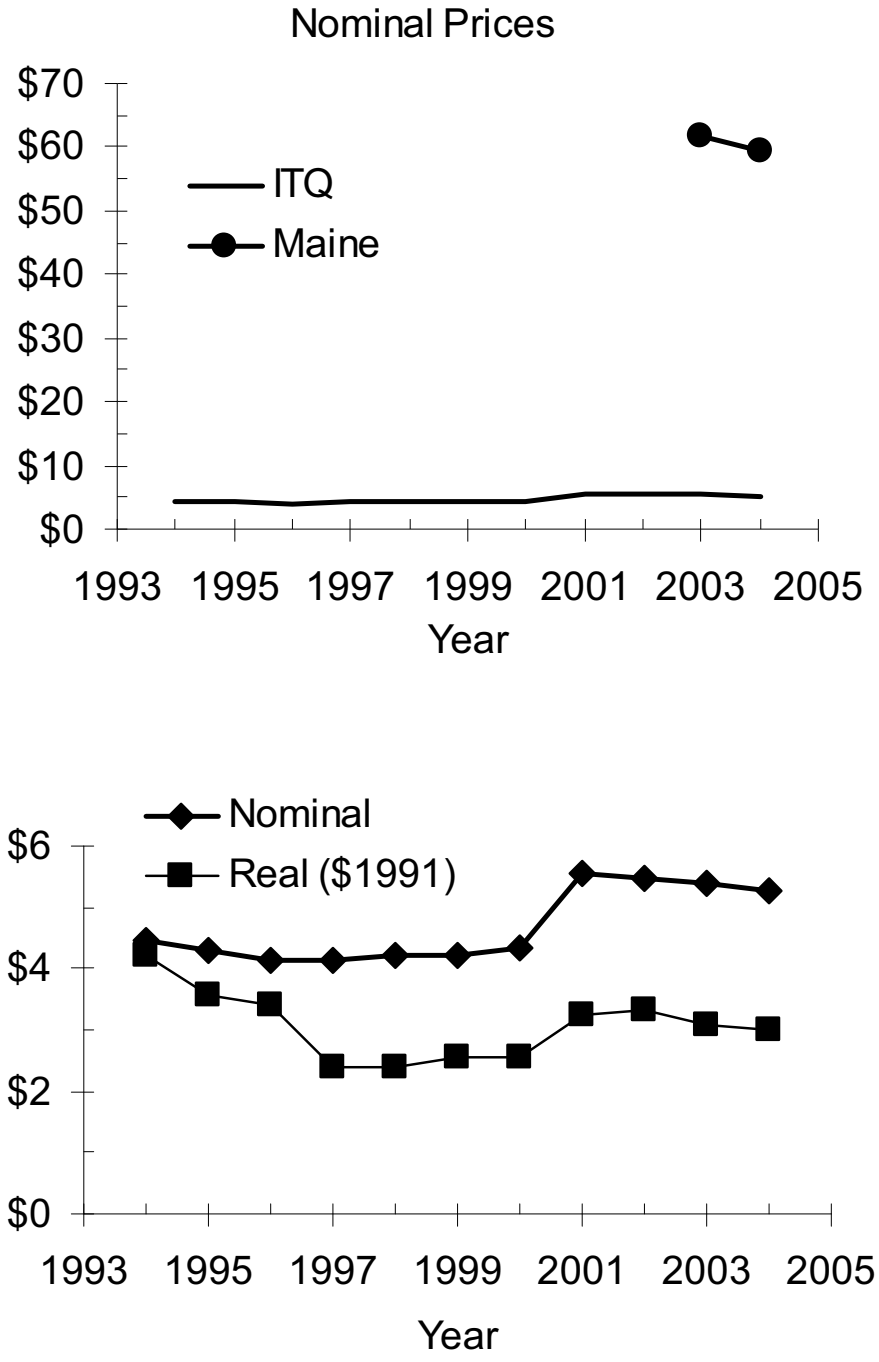

Figure A3. Real and nominal exvessel prices for ocean quahog in the ITQ and Maine fishery components.

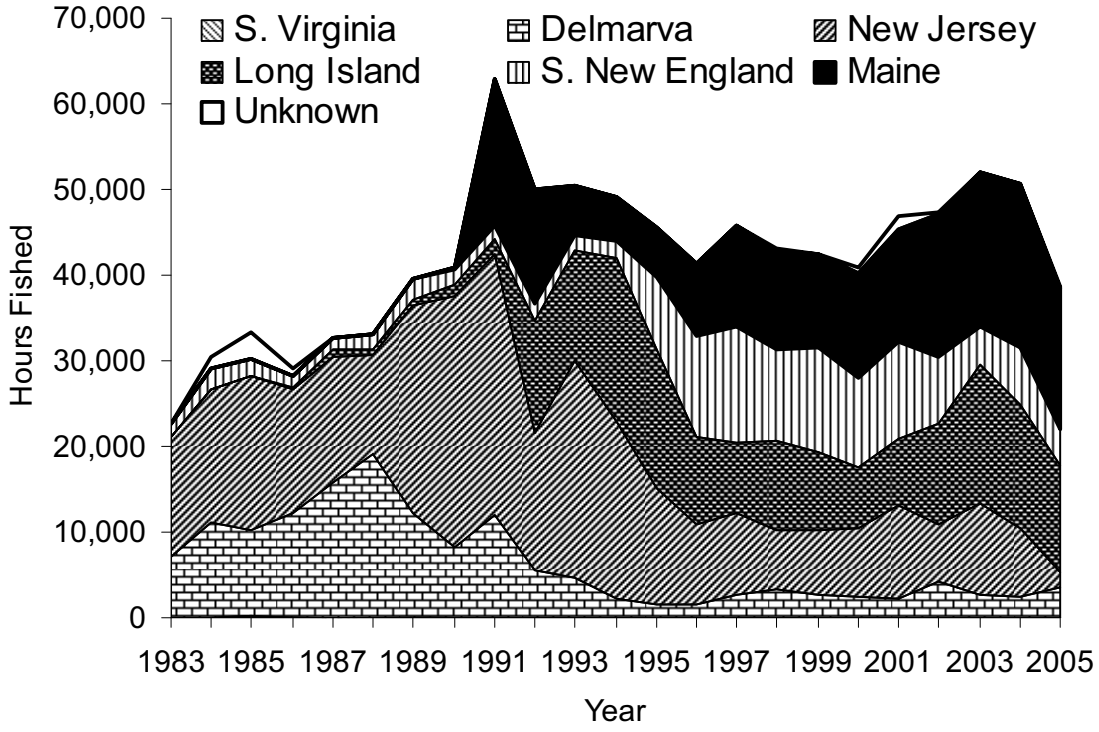

Figure A4. Hours fished for ocean quahog in the US EEZ during 1983-2005 based on logbook records.

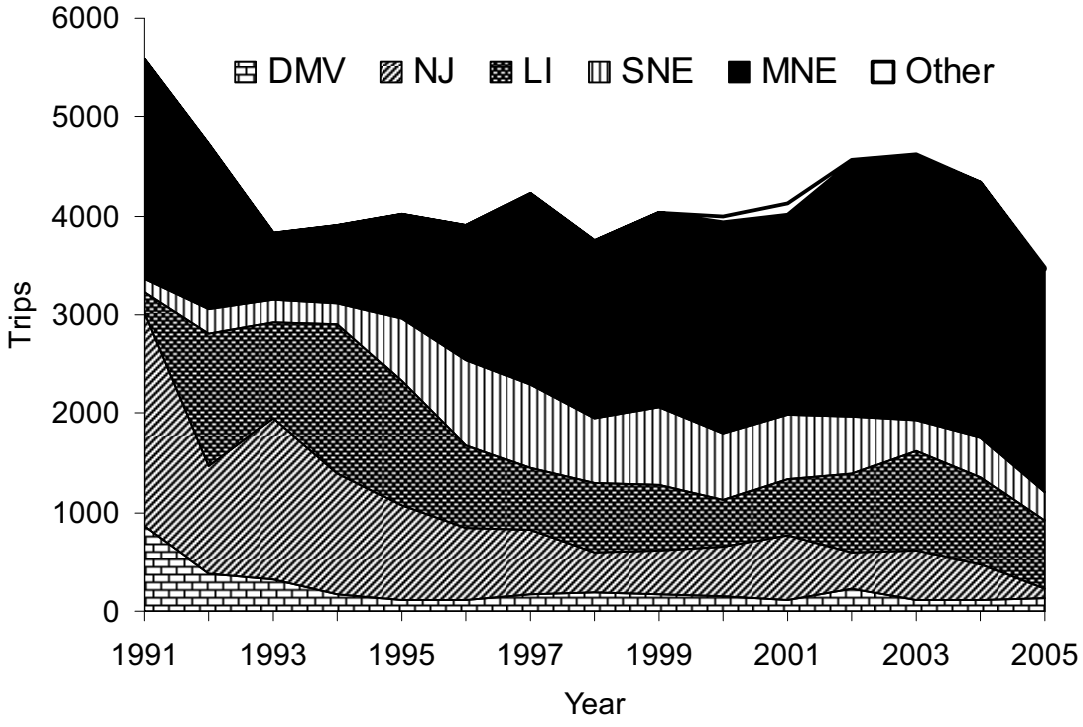

Figure A5. Number of trips for ocean quahog in the US EEZ during 1991-2004 based on logbook records.

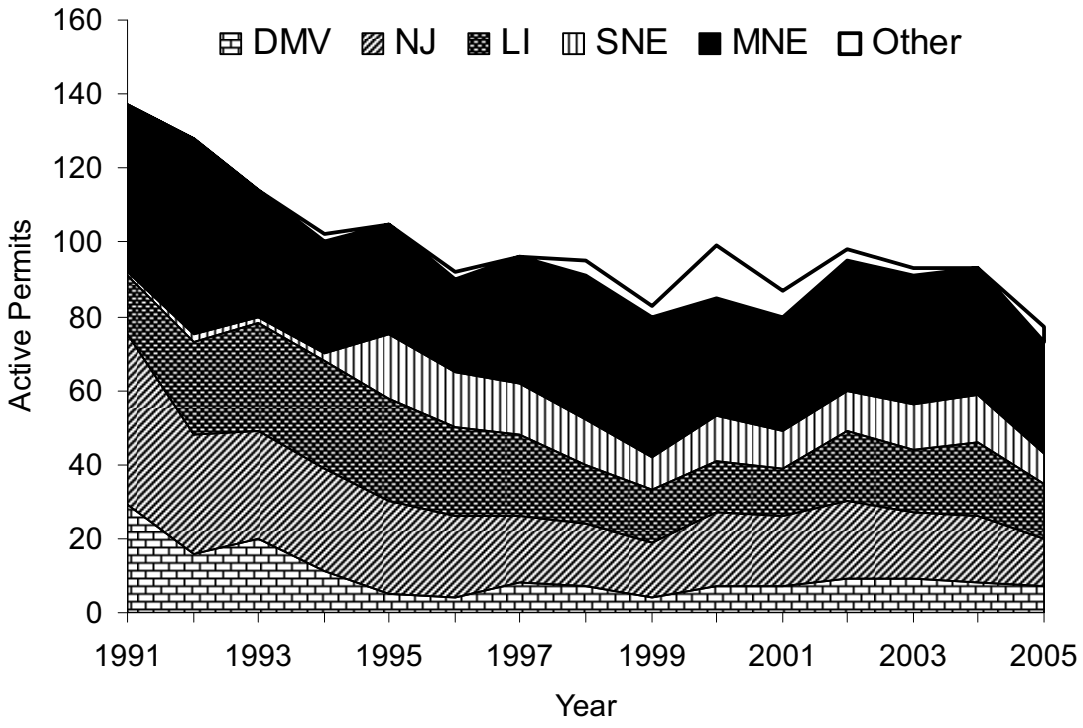

Figure A6. Number of active permits (fishing vessels) for ocean quahog in the US EEZ during 19910-2004 based on logbook records. The total number of permits in the graph for any year may exceed the total number of active permits in the fishery because some vessels fished in more than one area.

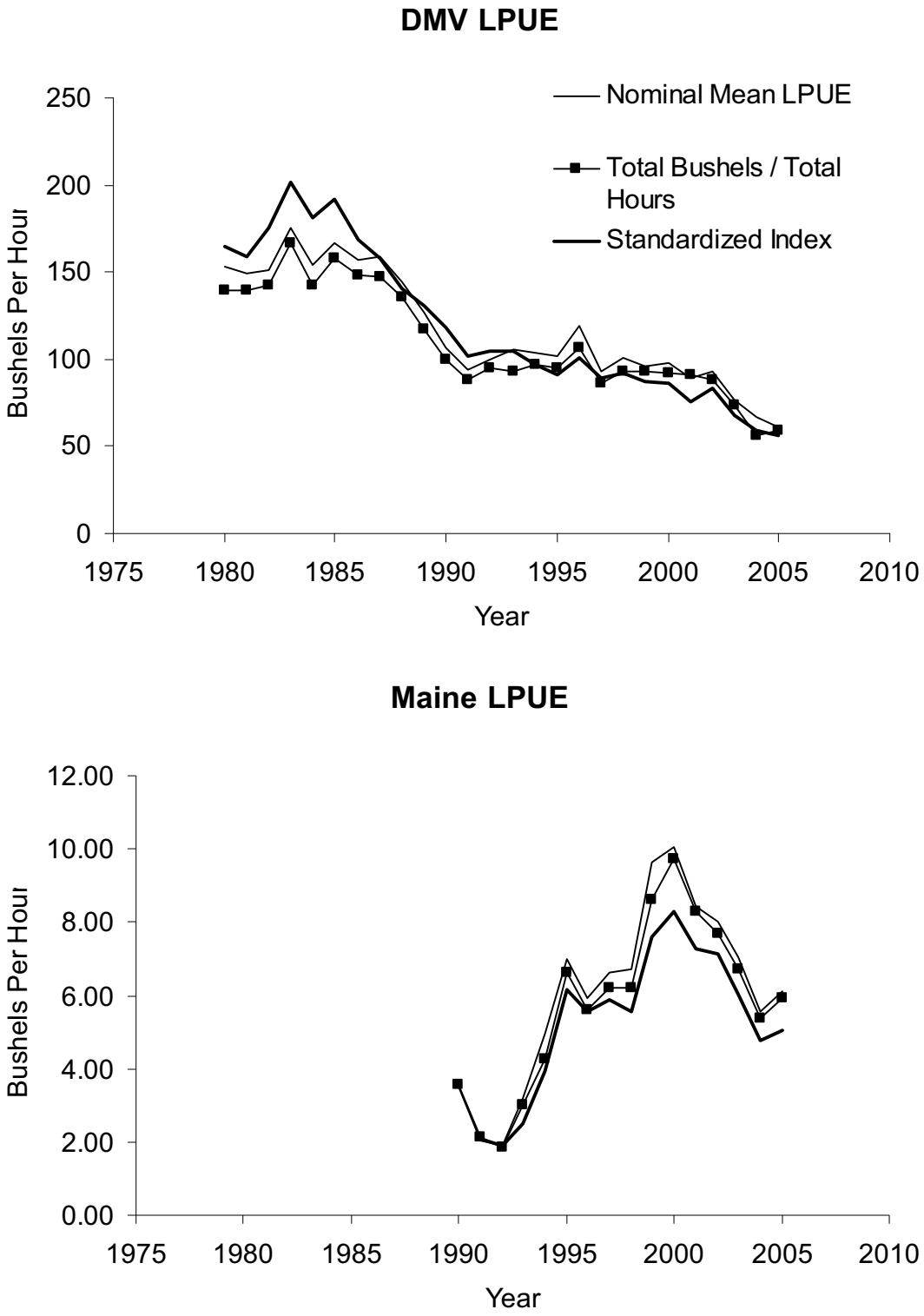

Figure A7. Trends in three measures of LPUE for ocean quahog in the DMV (ITQ bushels per hour) and MNE (Maine bushels per hour) stock assessment regions.

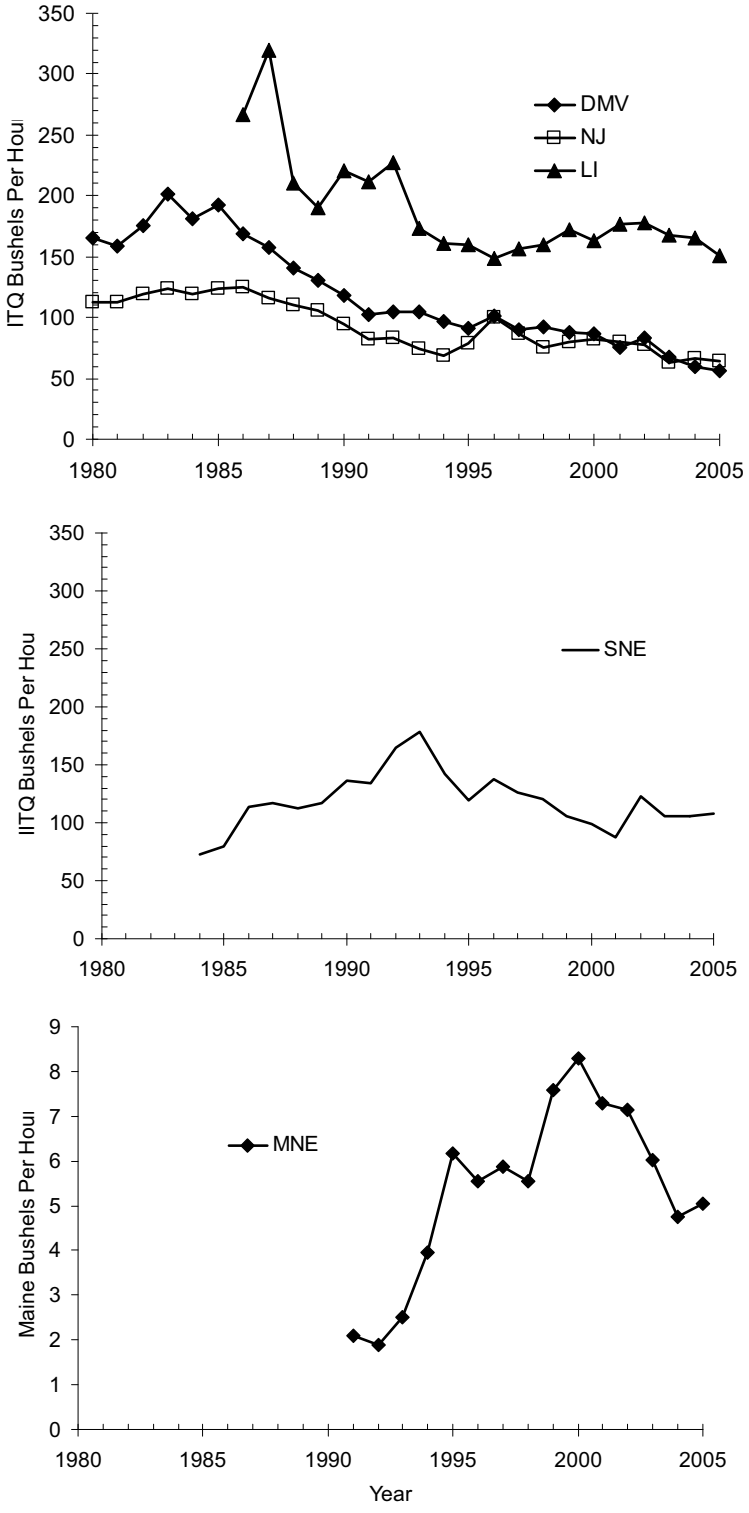

Figure A8. Trends in standardized LPUE for ocean quahog during 1980-2005 by stock assessment region.

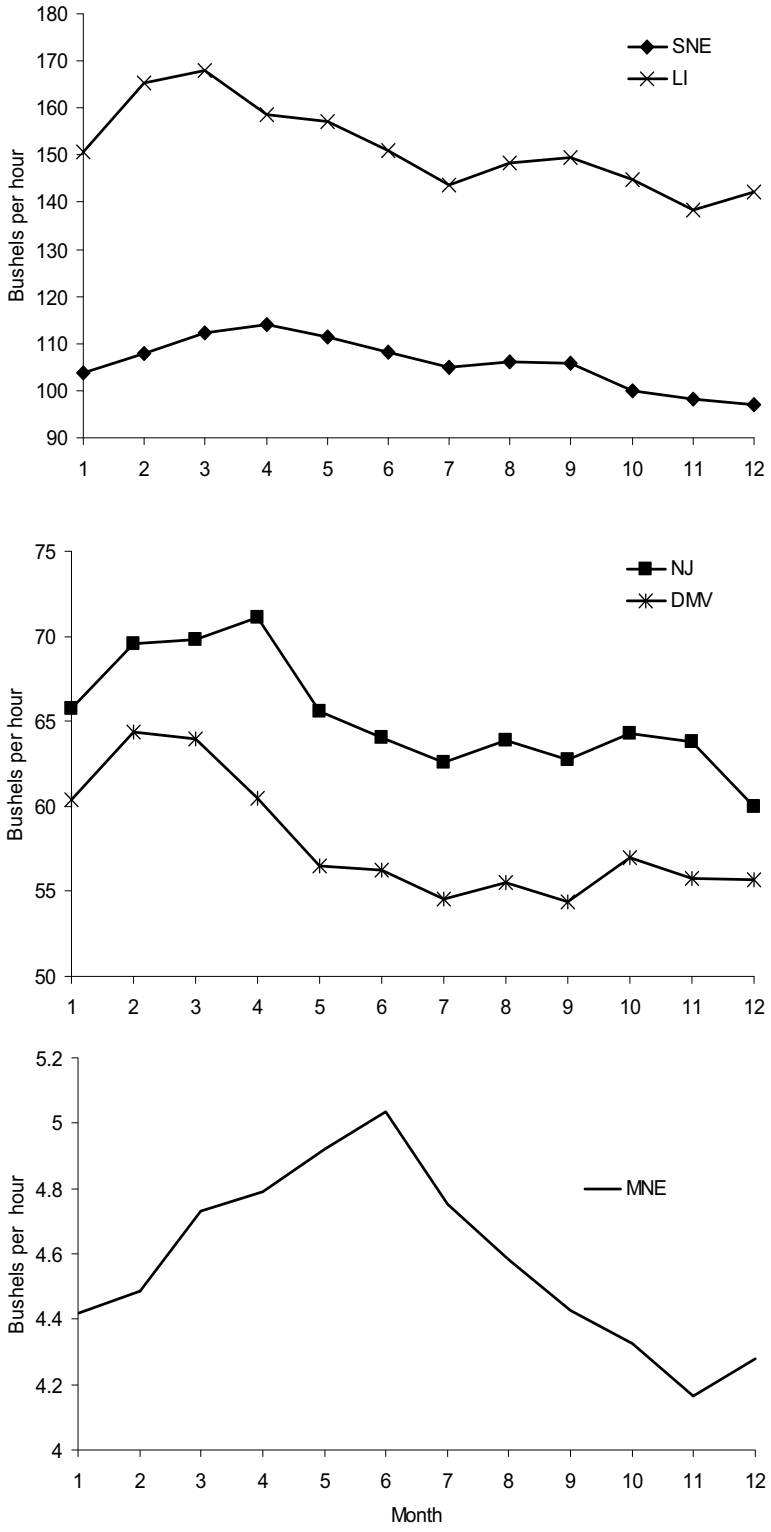

Figure A9. Trends in standardized LPUE month effects for ocean quahog during 1980-2005 by stock assessment region.

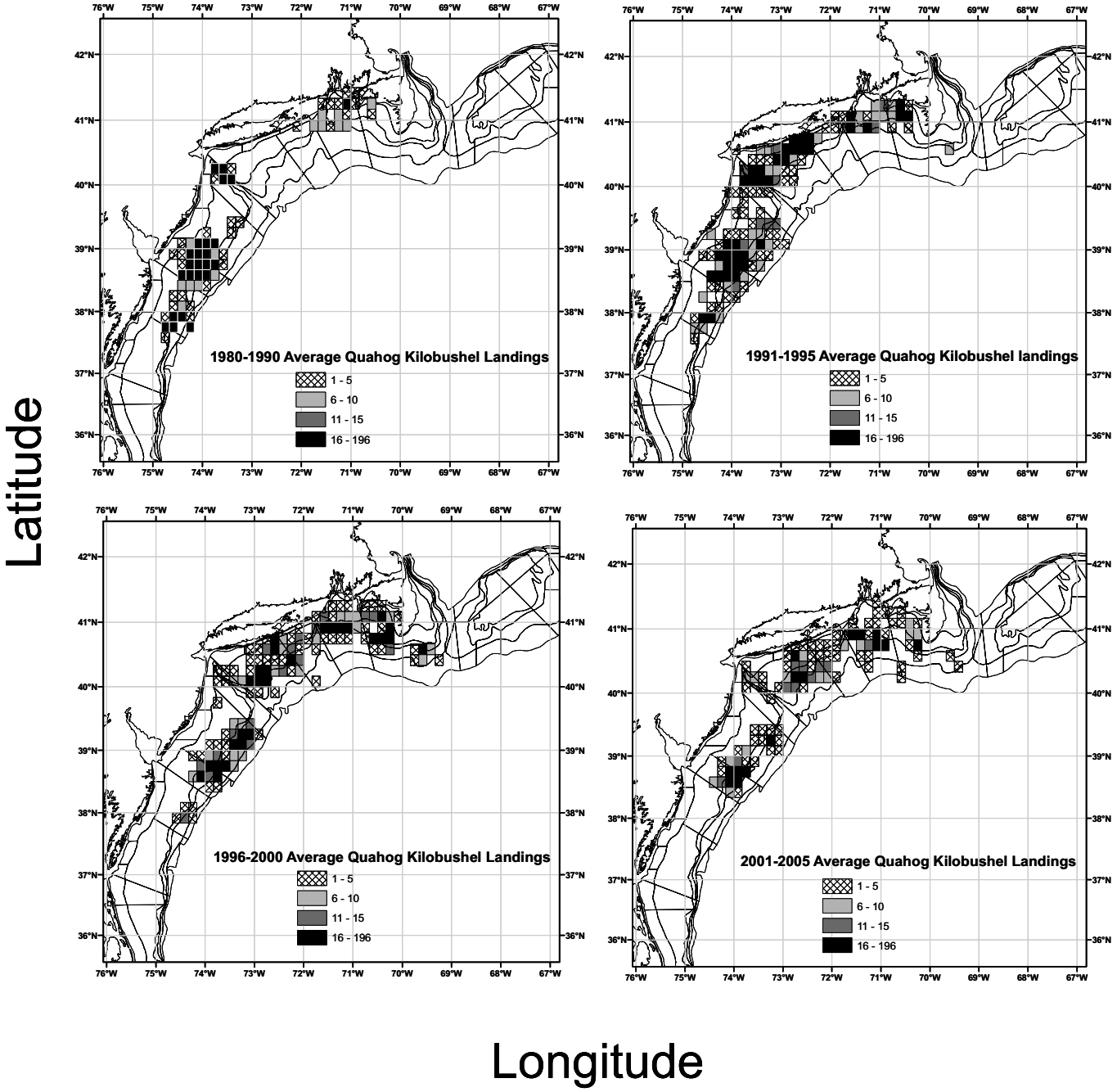

Figure A10. Spatial patterns in average annual landings (1000 ITQ bushels y^{-1}) for ocean quahog from logbook records. Data in TNMS far offshore reflect errors in logbook data.

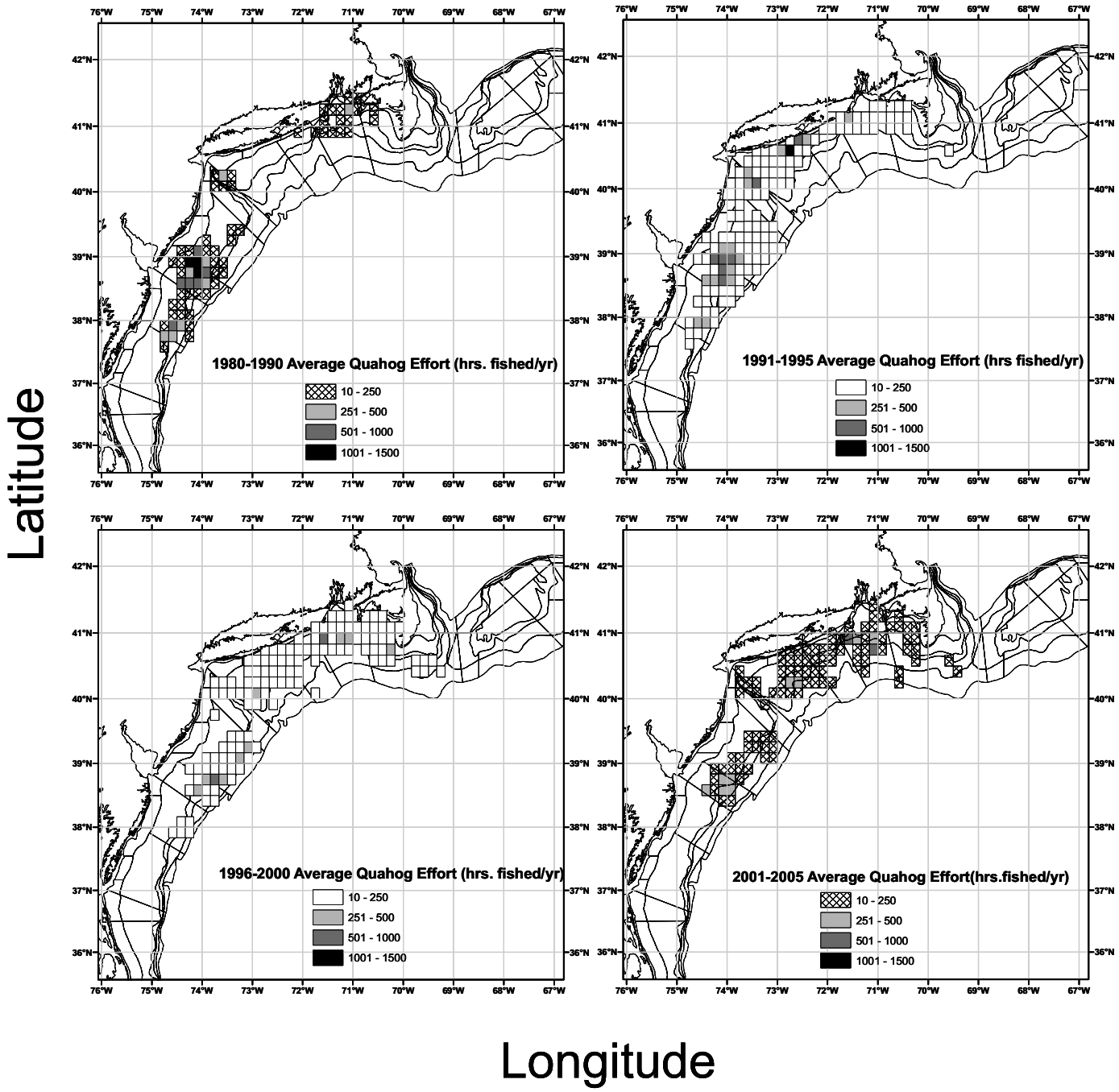

Figure A11. Spatial patterns in average annual fishing effort (hours fished y^{-1}) for ocean quahog from logbook records. Data in TNMS far offshore reflect errors in logbook data.

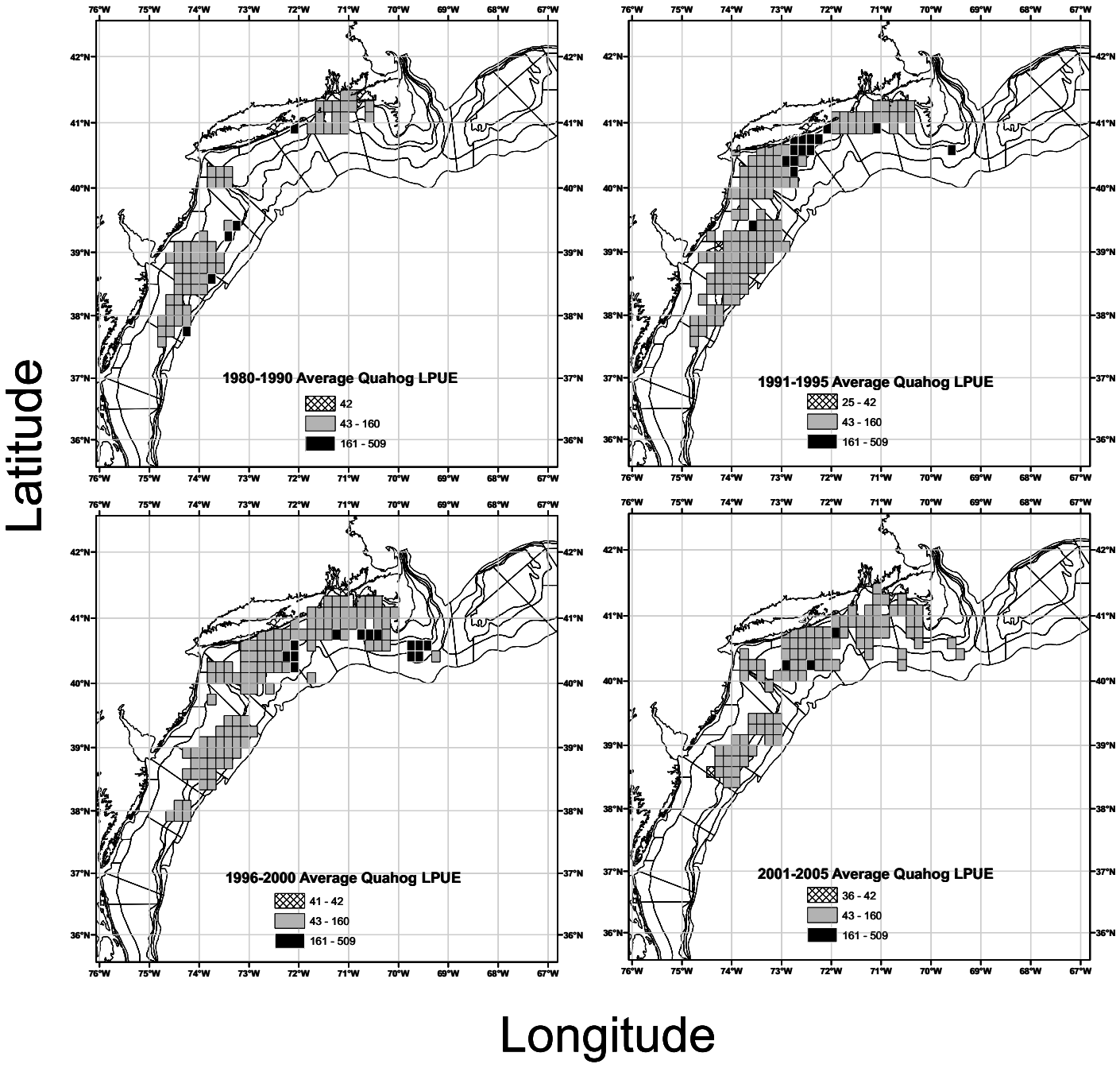

Figure A12. Spatial patterns in average LPUE (ITQ bushels per hours fished) for ocean quahog from logbook records. Data in TNMS far offshore reflect errors in logbook data.

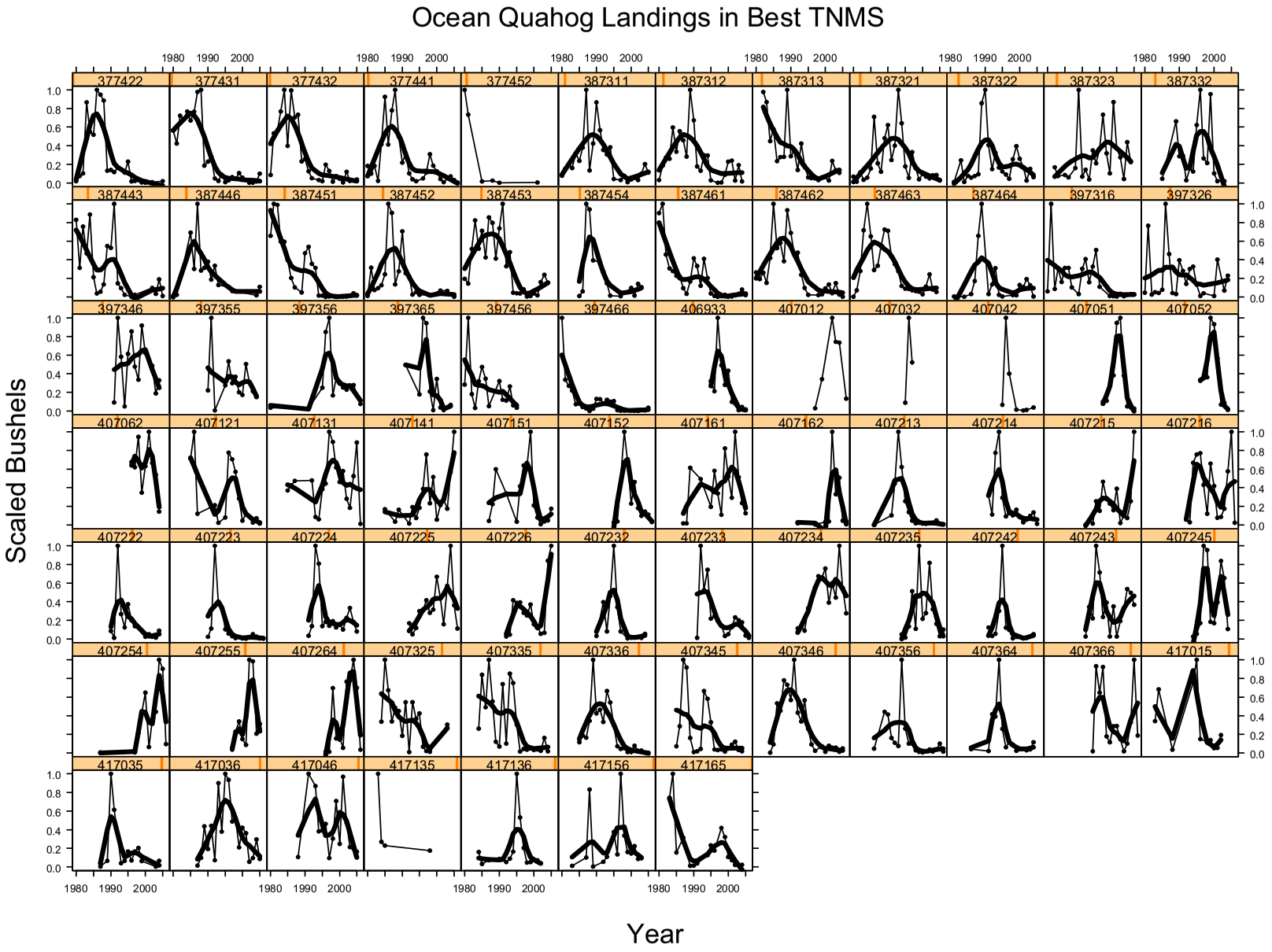

Figure A13. Trends in total annual landings (ITQ bu y^{-1}, vessel ton class 3-4) for ocean quahog in important TNMS during 1980-2005.

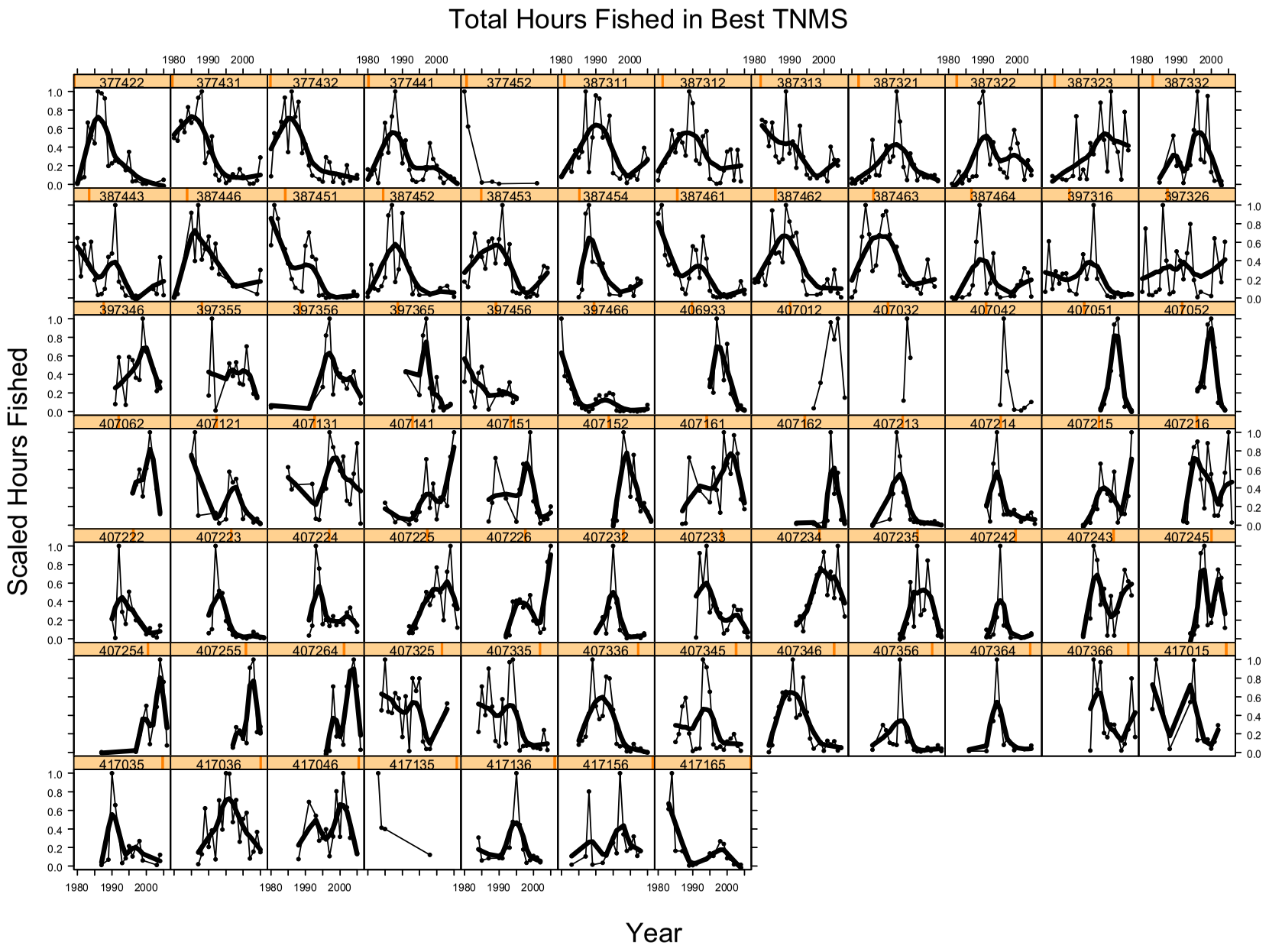

Figure A14. Trends in total annual fishing effort (hours fished y^{-1}, vessel ton class 3-4) for ocean quahog in important TNMS during 1980-2005.

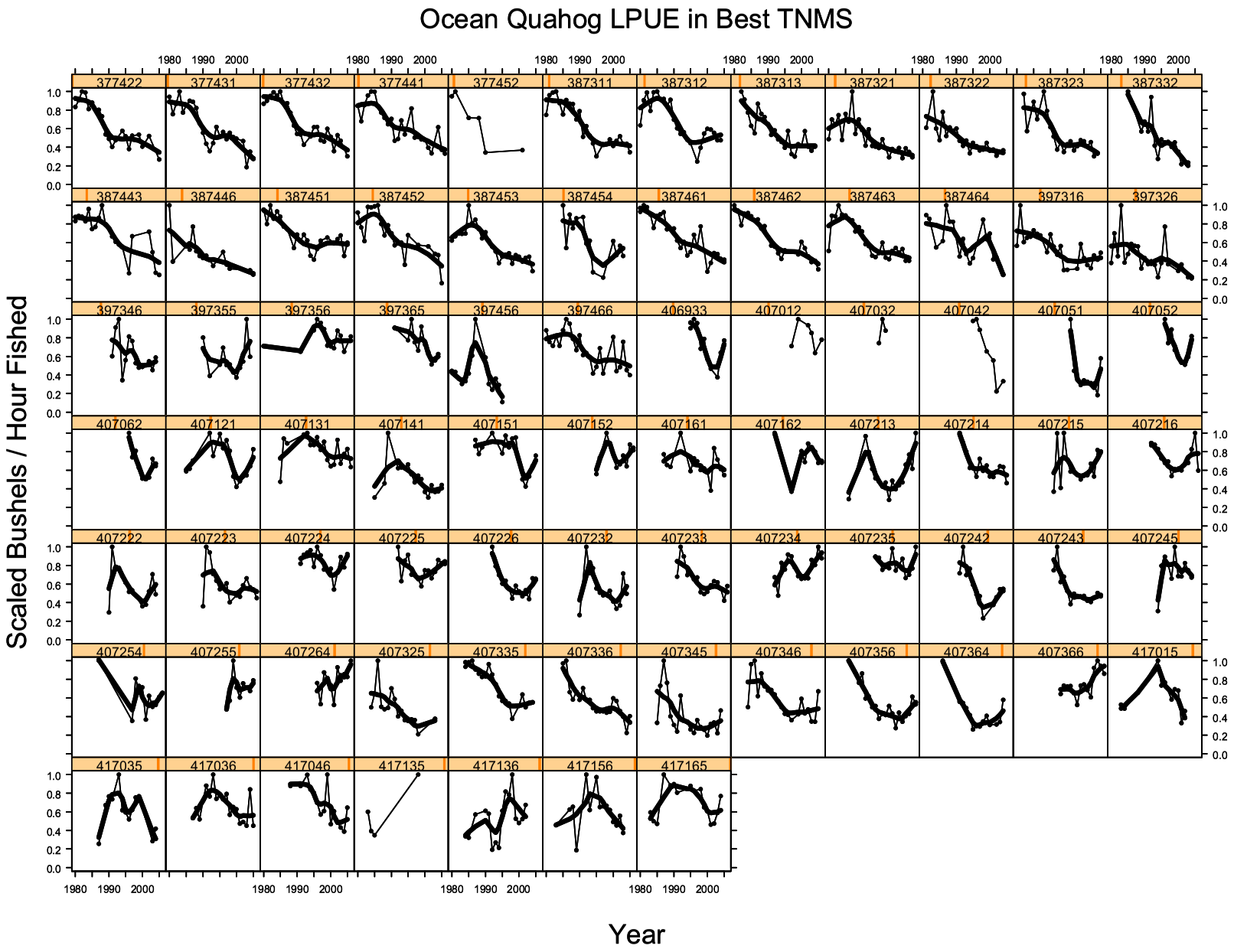

Figure A15. Trends in annual LPUE (ITQ bushels per hours fished, vessel ton class 3-4) for ocean quahog in important TNMS during 1980-2005.

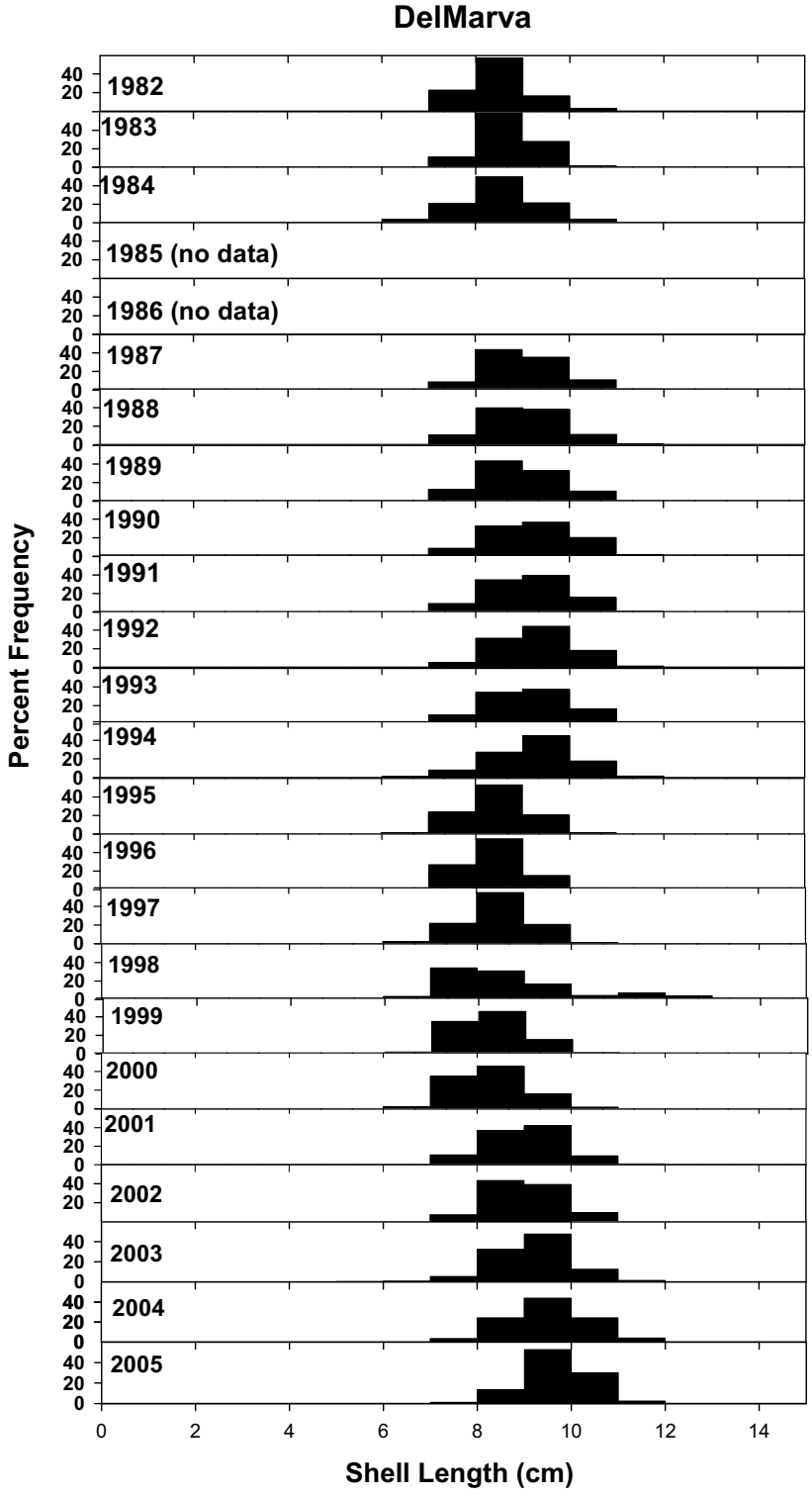

Figure A16. Commercial length composition data for ocean quahog landed in the DMV stock assessment region.

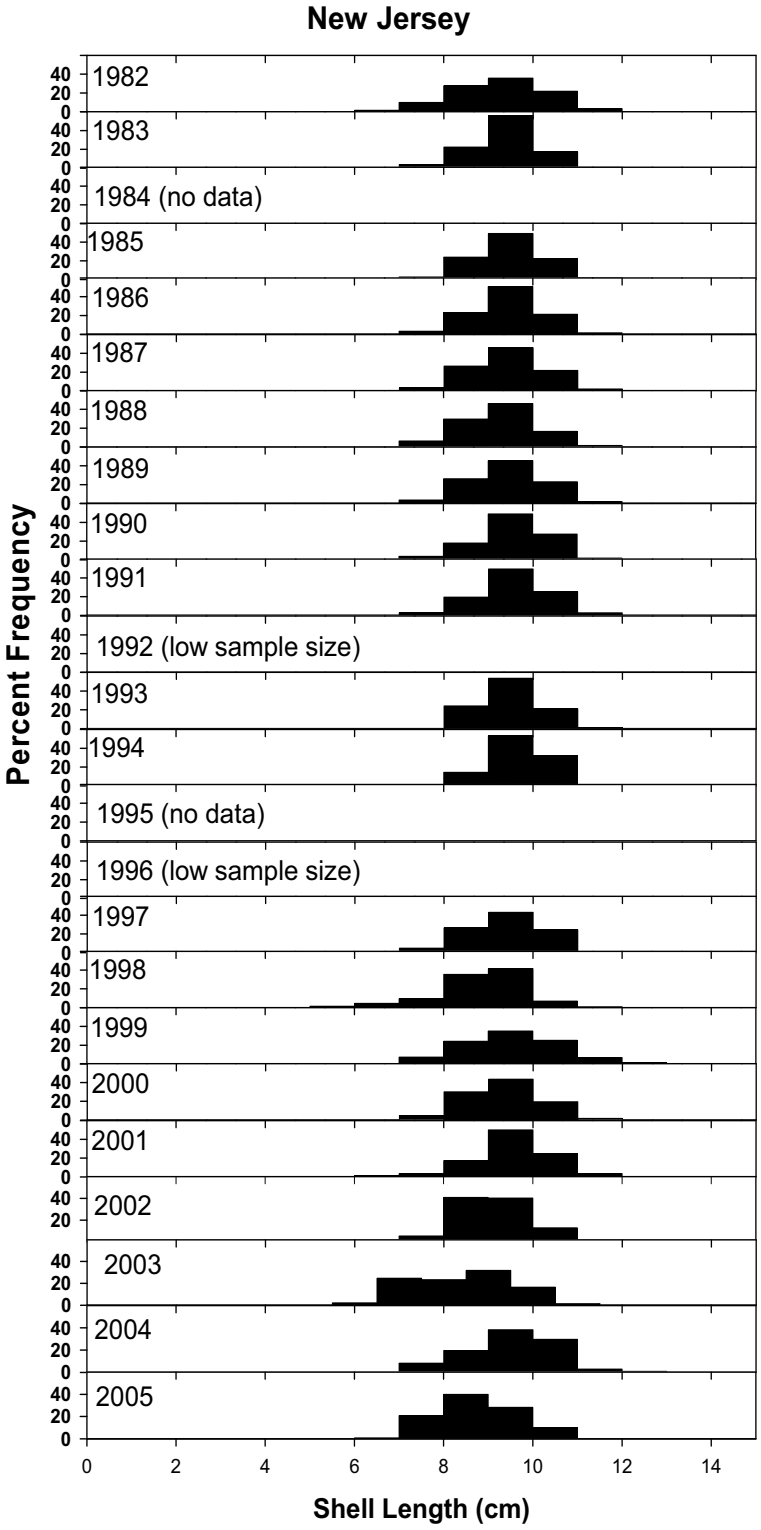

Figure A17. Commercial length composition data for ocean quahog landed in the NJ stock assessment region.

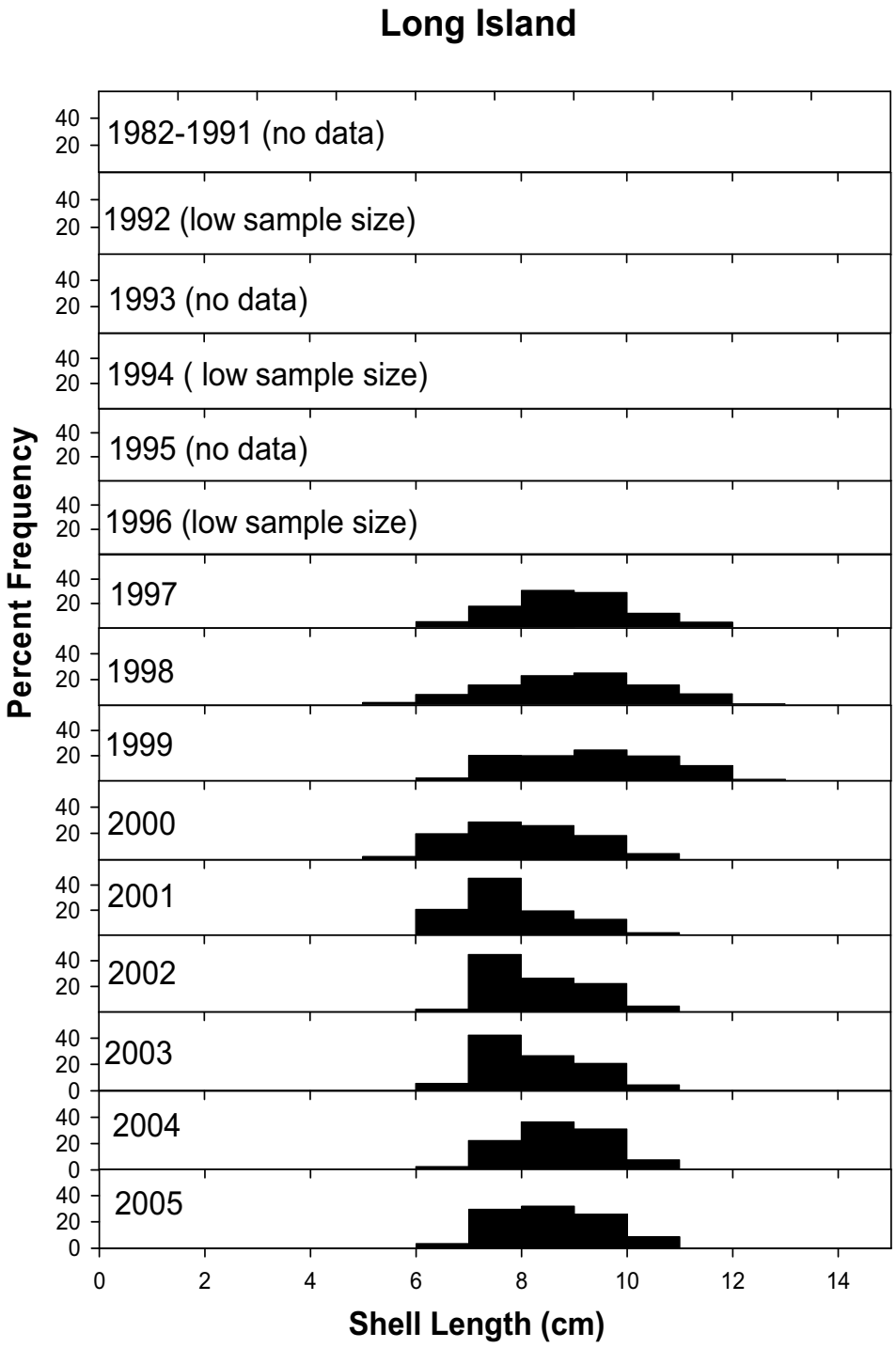

Figure A18. Commercial length composition data for ocean quahog landed in the LI stock assessment region.

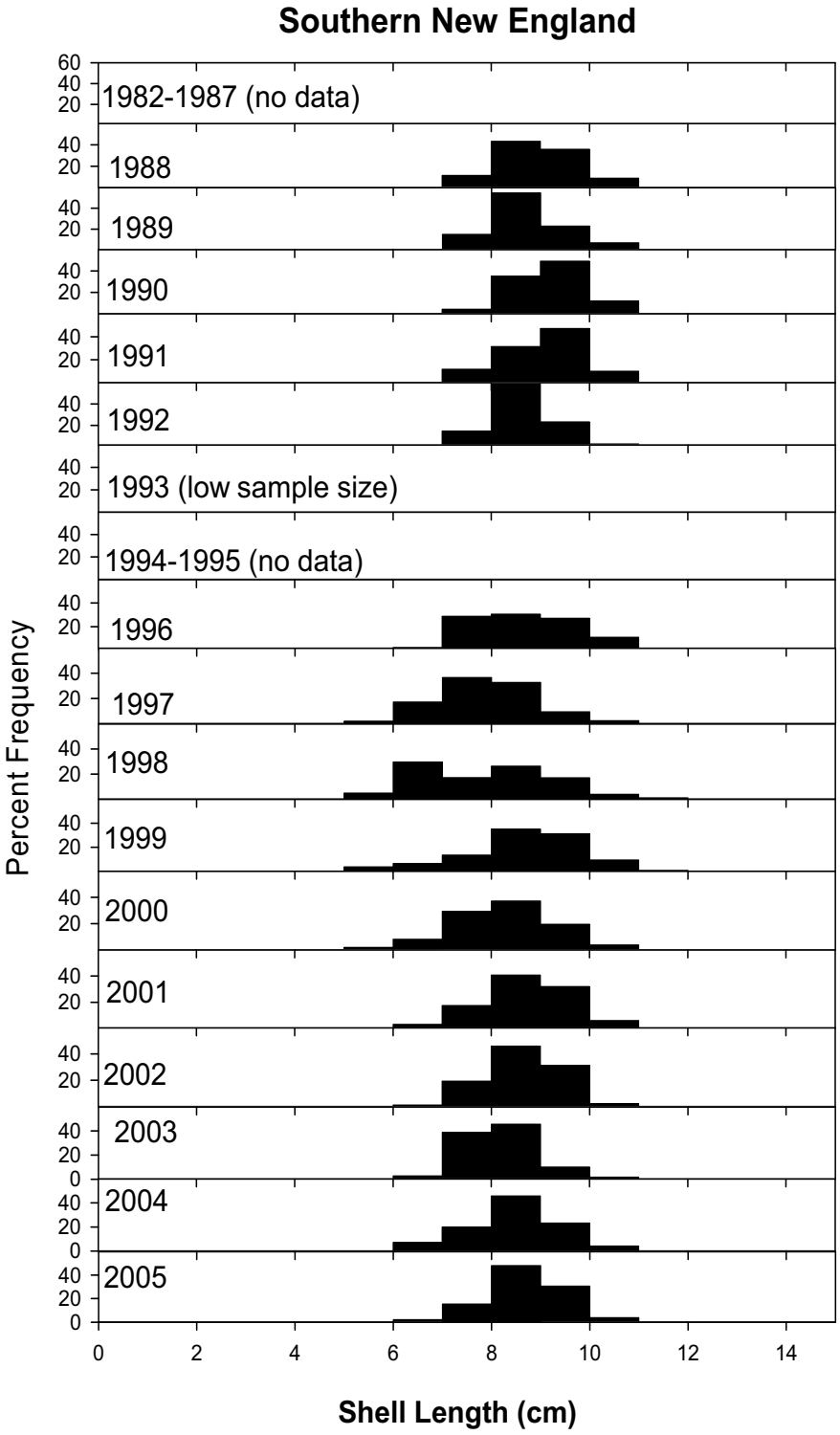

Figure A19. Commercial length composition data for ocean quahog landed in the SNE stock assessment region.

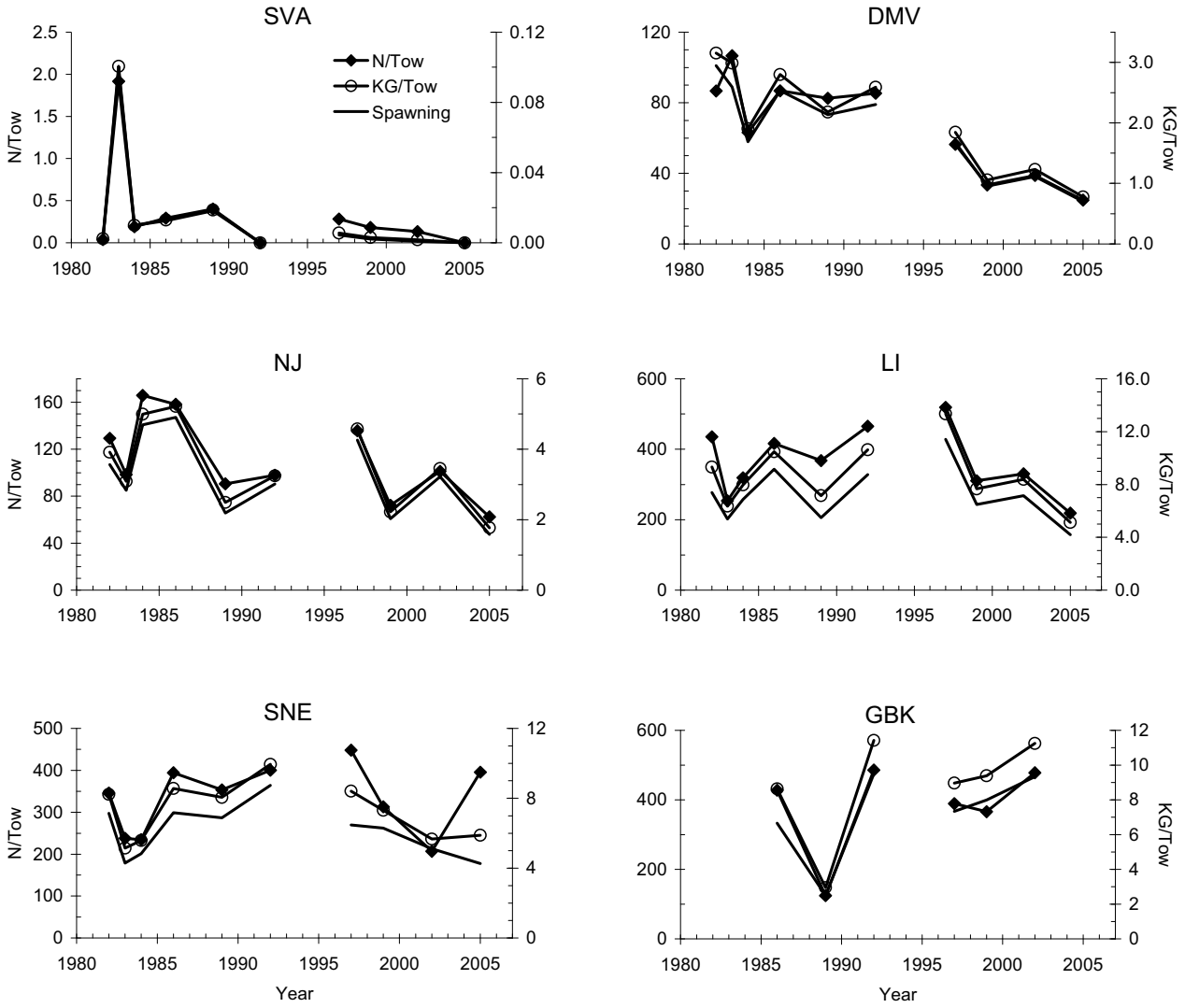

Figure A20. NEFSC clam survey trends for ocean quahog stock abundance (mean n/tow), biomass (mean kg/tow), and spawning biomass (mean kg/tow) during 1982-2005. Data for 1994 are omitted because of electrical problems with pump voltage that artificially increased dredge efficiency. Survey data shown in graphs were adjusted based on survey selectivity to estimate trends for the entire stock.

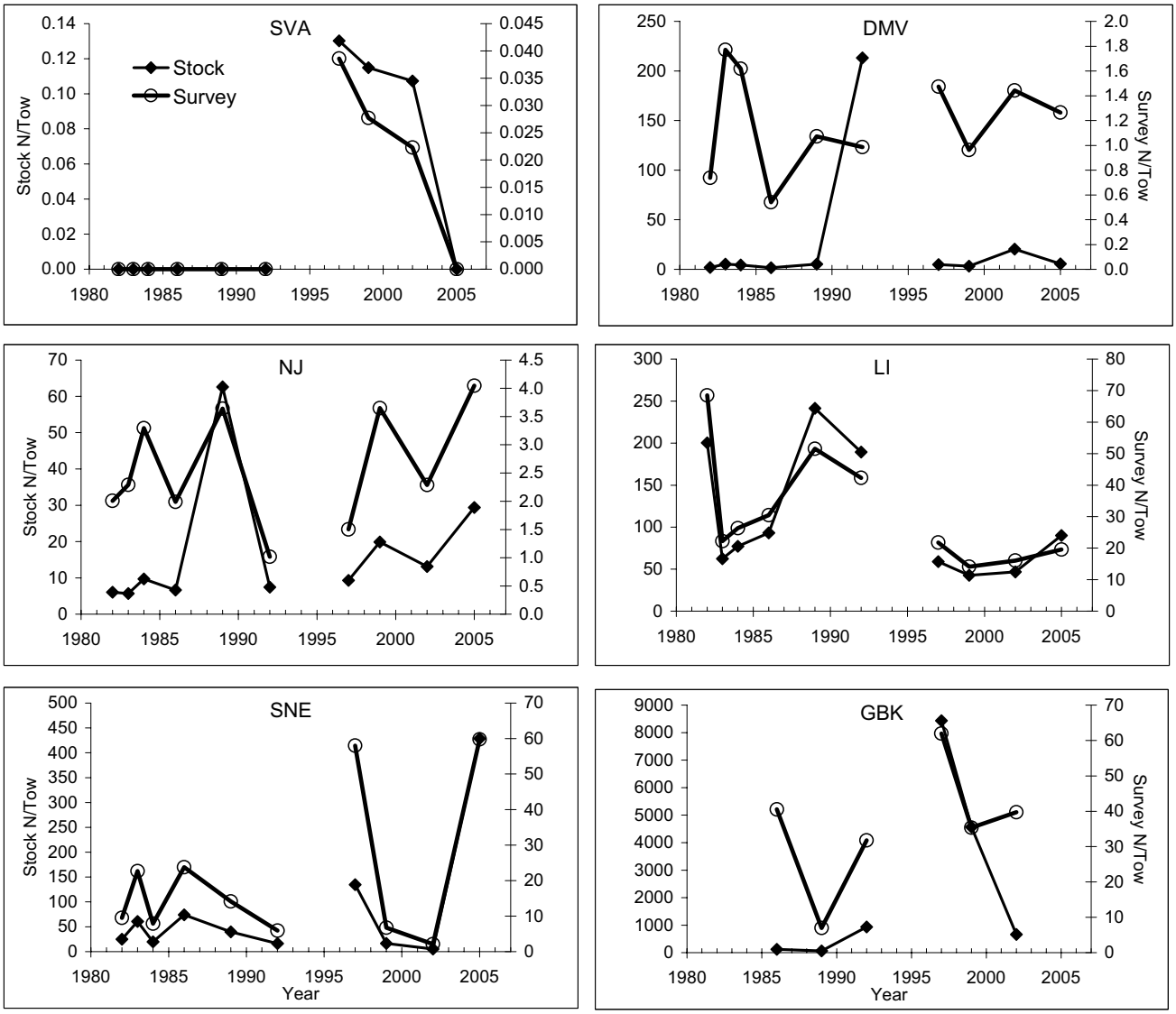

Figure A21. NEFSC clam survey trends for ocean quahog recruit (<70 mm SL) abundance (mean n/tow) during 1982-2005. Trends are shown with ("Stock") and without ("Survey") corrections for survey dredge selectivity. Data for 1994 are omitted because of electrical problems with pump voltage that artificially increased dredge efficiency. The apparent outlier for stock n/tow in DMV during 1992 is due to a relatively large catch of small ocean quahog which was increased substantially when adjusted for survey dredge selectivity.

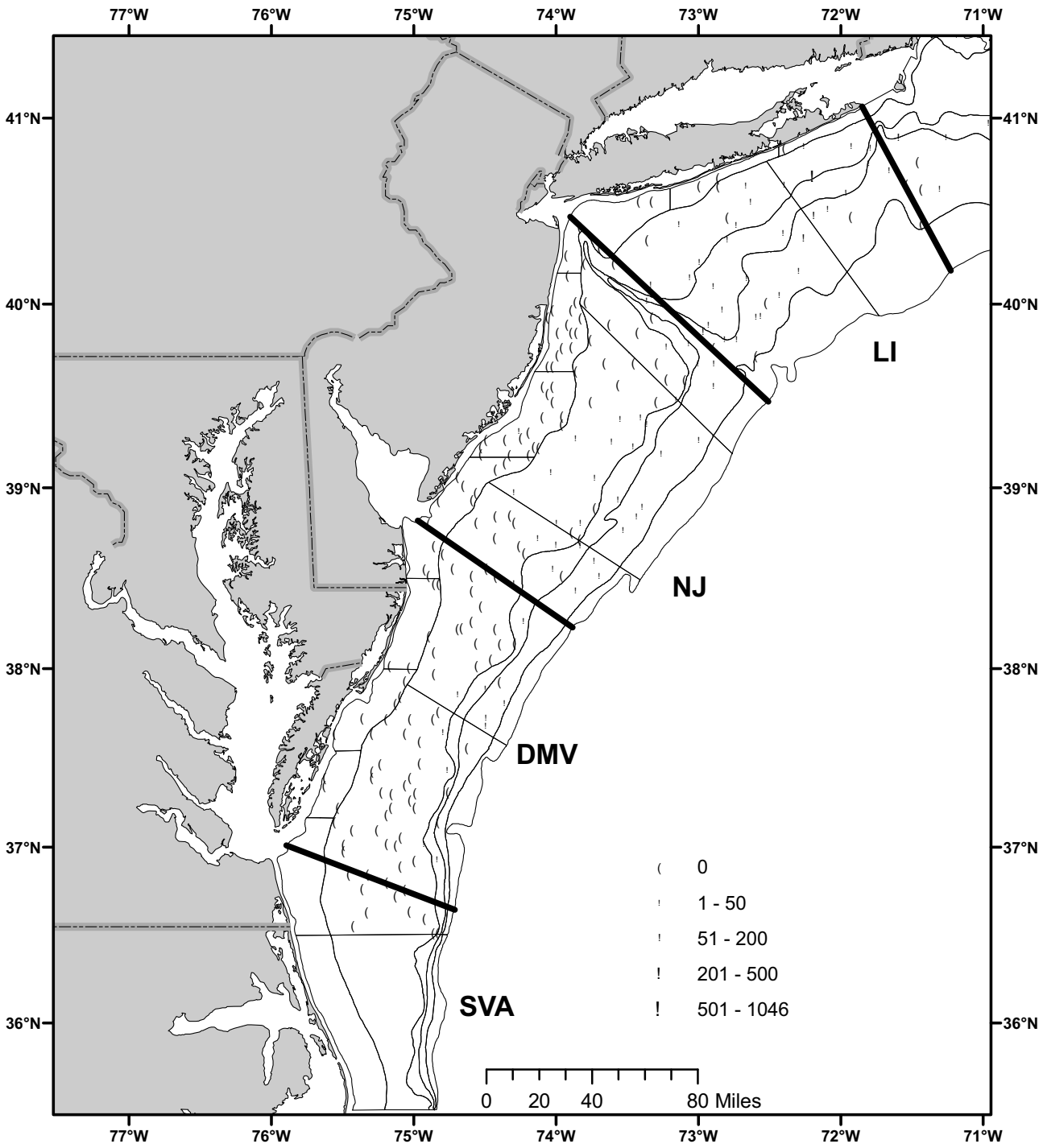

Figure A22. Location and size of recruit ocean quahog (<70 mm) catches in 2005 NEFSC clam survey, between Long Island and Cape Hatteras.

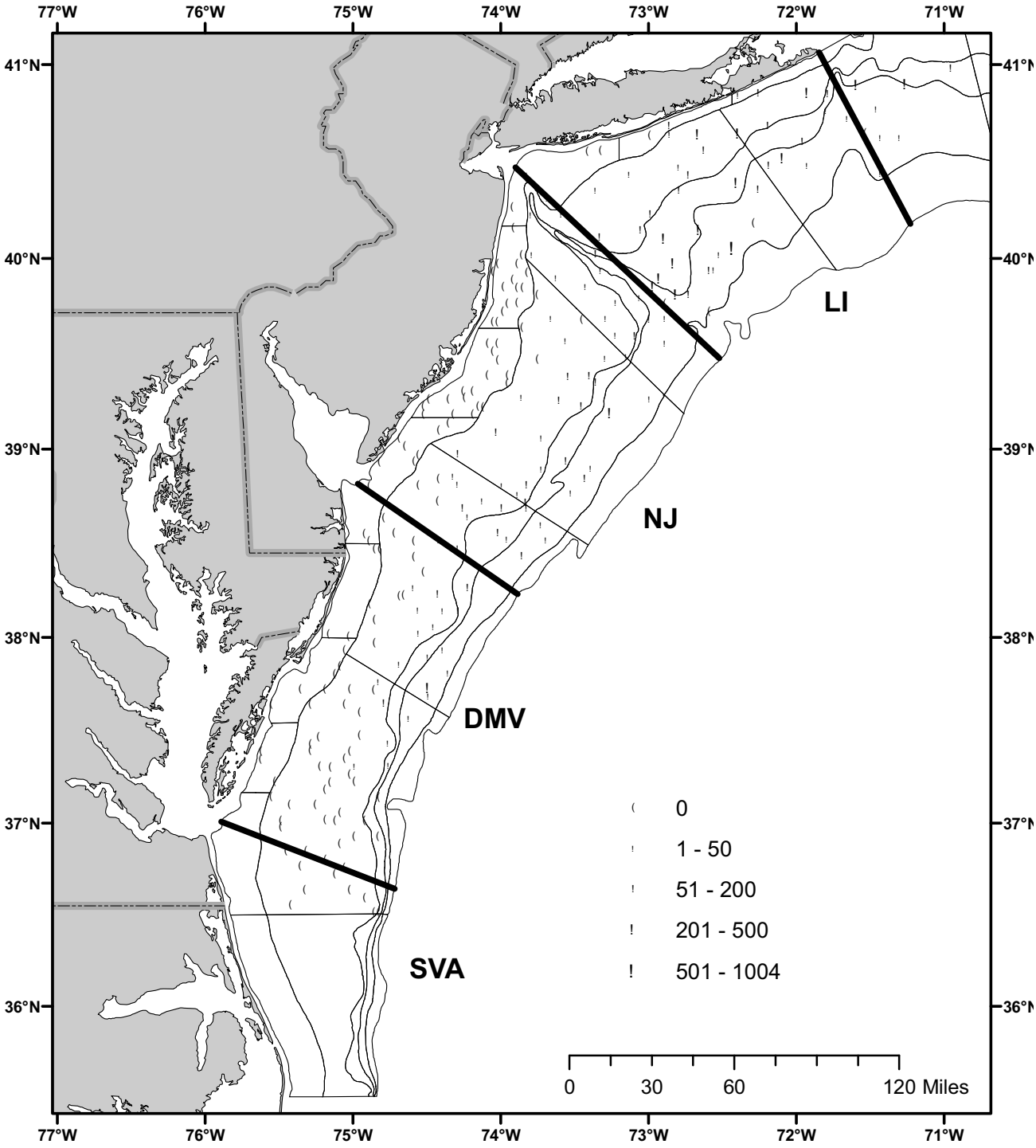

Figure A23. Location and size of large ocean quahog (70+ mm) catches in 2005 NEFSC clam survey, between Long Island and Cape Hatteras.

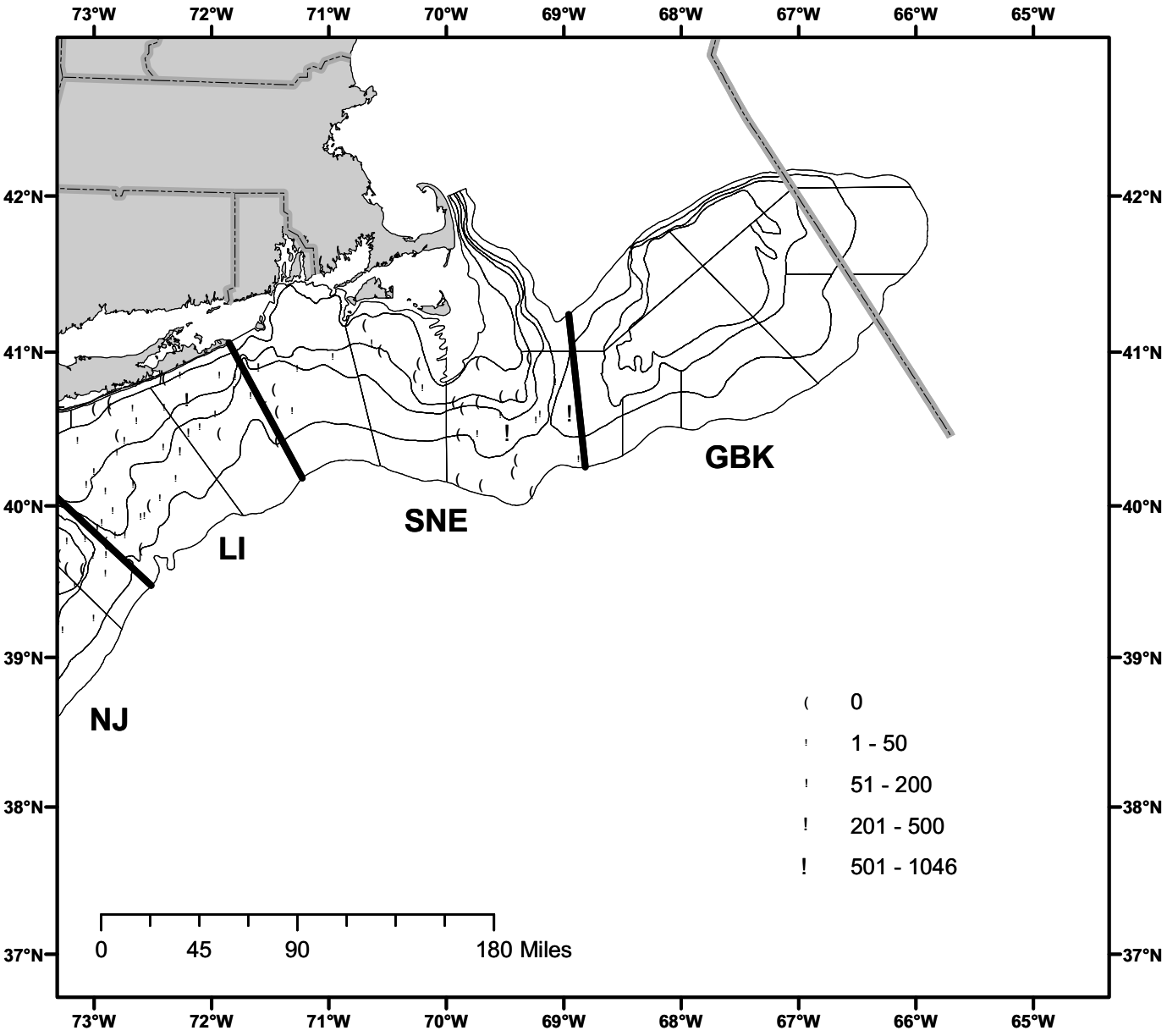

Figure A24. Location and size of recruit ocean quahog (<70 mm) catches in 2005 NEFSC clam survey, between Georges Banks and Long Island.

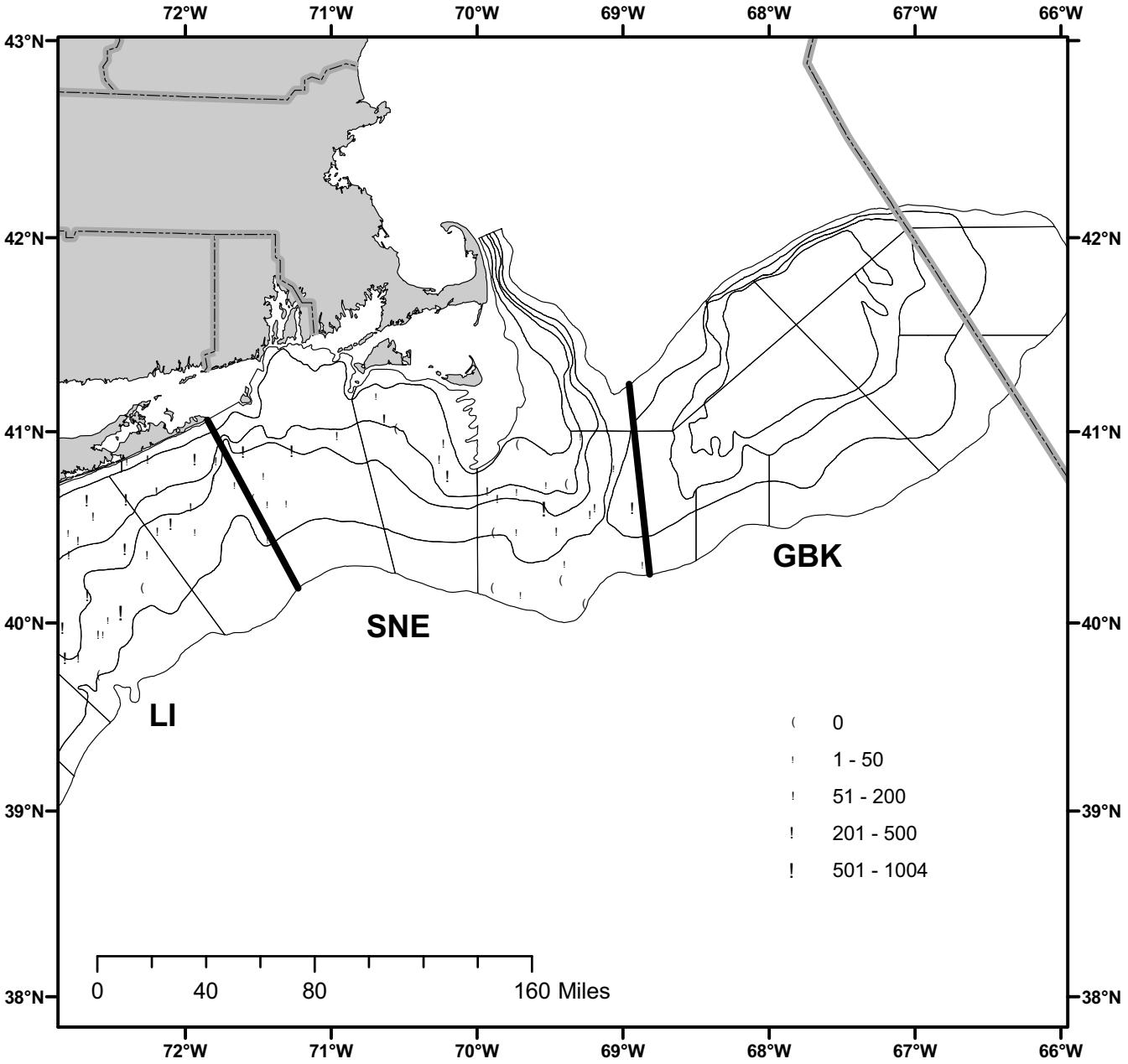

Figure A25. Location and size of large ocean quahog (70+ mm) catches in 2005 NEFSC clam survey, between Georges Bank and Long Island.

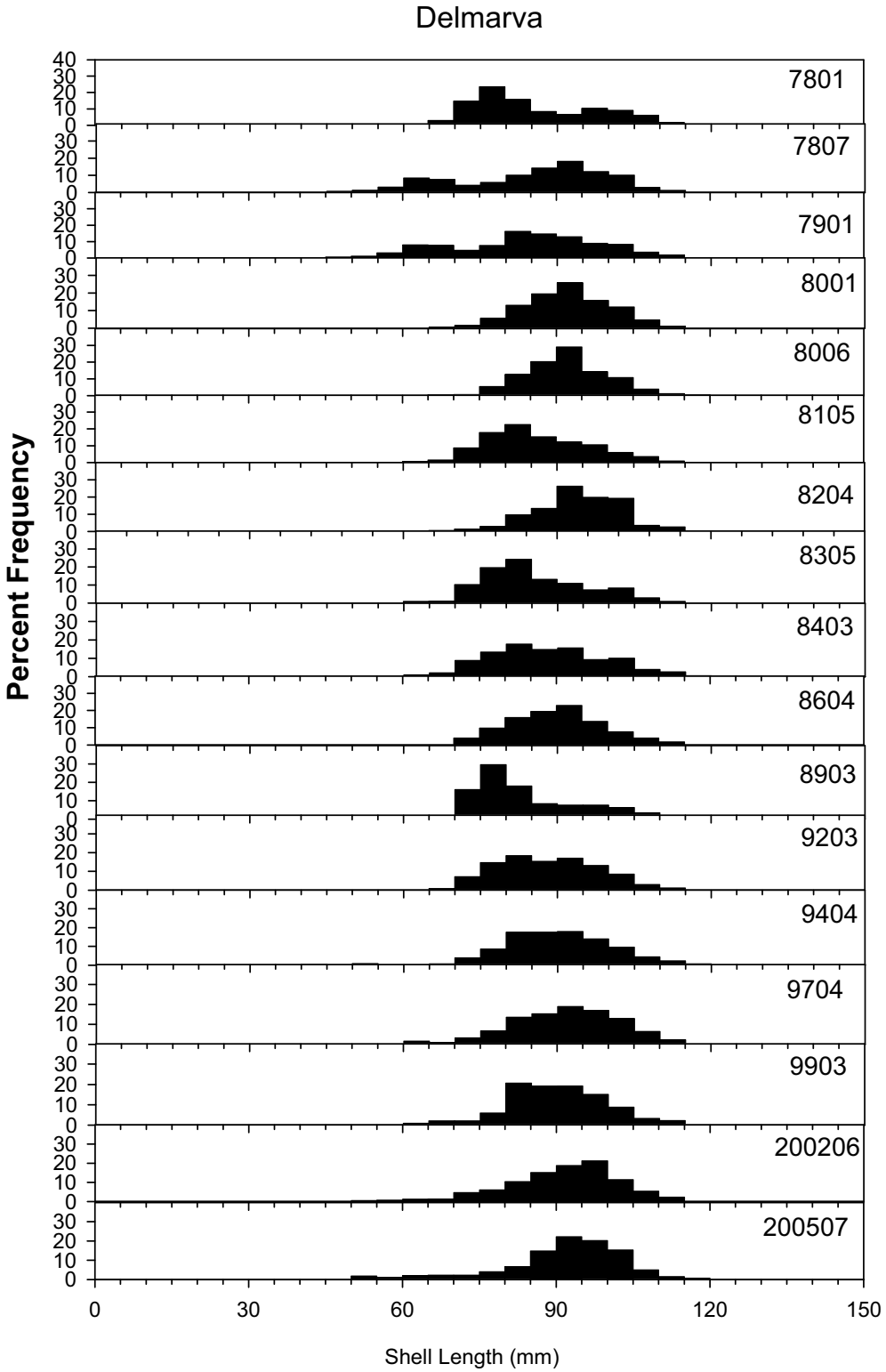

Figure A26. Length composition for ocean quahog in NEFSC clam surveys, by region. Frequencies are proportional to mean numbers per tow at length, without adjustment for survey dredge selectivity.

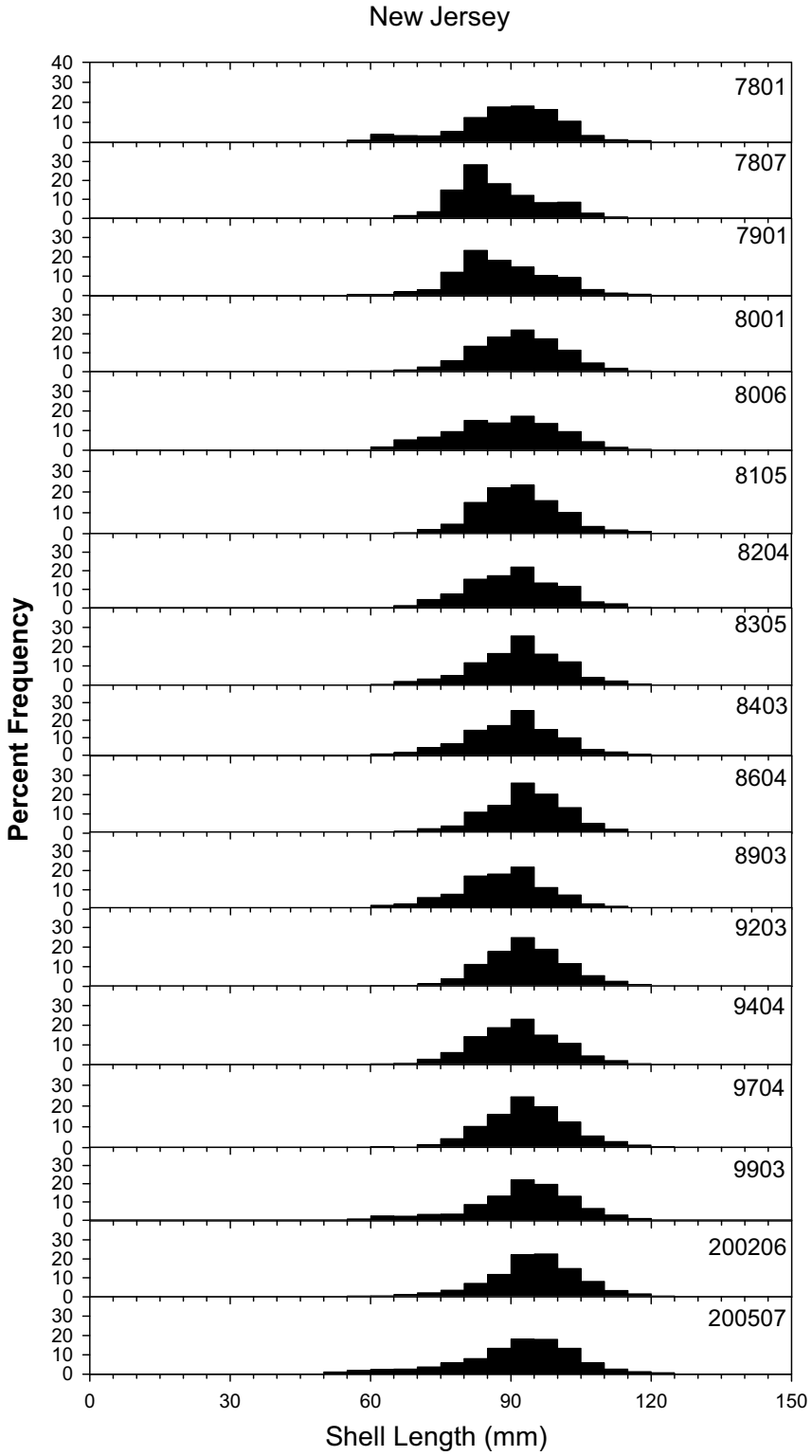

Figure A26 (continued)

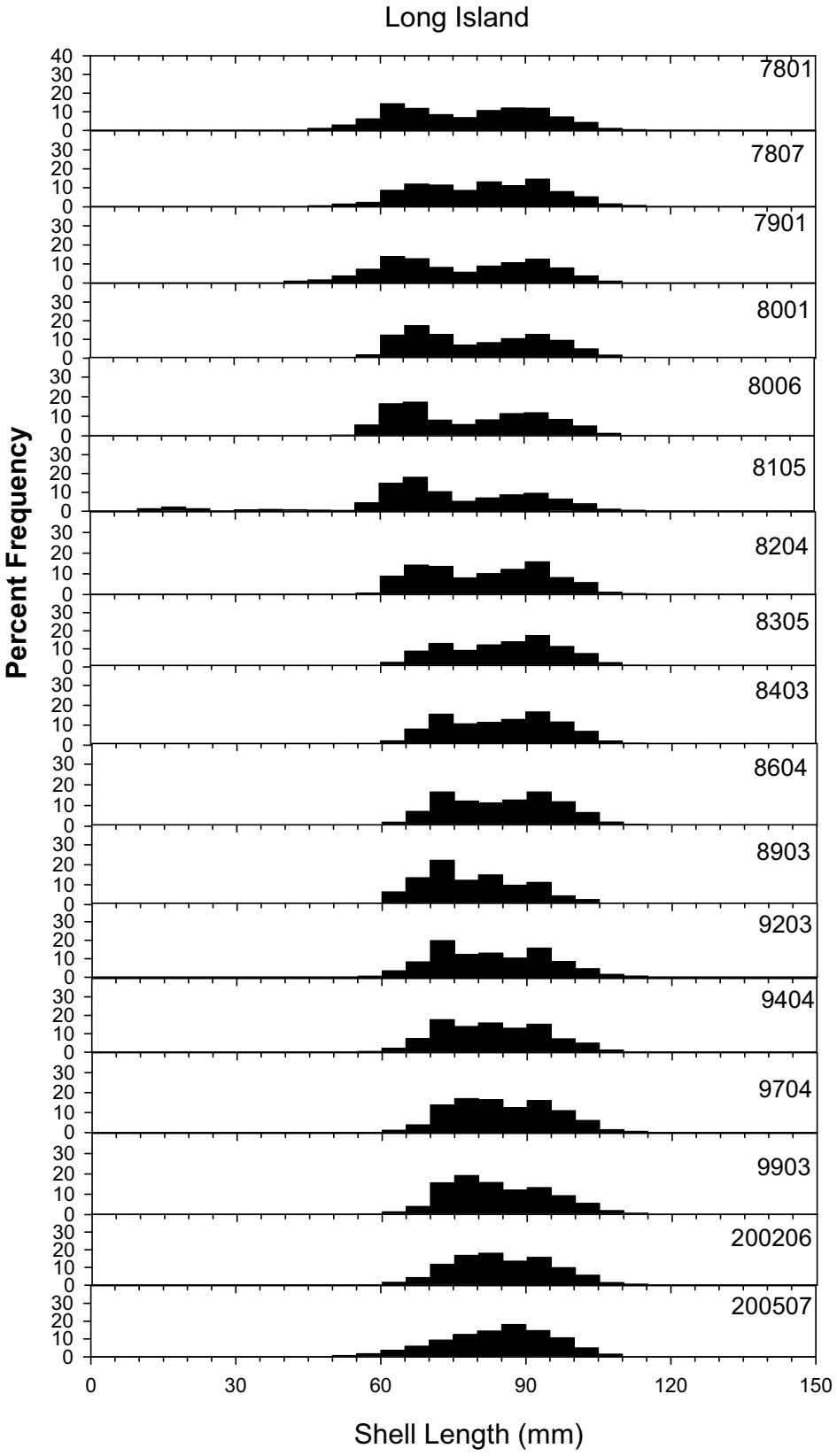

Figure A26 (continued)

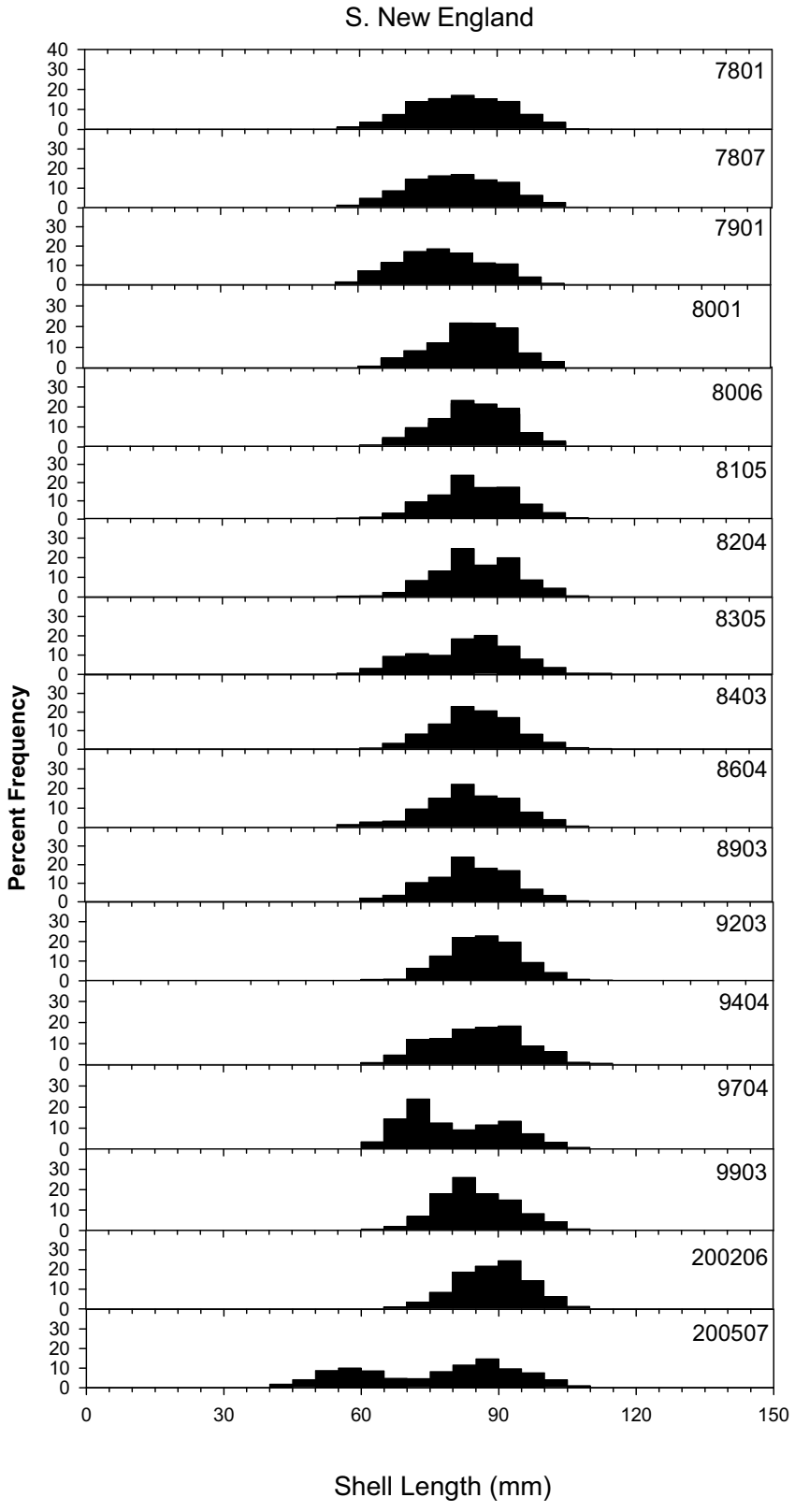

Figure A26 (continued)

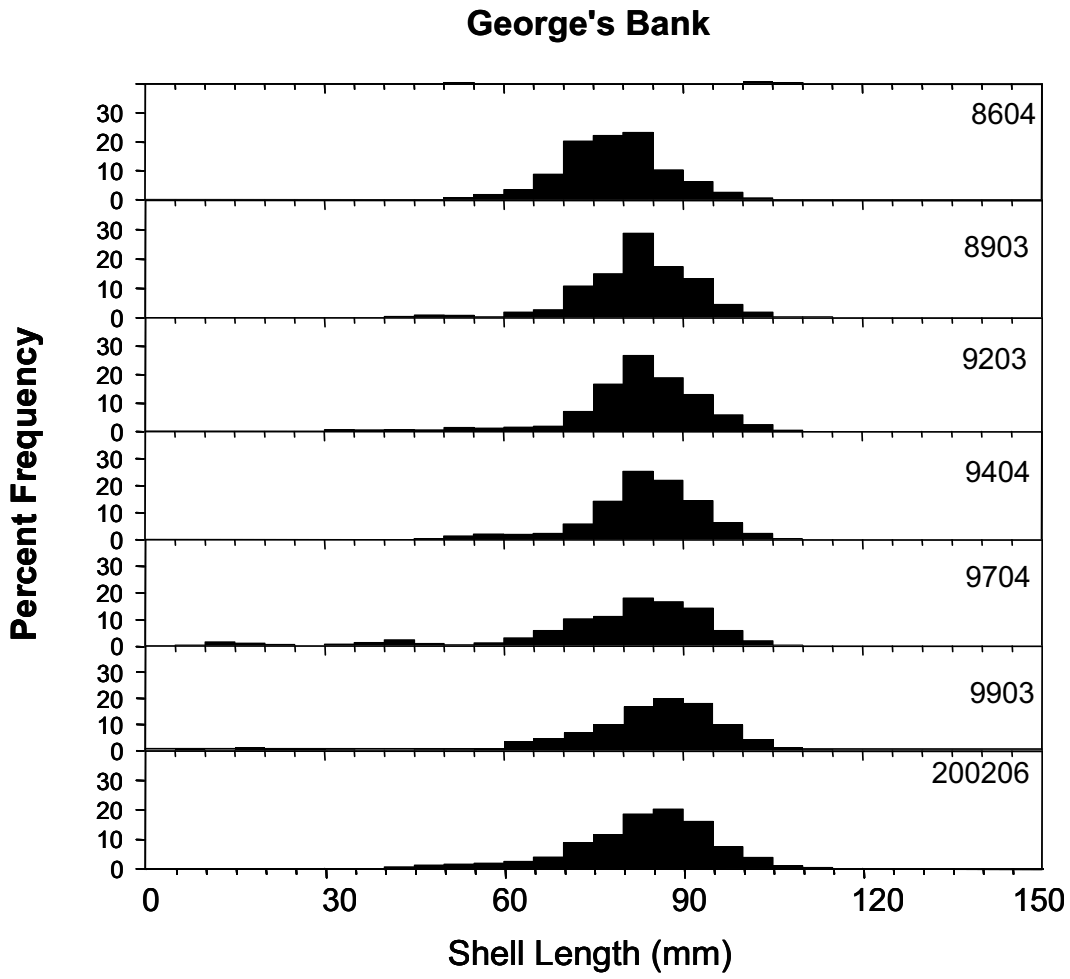

Figure A26 (continued)

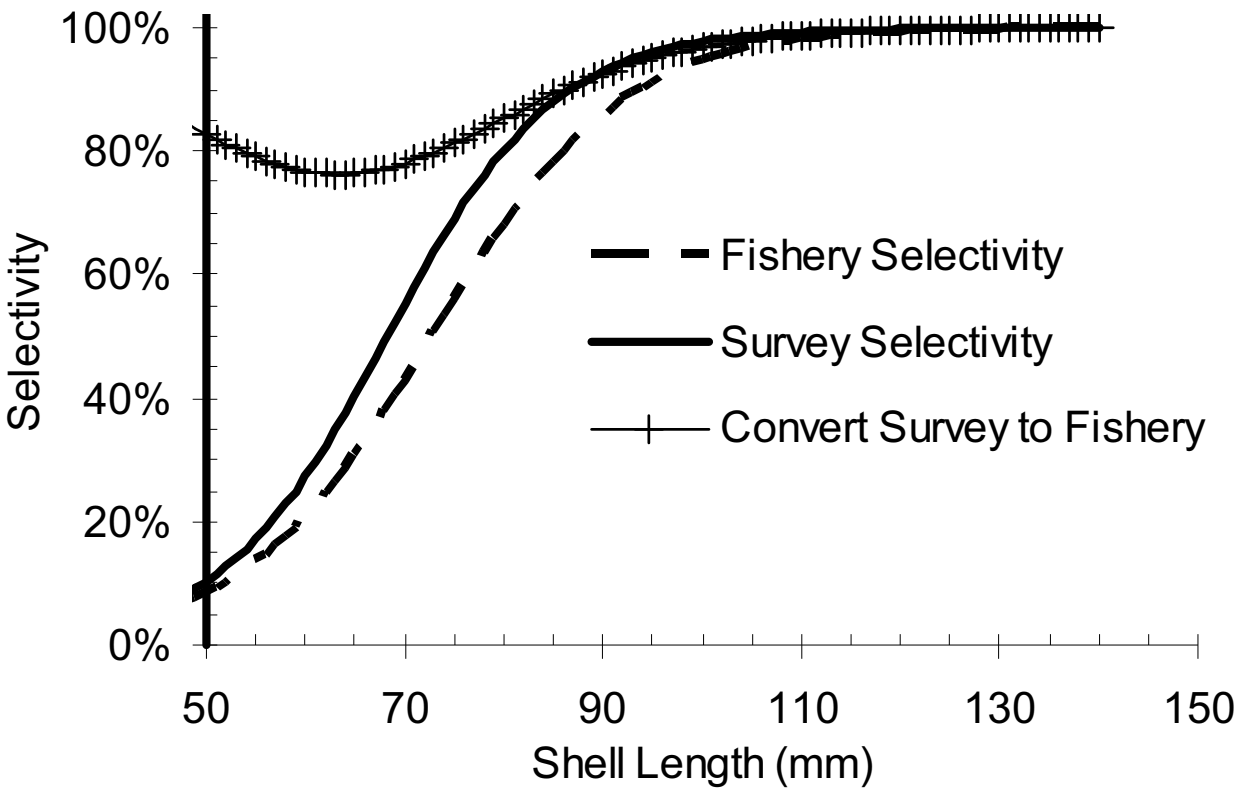

Figure A27. Fishery and survey selectivity curves for ocean quahog. The ratio of the fishery and survey selectivity curves, which can be used to convert survey abundance at size directly to fishable abundance at size, is also shown.

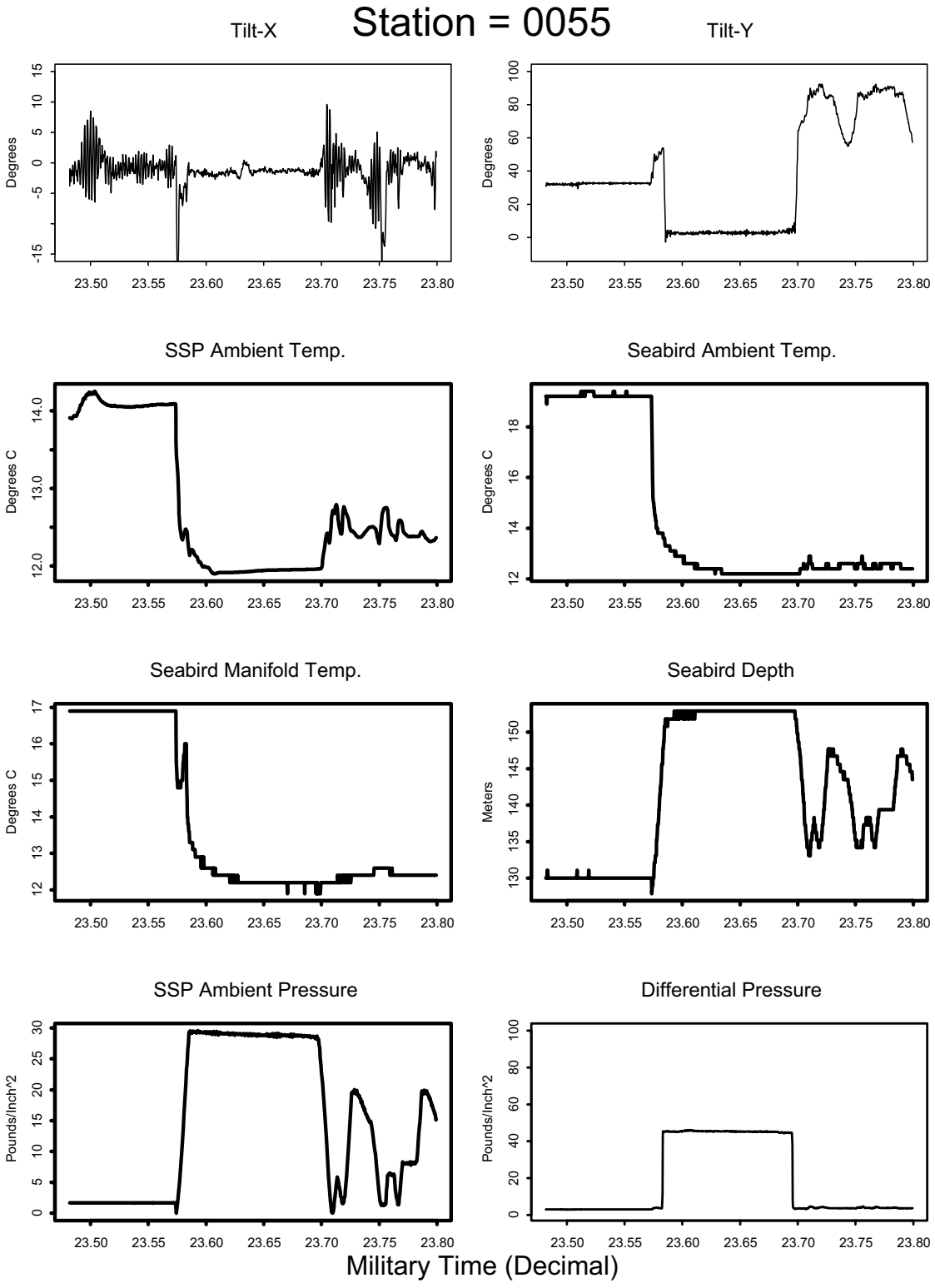

Figure A28. Survey sensor package data for an NEFSC clam survey tow with acceptable dredge performance.

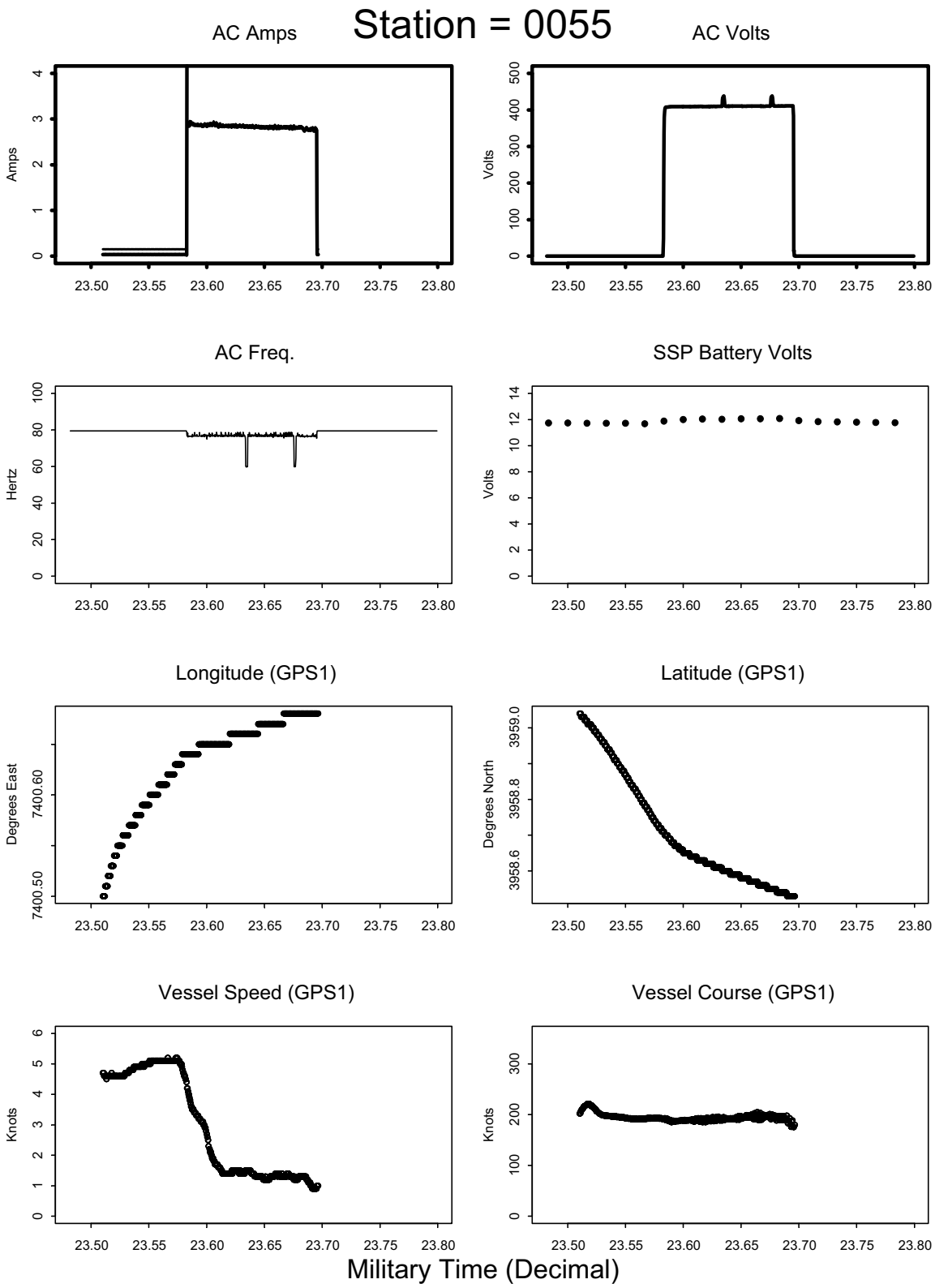

Figure A28. (continued)

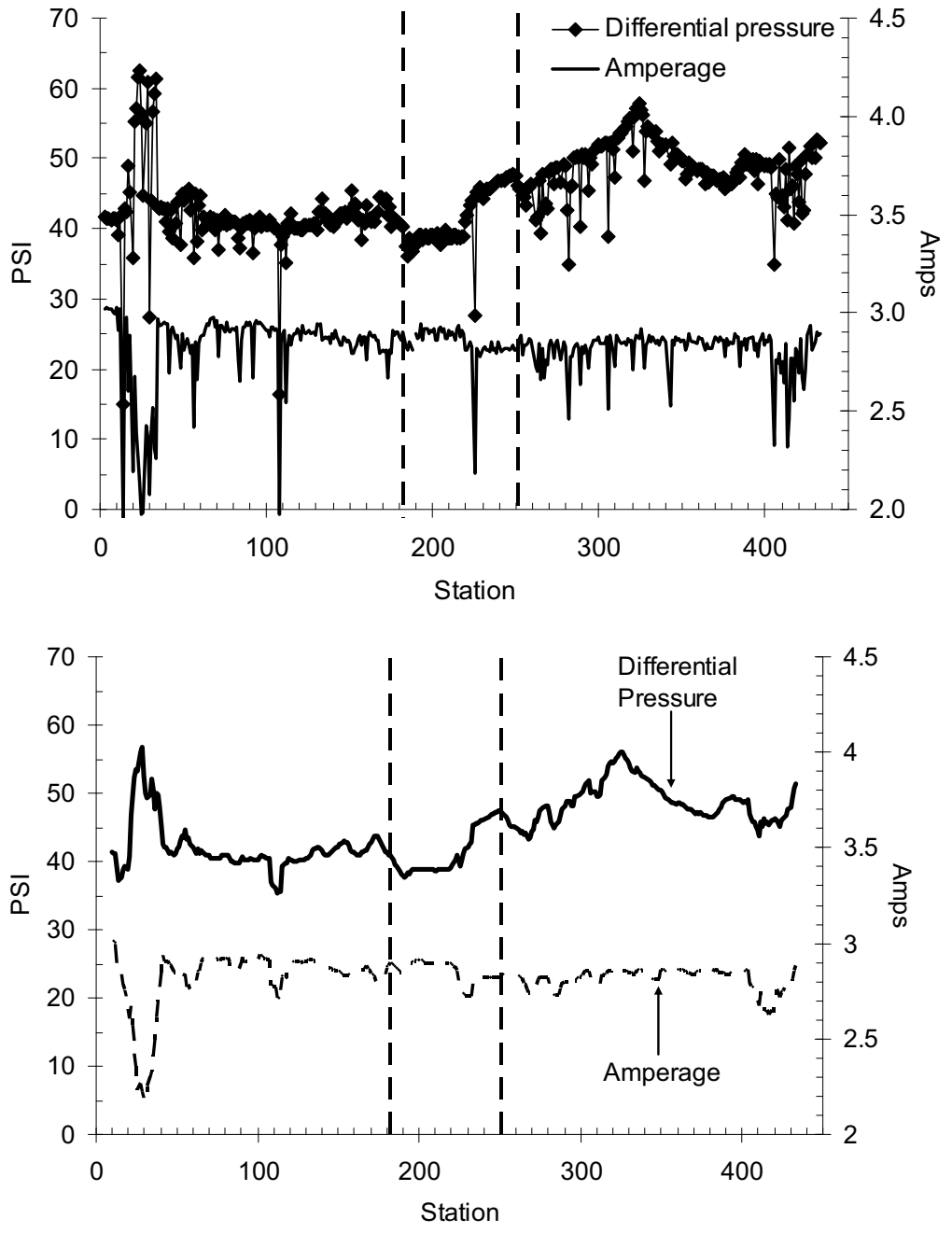

Figure A29. Differential pressure and amperage measured by sensors on the survey dredge during the 2005 NEFSC clam survey. Vertical lines separate the first, second and third legs. *Top*: Mean values for each station. *Bottom*: Mean values for each station smoothed by a seven point moving average.

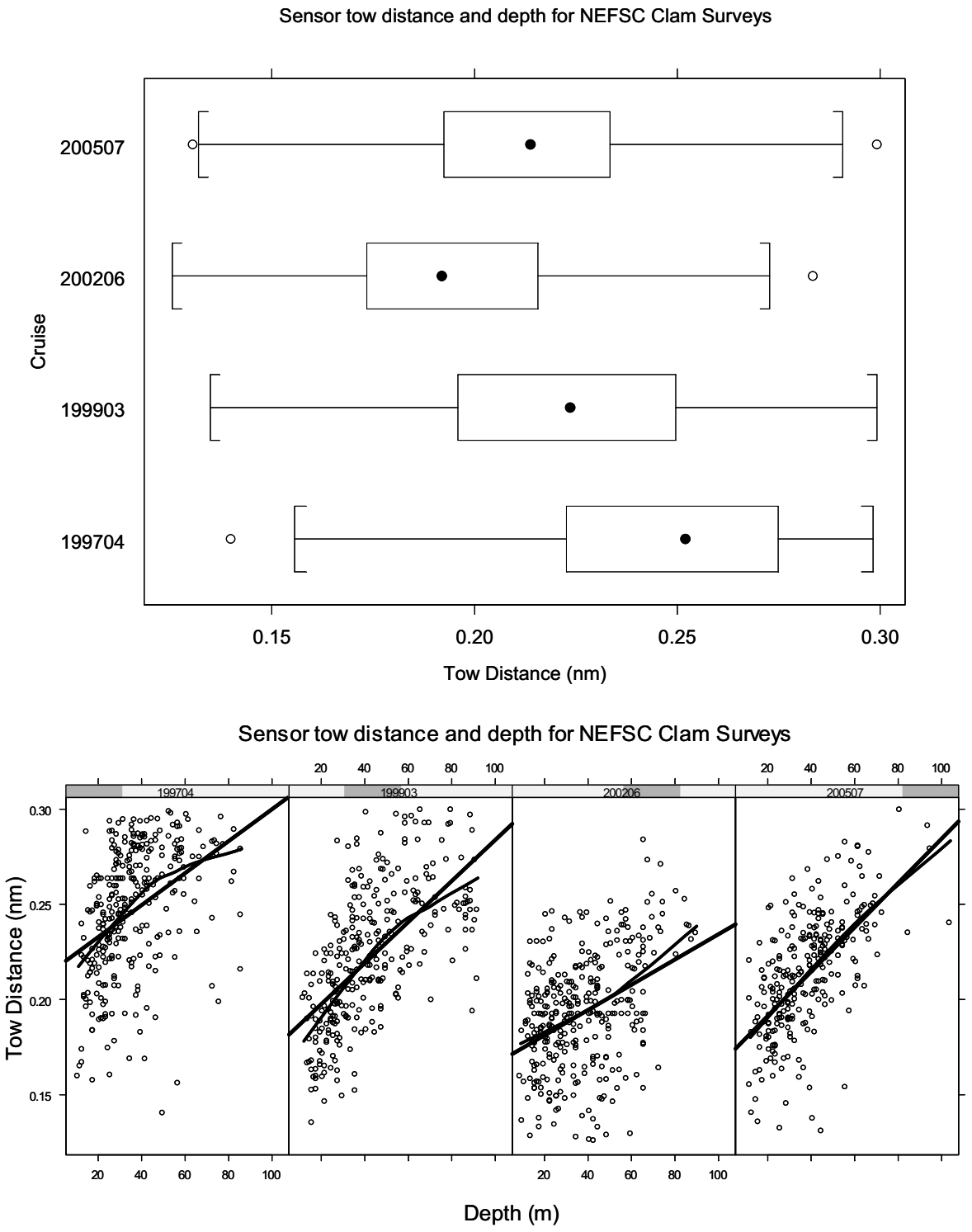

Figure A30. Tow distance measurements for NEFSC clam surveys from sensor data (top) and tow distance as a function of depth (bottom). Straight lines in the bottom panel show the best regression model. Curved lines are from loess regression and are intended to show trends.

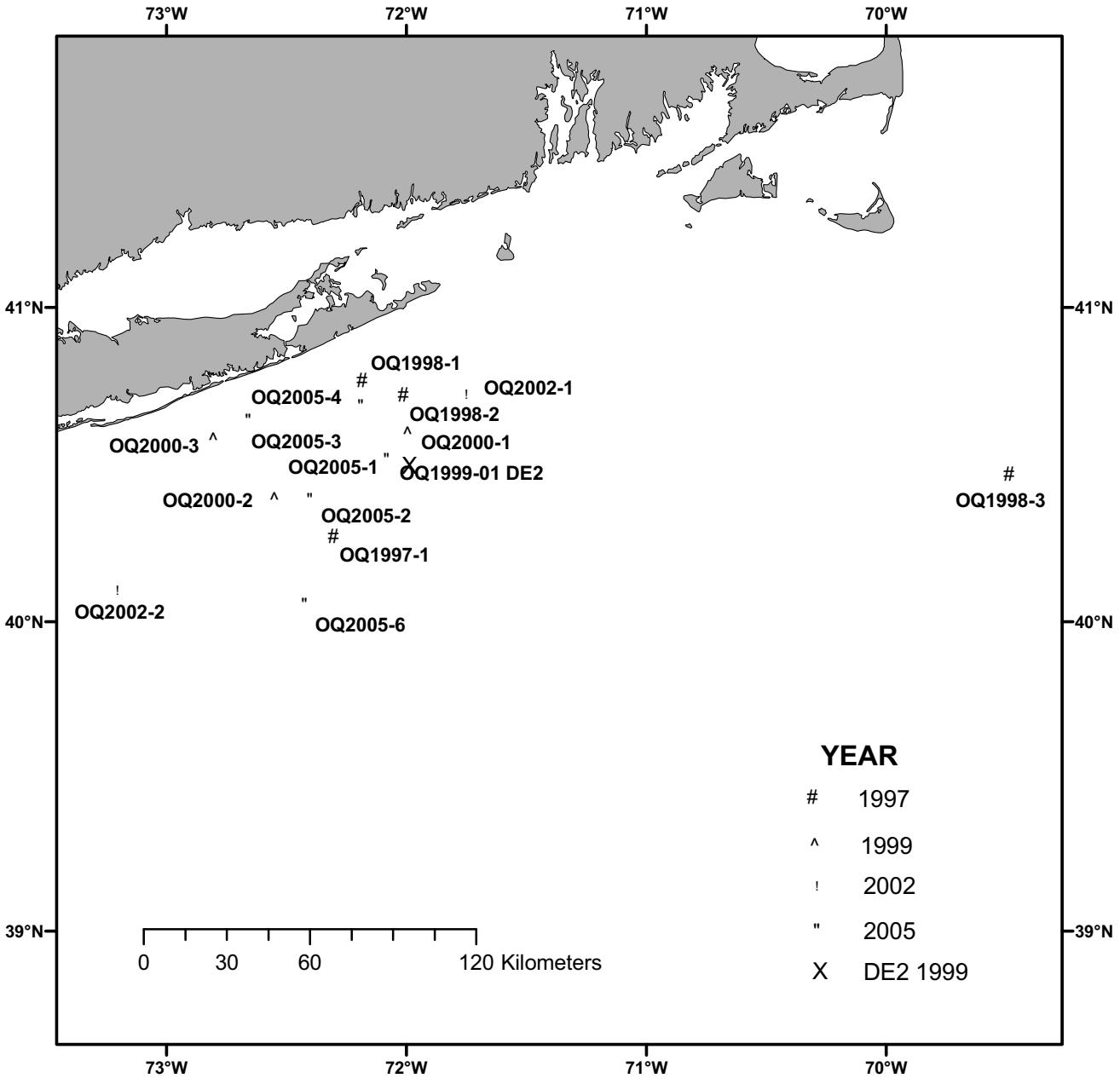

Figure A31a. Locations of ocean quahog depletion experiments off the Long Island area, 1997-2005.

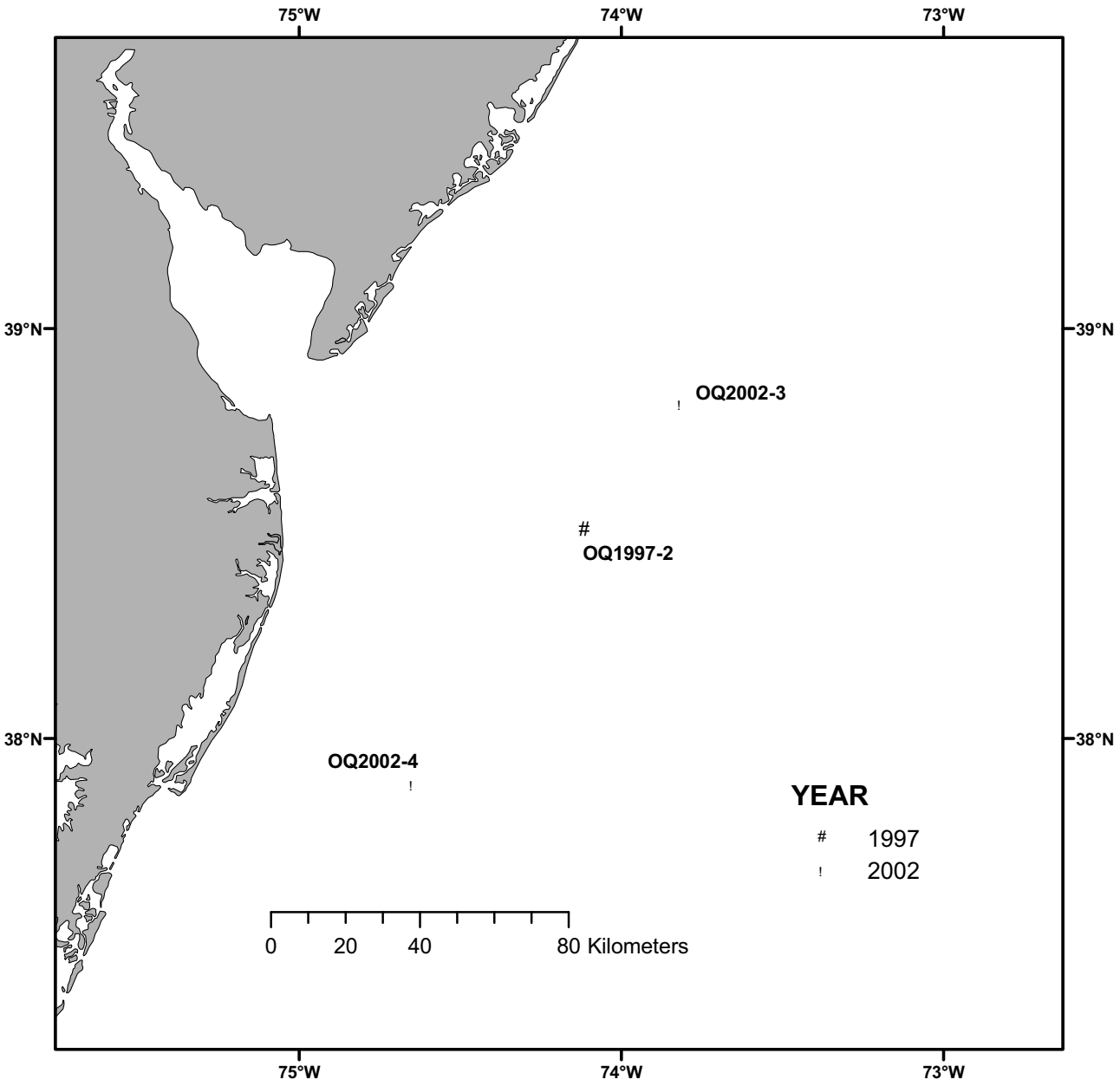

Figure A31b. Locations of ocean quahog depletion experiments off the New Jersey-Delmarva area, 1997-2005.

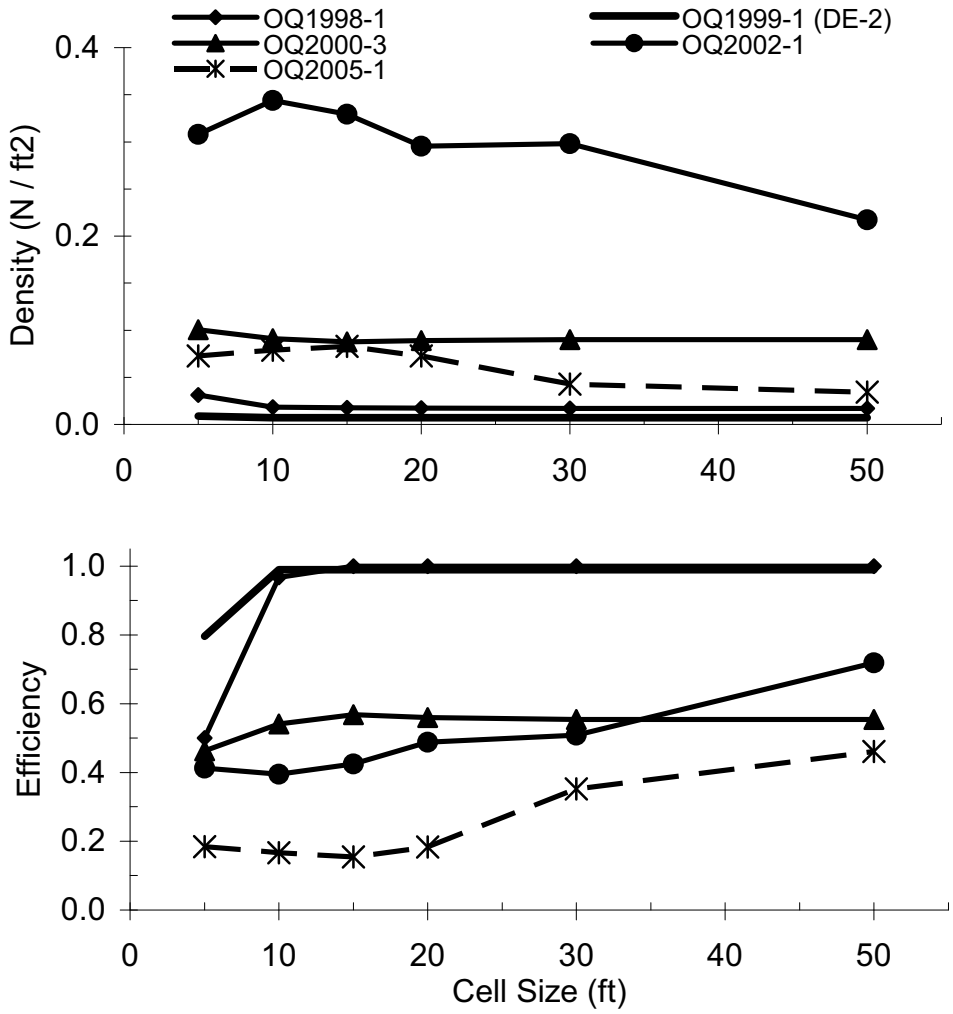

Figure A32. Sensitivity of Patch model estimates of ocean quahog density and dredge efficiency from depletion experiments and the Patch model. All of the experiments shown in the figure except OQ1999-1 (DE-2) were commercial experiments with a 10 ft dredge. The OQ1999-1 (DE-2) experiment was a Delaware II depletion experiment using a 5 ft dredge. The default cell size for Patch model analysis was 20 ft in all cases.

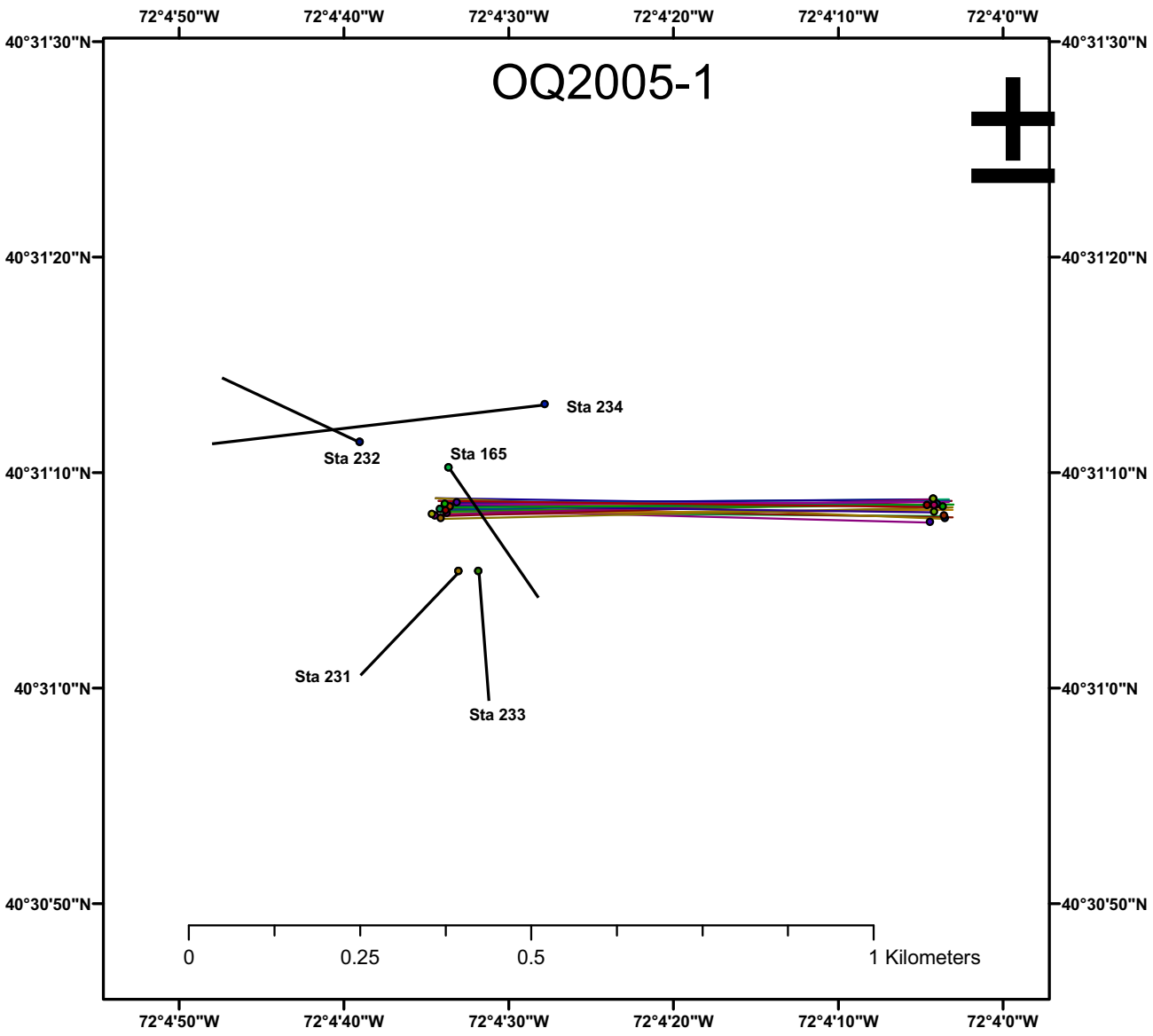

Figure A33. Setup and depletion tows for the OQ2005-1 ocean quahog depletion study. Setup tows by the *R/V Delaware II* are identified by station numbers. Depletion tows by the *F/V Lisa Kim* are tightly clustered along parallel tracks. Tow paths appear straight because they are shown as straight lines between start and stop points.

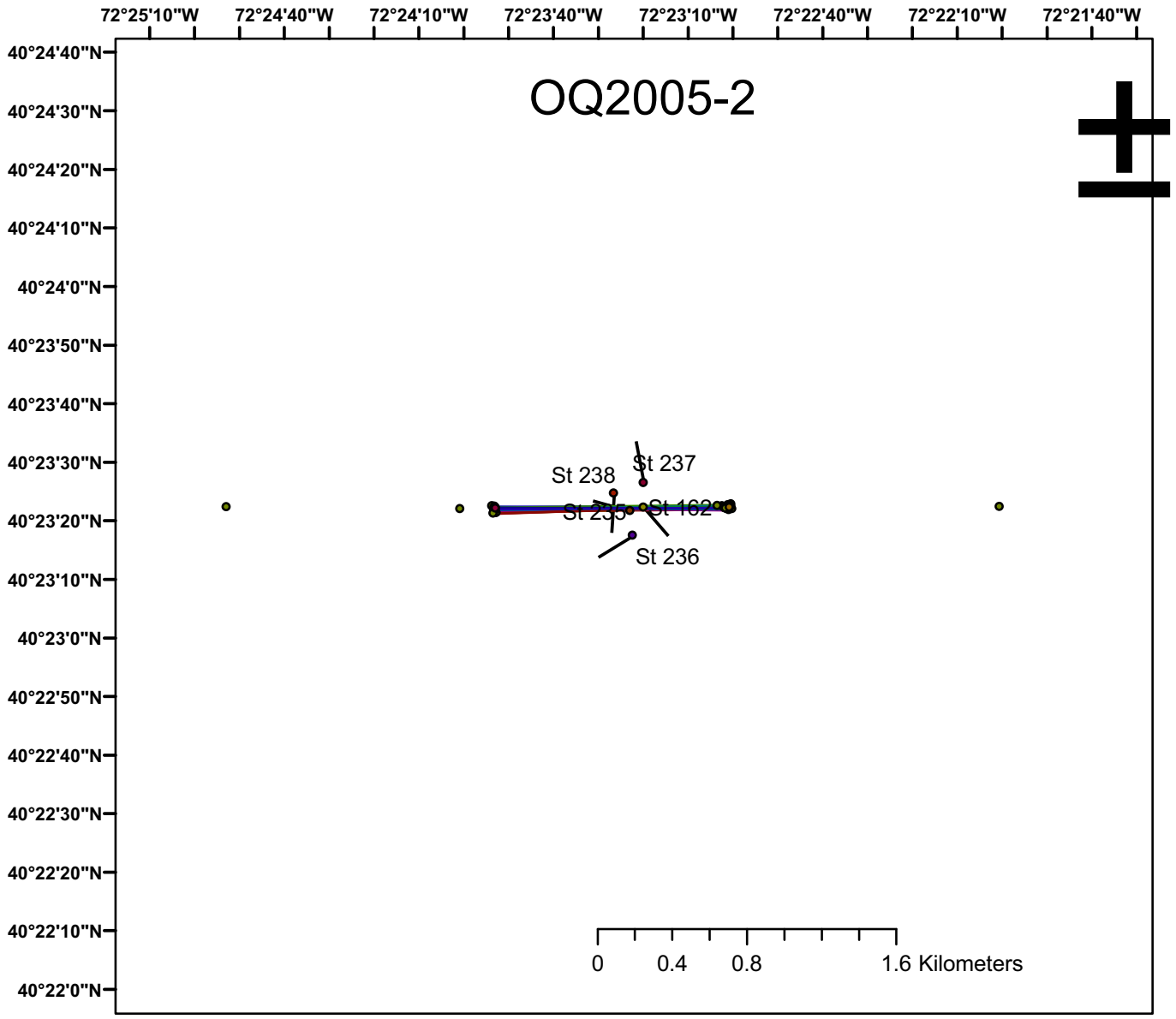

Figure A34. Setup and depletion tows for the OQ2005-2 ocean quahog depletion study. Setup tows by the *R/V Delaware II* are identified by station numbers. Depletion tows by the *F/V Lisa Kim* are tightly clustered along parallel tracks. Tow paths appear straight because they are shown as straight lines between start and stop points.

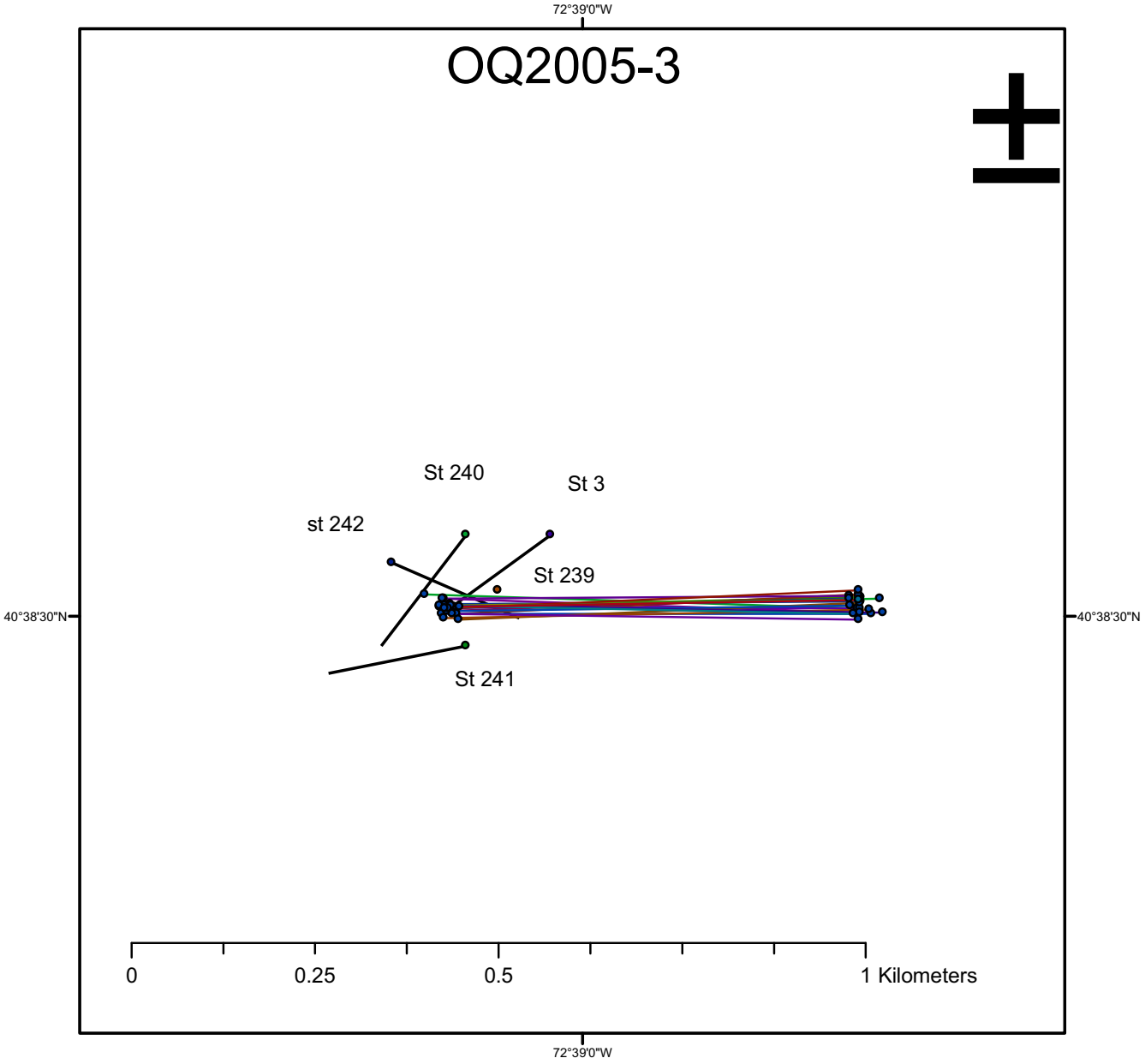

Figure A35. Setup and depletion tows for the OQ2005-3 ocean quahog depletion study. Setup tows by the *R/V Delaware II* are identified by station numbers. Depletion tows by the *F/V Lisa Kim* are tightly clustered along parallel tracks. Tow paths appear straight because they are shown as straight lines between start and stop points.

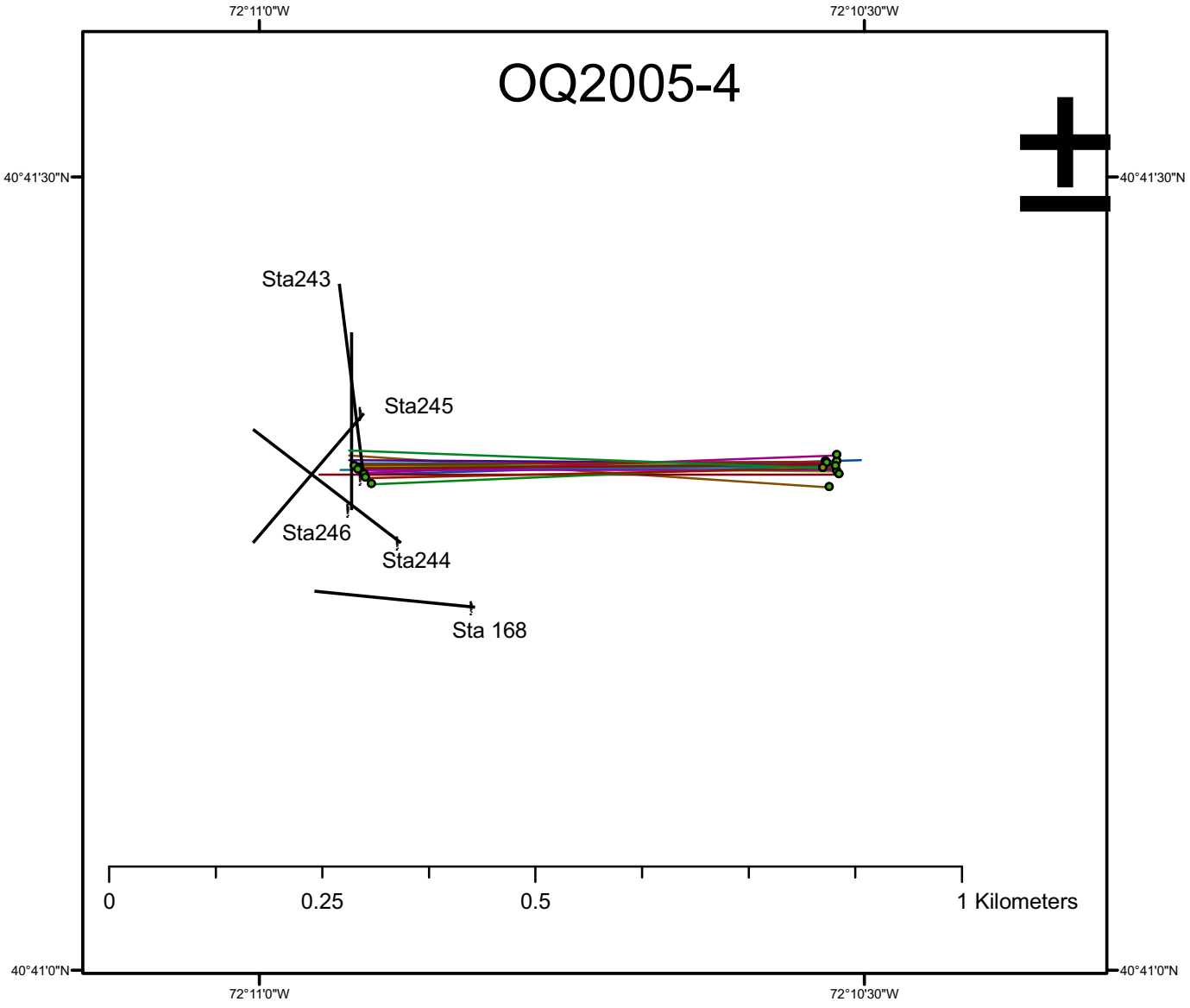

Figure A36. Setup and depletion tows for the OQ2005-4 ocean quahog depletion study. Setup tows by the *R/V Delaware II* are identified by station numbers. Depletion tows by the *F/V Lisa Kim* are tightly clustered along parallel tracks. Tow paths appear straight because they are shown as straight lines between start and stop points.

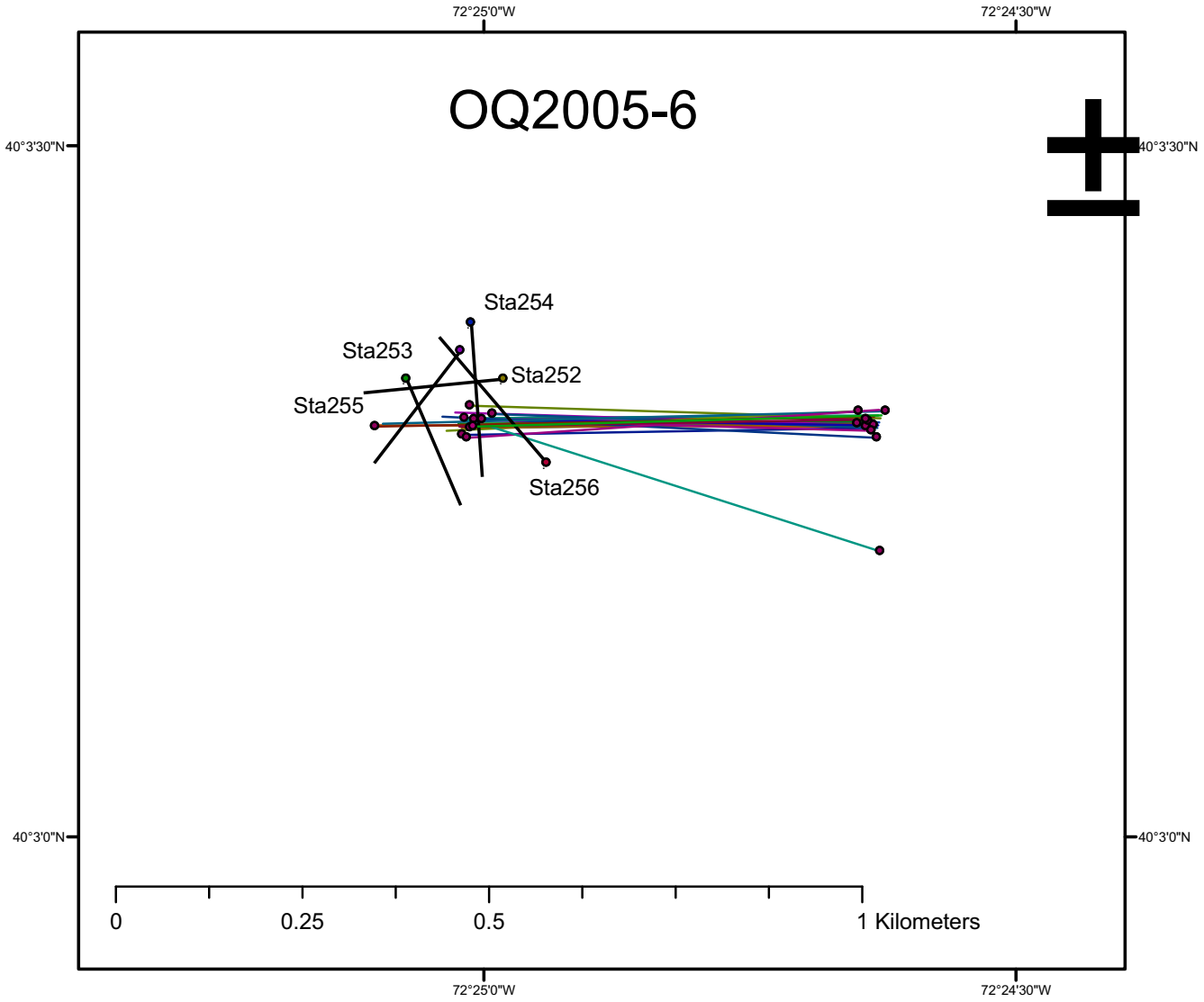

Figure A37. Setup and depletion tows for the OQ2005-6 ocean quahog depletion study. Setup tows by the *R/V Delaware II* are identified by station numbers. Depletion tows by the *F/V Lisa Kim* are tightly clustered along parallel tracks. Tow paths appear straight because they are shown as straight lines between start and stop points.

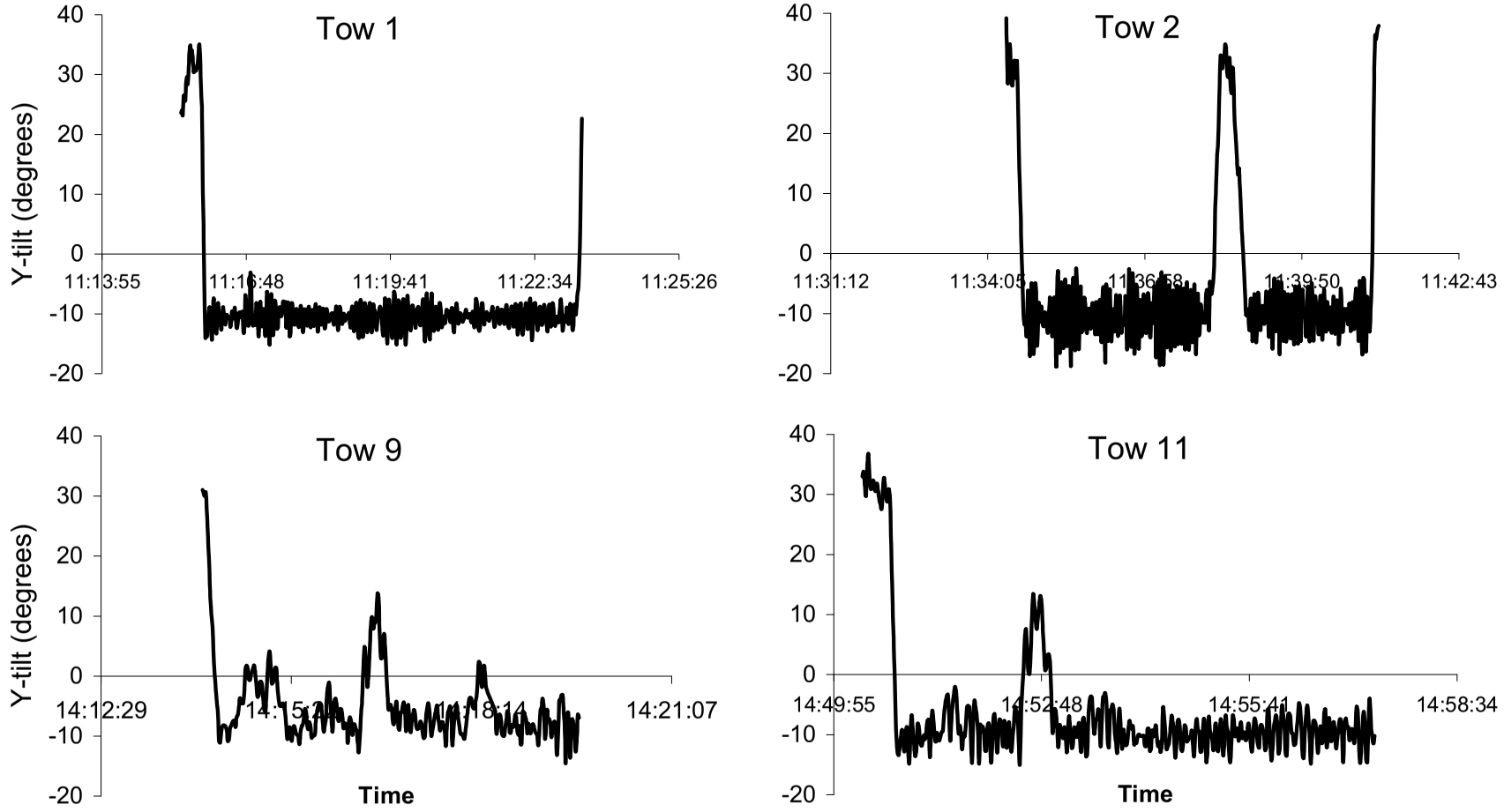

Figure A38. Inclinometer data for selected tows by a commercial dredge at depletion experiment site OQ2005-06, which was carried out in relatively deep water with a short pump hose and under choppy conditions. Data missing at end of tows 9-11 because of low sensor batteries.

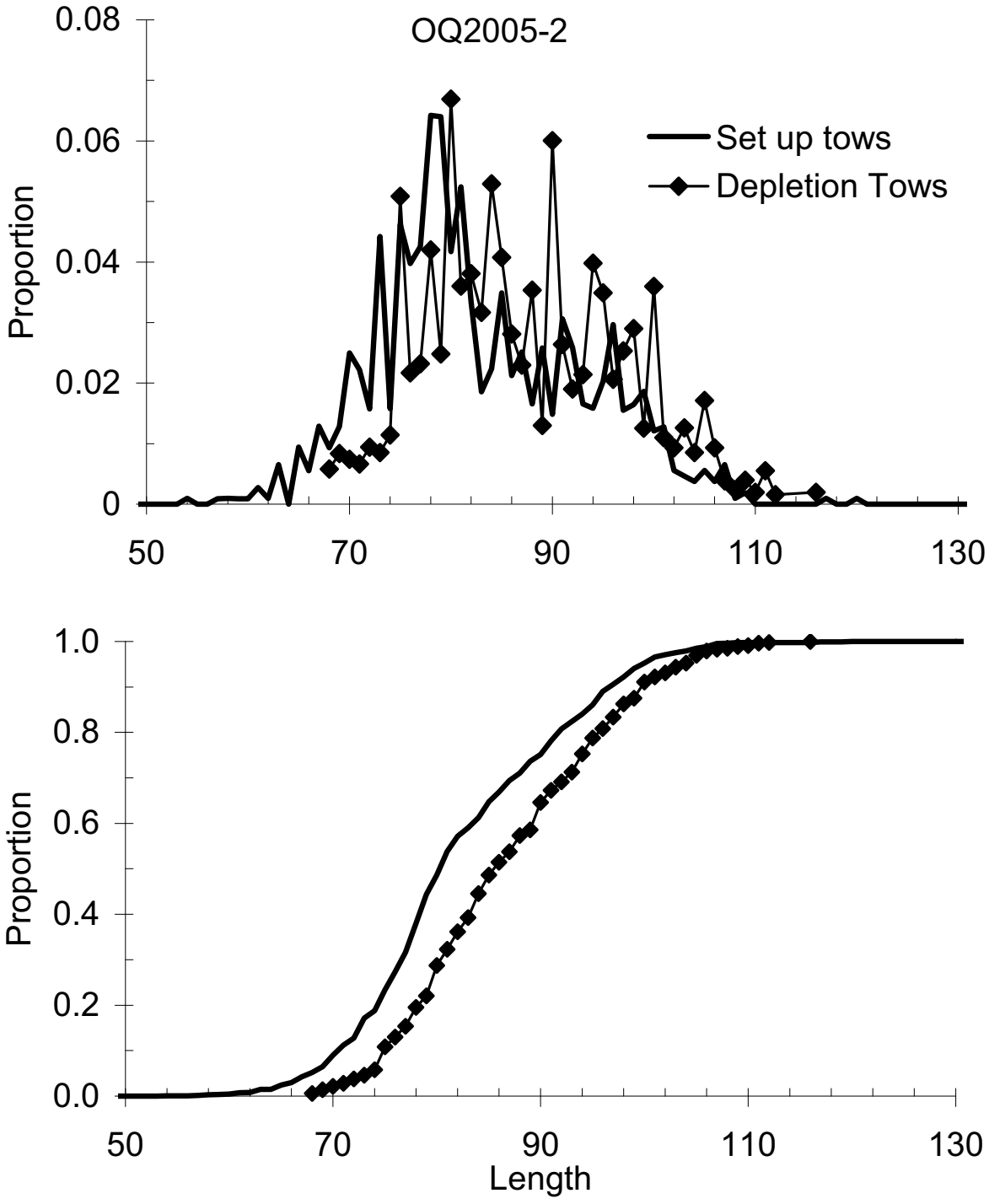

Figure A39. Length composition data from setup and depletion tows at a typical 2005 depletion site for ocean quahog (OQ2005-02).

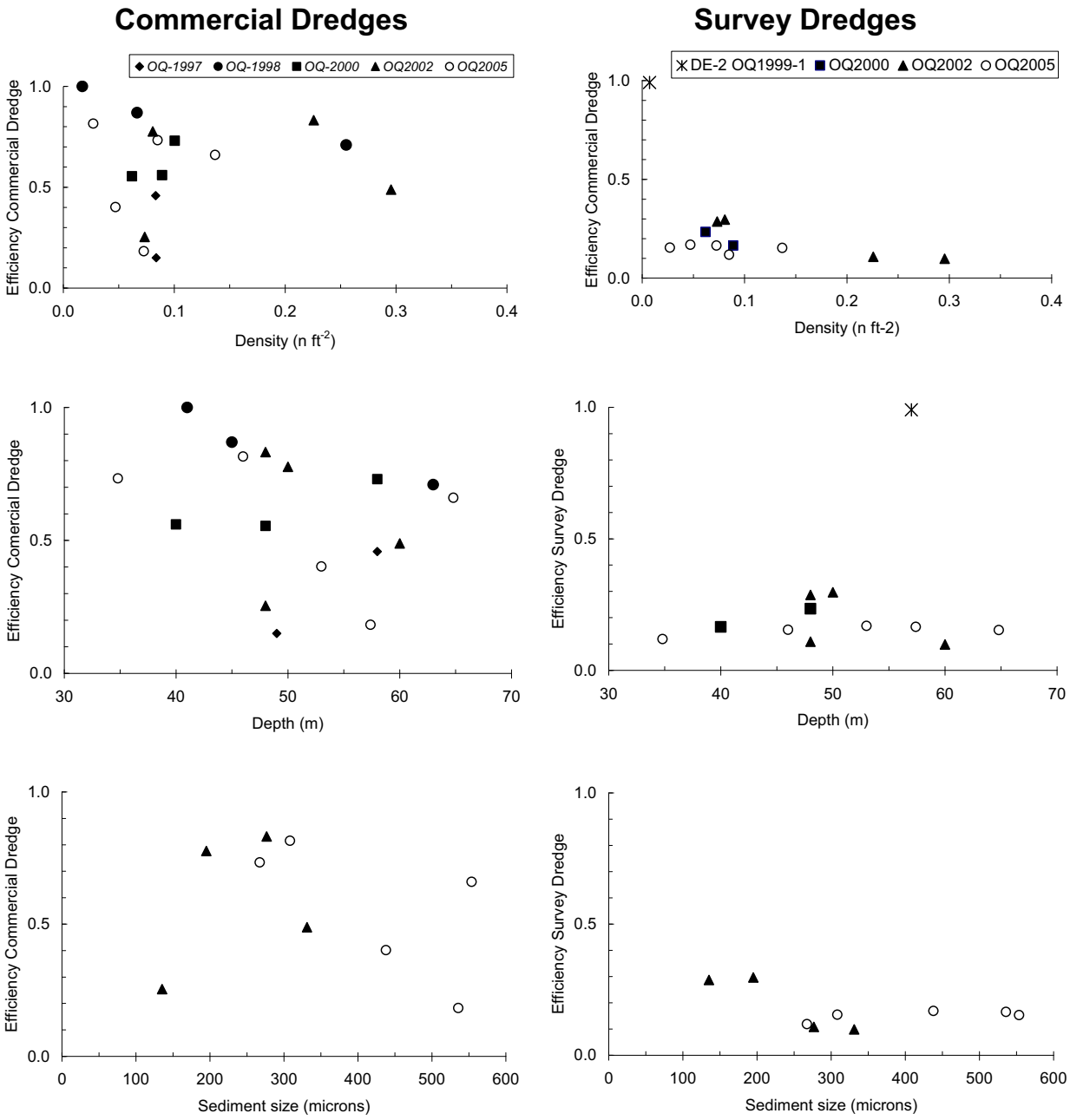

Figure A40. Patch model dredge efficiency estimates vs. depth, estimated density from the Patch model and mean sediment size for ocean quahog in hydraulic dredges used on commercial vessels during depletion studies and the hydraulic dredge used during research surveys by the *F/V Delaware II*. All data shown in plots on the left hand side are efficiency estimates for commercial vessels used in depletion studies. All data shown in plots on the right hand side are efficiency estimates for the R/V Delaware II based on commercial depletion estimates with setup tows by the Delaware II or, in the case of "DE-2 OQ1999-1", a depletion study carried out directly by the R/V Delaware II.

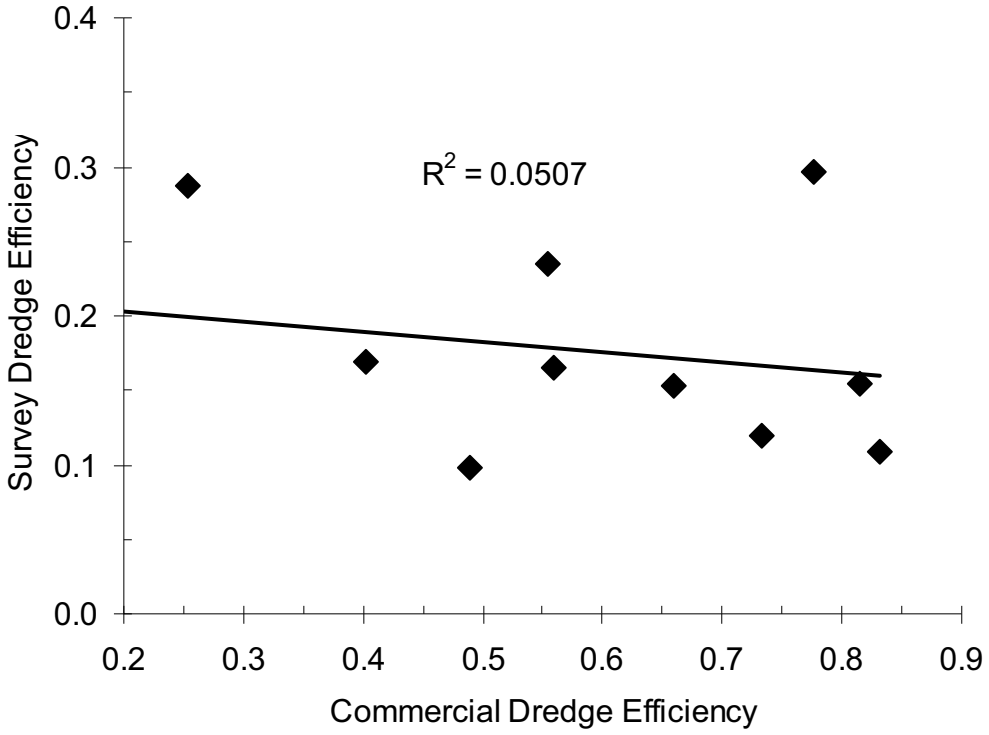

Figure A41. Survey dredge efficiency estimates for ocean quahog from depletions studies by commercial vessels and by the R/V Delaware II.

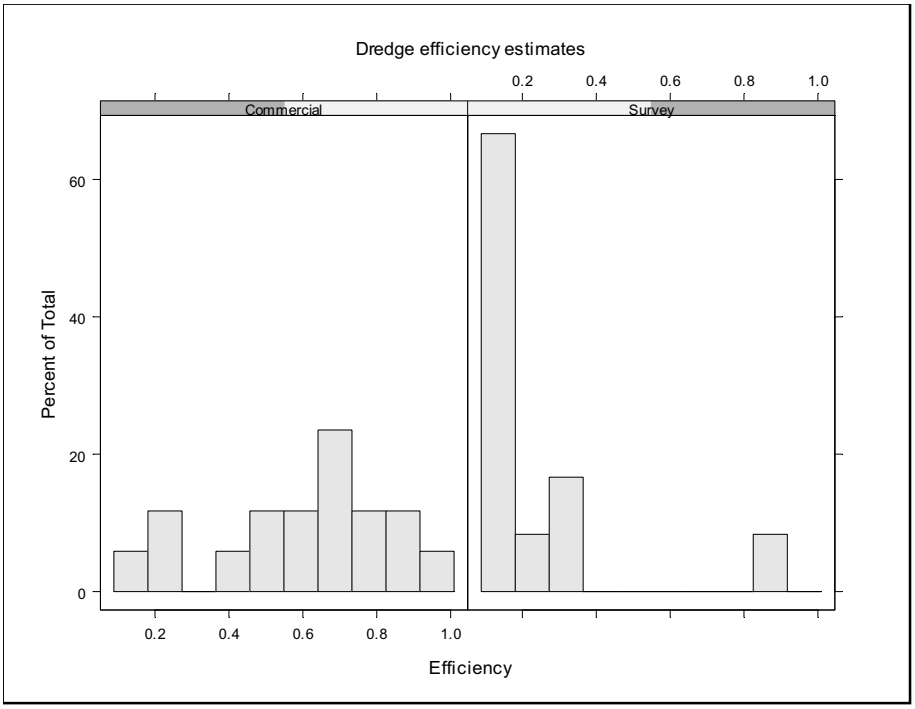

Figure A42. Distribution of survey dredge efficiency estimates for ocean quahog from depletion studies by commercial vessels and by the survey vessel (*R/V Delaware II*).

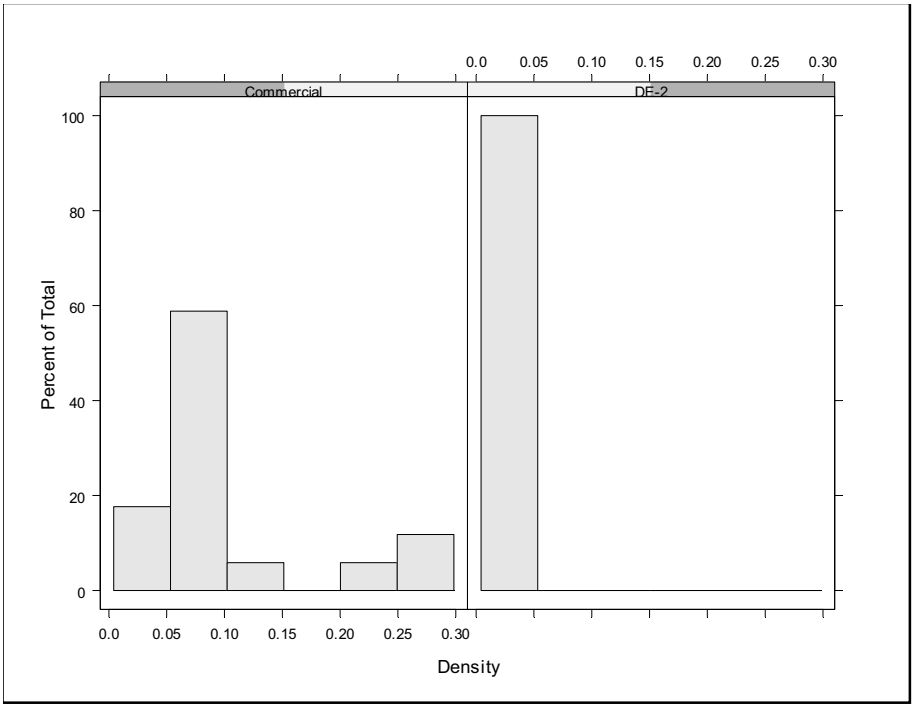

Figure A43. Distribution of ocean quahog density estimates (n ft^{-2}) for ocean quahog 90+ mm SL from depletion studies by commercial vessels and by the survey vessel (*R/V Delaware II*).

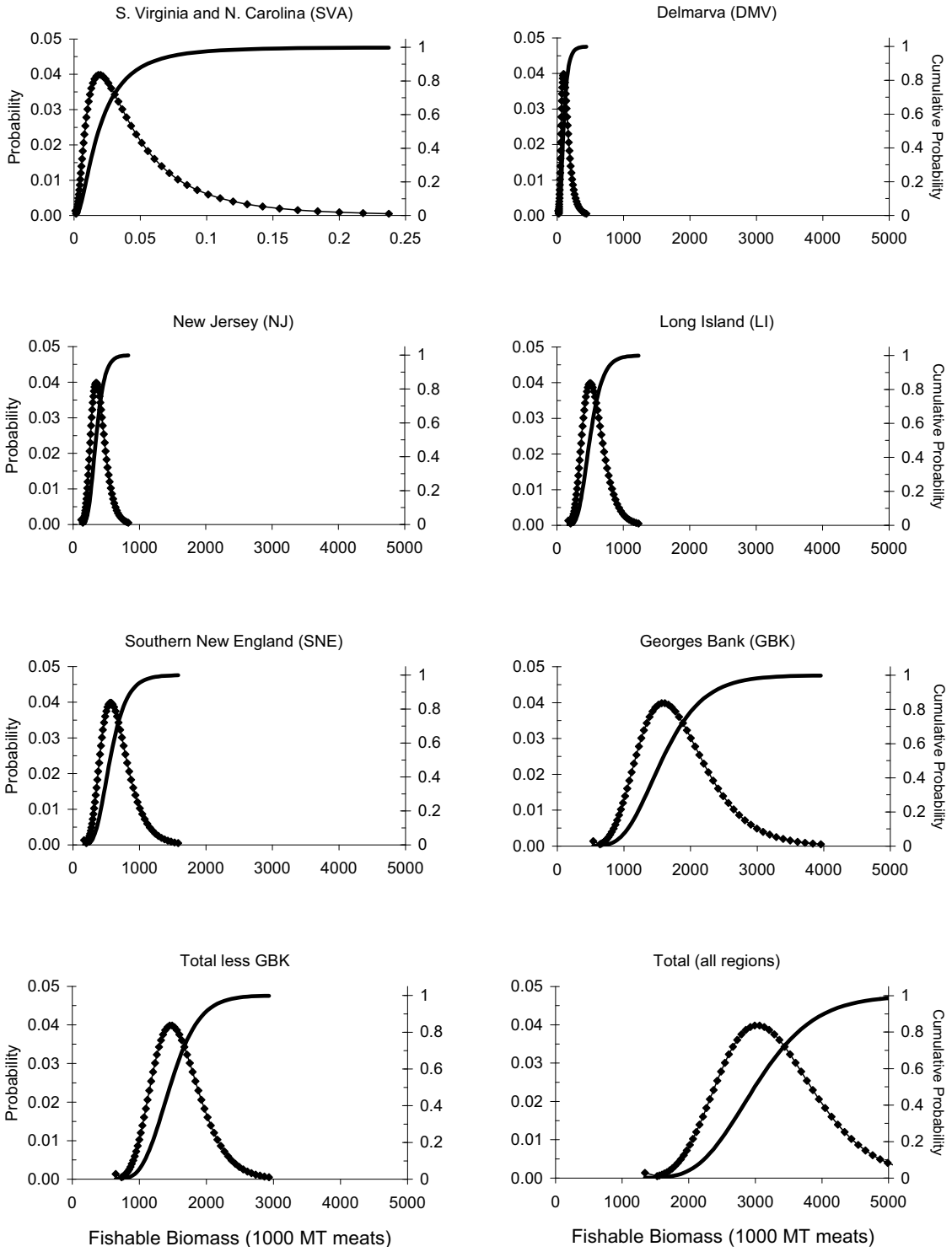

Figure A44. Uncertainty in efficiency corrected swept area biomass estimates for fishable ocean quahog during 2005. Note that the x-axis differs in the panel for SVA but is the same in all other panels to facilitate comparisons.

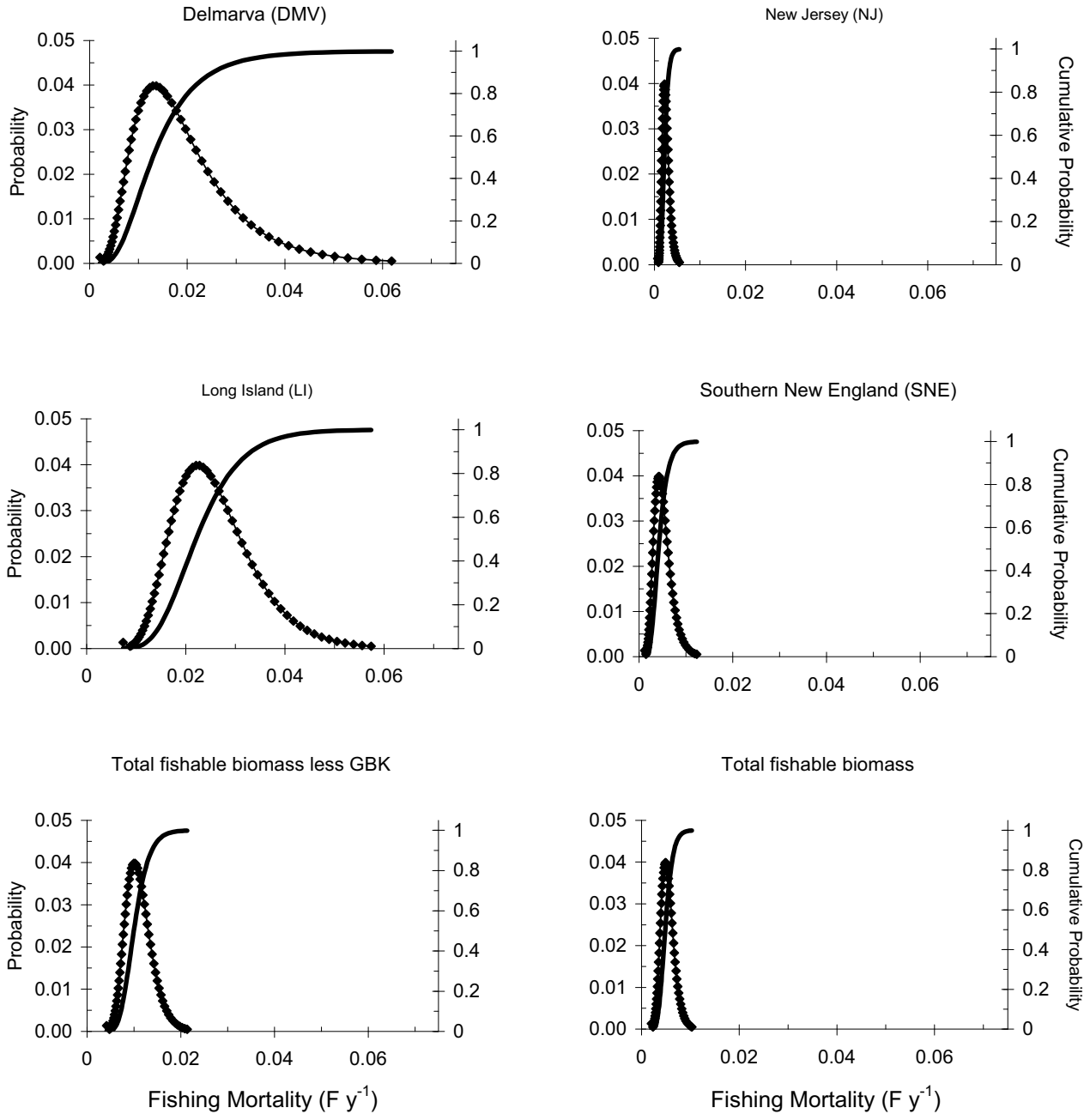

Figure A45. Uncertainty in fishing mortality estimates for ocean quahog during 2005 based on catch data and efficiency corrected swept-area biomass. X-axes are scaled to the same maximum to facilitate comparisons.

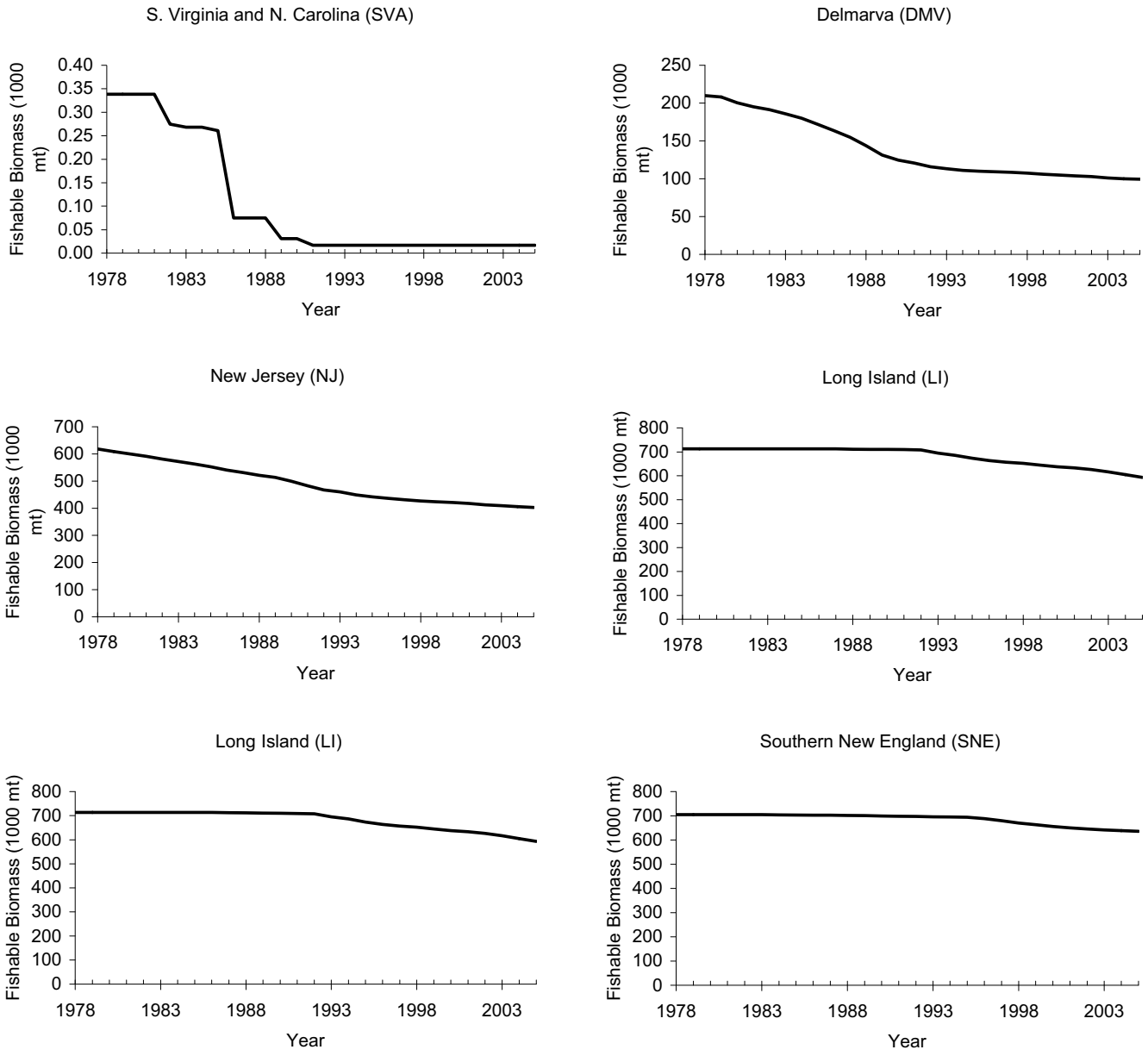

Figure A46. Trends in fishable biomass for ocean quahog from the "VPA" model, by region.

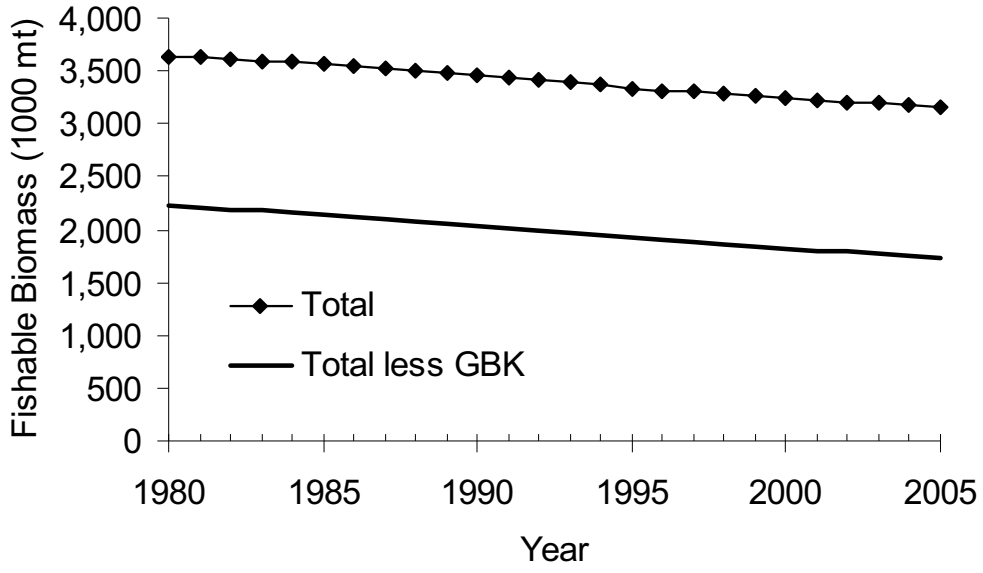

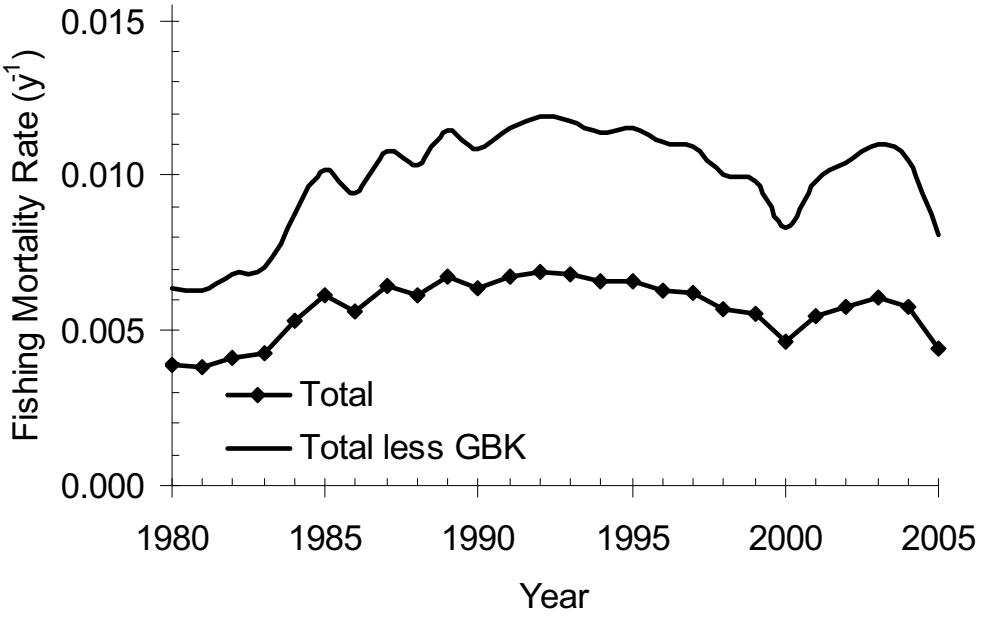

Figure A47. Trends in fishable biomass and fishing mortality for ocean quahog from the "VPA" model.

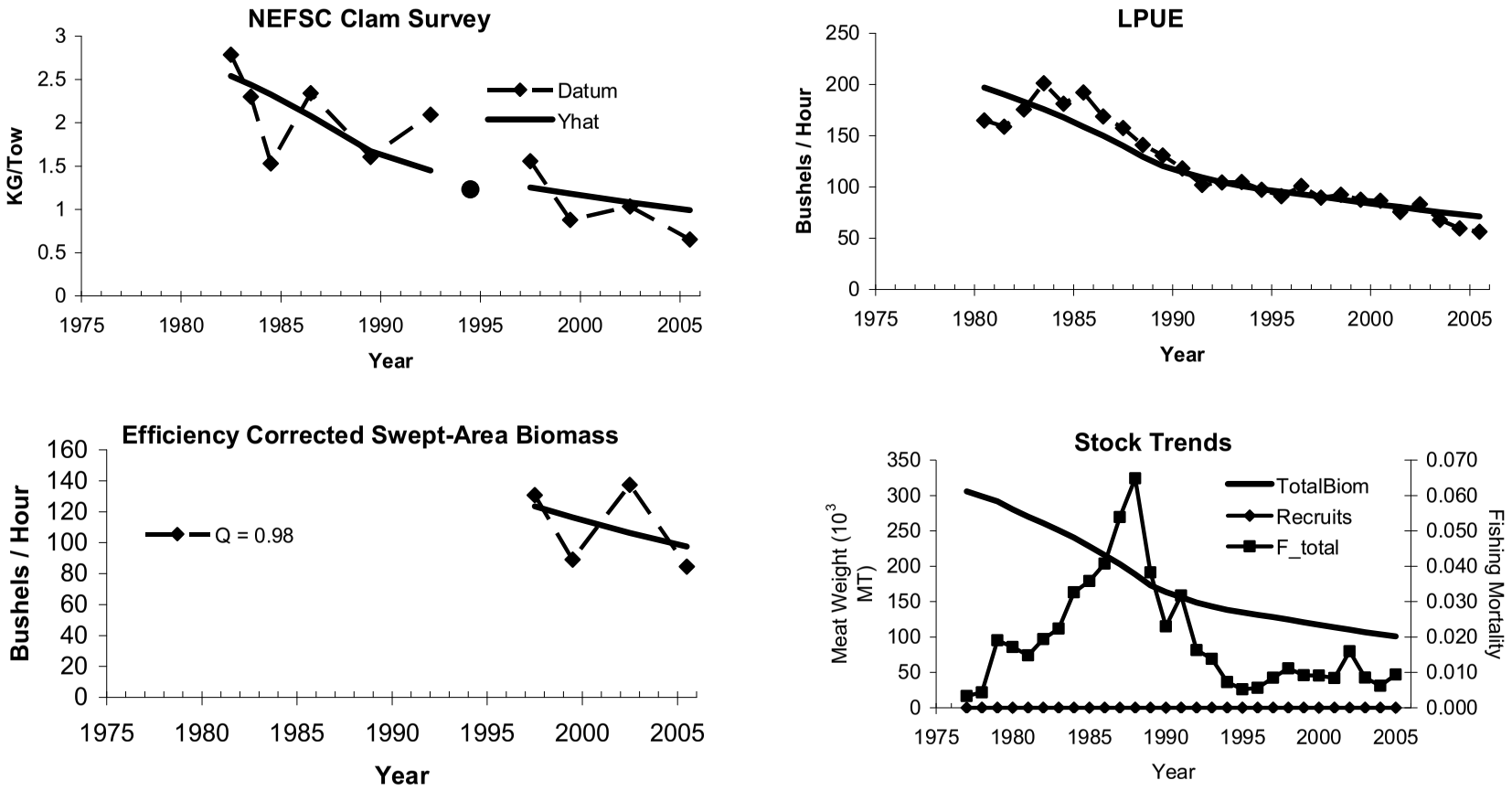

Figure A48. KLAMZ model results for ocean quahog in the DMV stock assessment region. The bottom right panel shows population estimates. Other panels show goodness of fit to trend data. The survey scaling parameter estimate for efficiency corrected swept-area biomass data used as prior information is shown in the bottom left panel. Trends in efficiency corrected swept area biomass and LPUE data did not affect model estimates and are shown for comparison only.

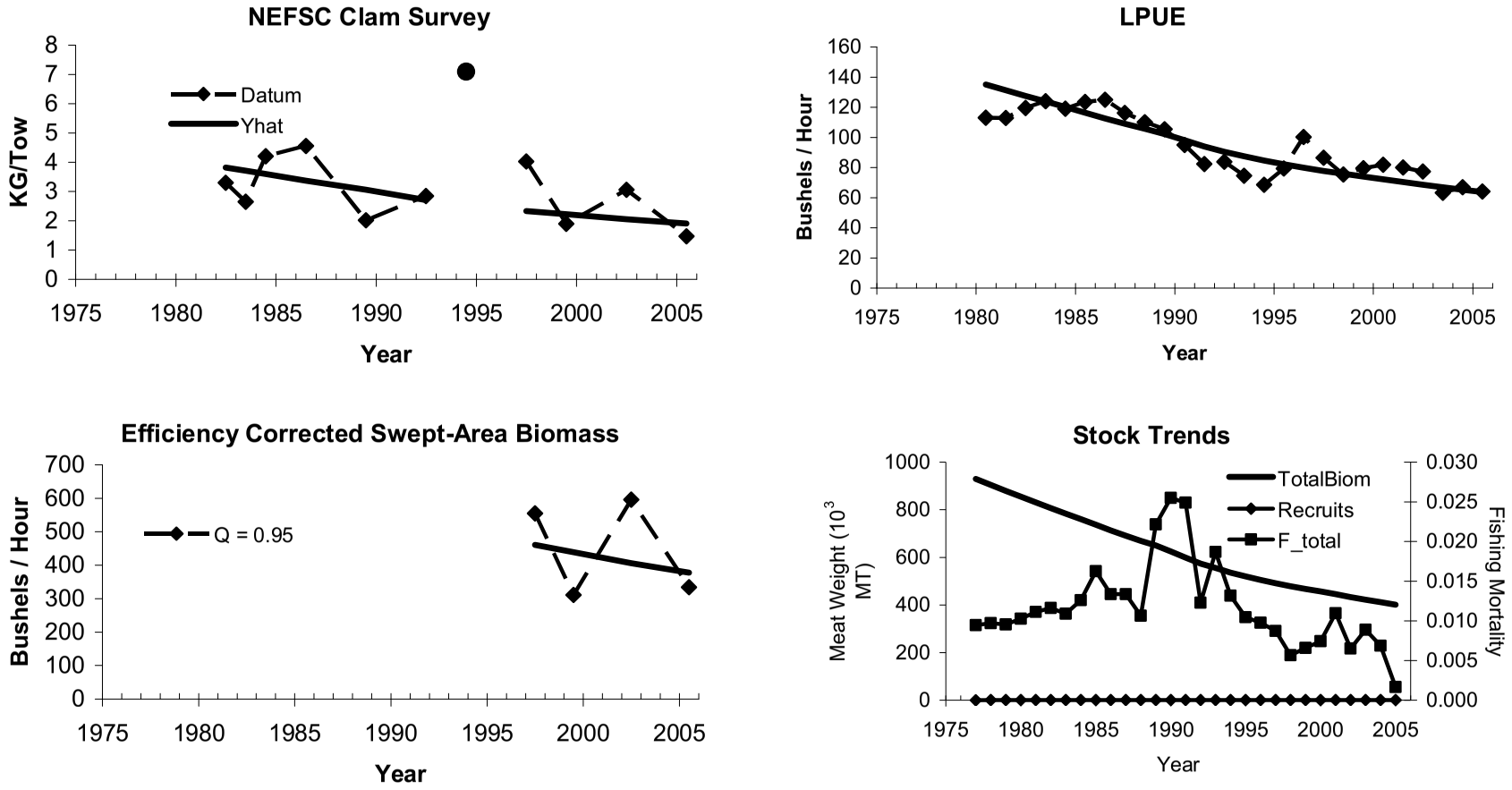

Figure A49. KLAMZ model results for ocean quahog in the NJ stock assessment region. The bottom right panel shows population estimates. Other panels show goodness of fit to trend data. The survey scaling parameter estimate for efficiency corrected swept-area biomass data used as prior information is shown in the bottom left panel. Trends in efficiency corrected swept area biomass and LPUE data did not affect model estimates and are shown for comparison only.

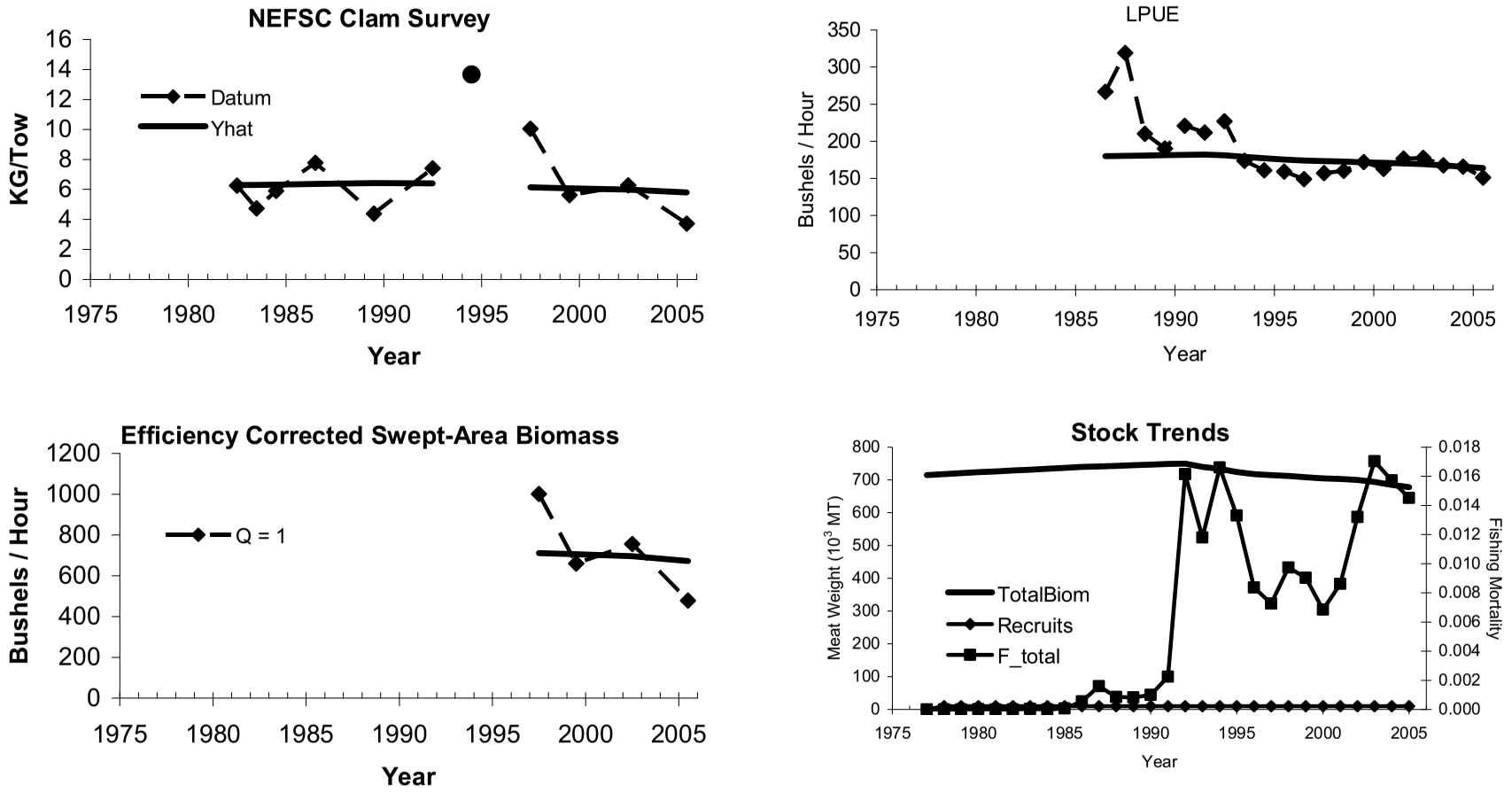

Figure A50. KLAMZ model results for ocean quahog in the LI stock assessment region. The bottom right panel shows population estimates. Other panels show goodness of fit to trend data. The survey scaling parameter estimate for efficiency corrected swept-area biomass data used as prior information is shown in the bottom left panel. Trends in efficiency corrected swept area biomass and LPUE data did not affect model estimates and are shown for comparison only.

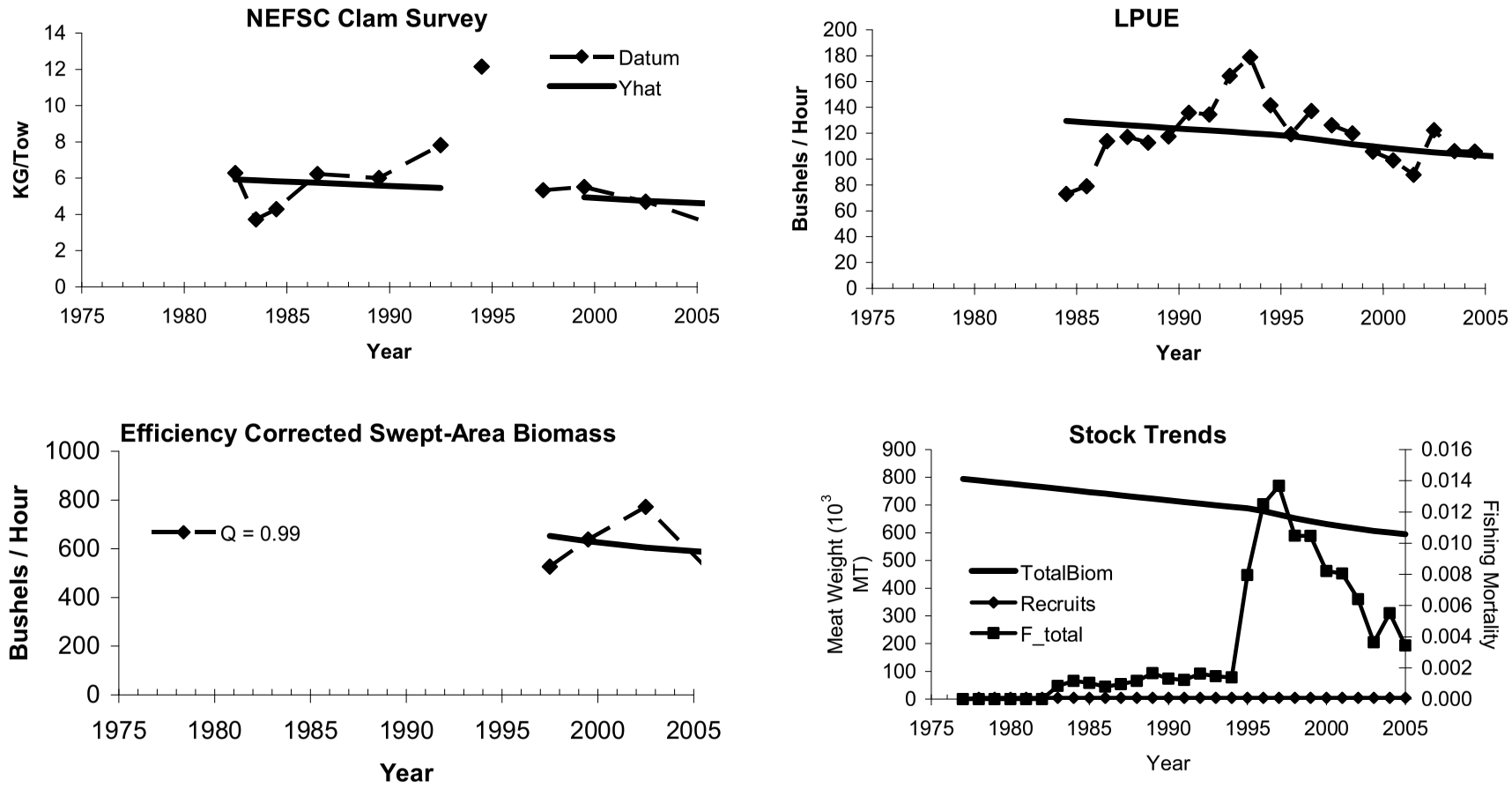

Figure A51. KLAMZ model results for ocean quahog in the SNE stock assessment region. The bottom right panel shows population estimates. Other panels show goodness of fit to trend data. The survey scaling parameter estimate for efficiency corrected swept-area biomass data used as prior information is shown in the bottom left panel. Trends in efficiency corrected swept area biomass and LPUE data did not affect model estimates and are shown for comparison only.

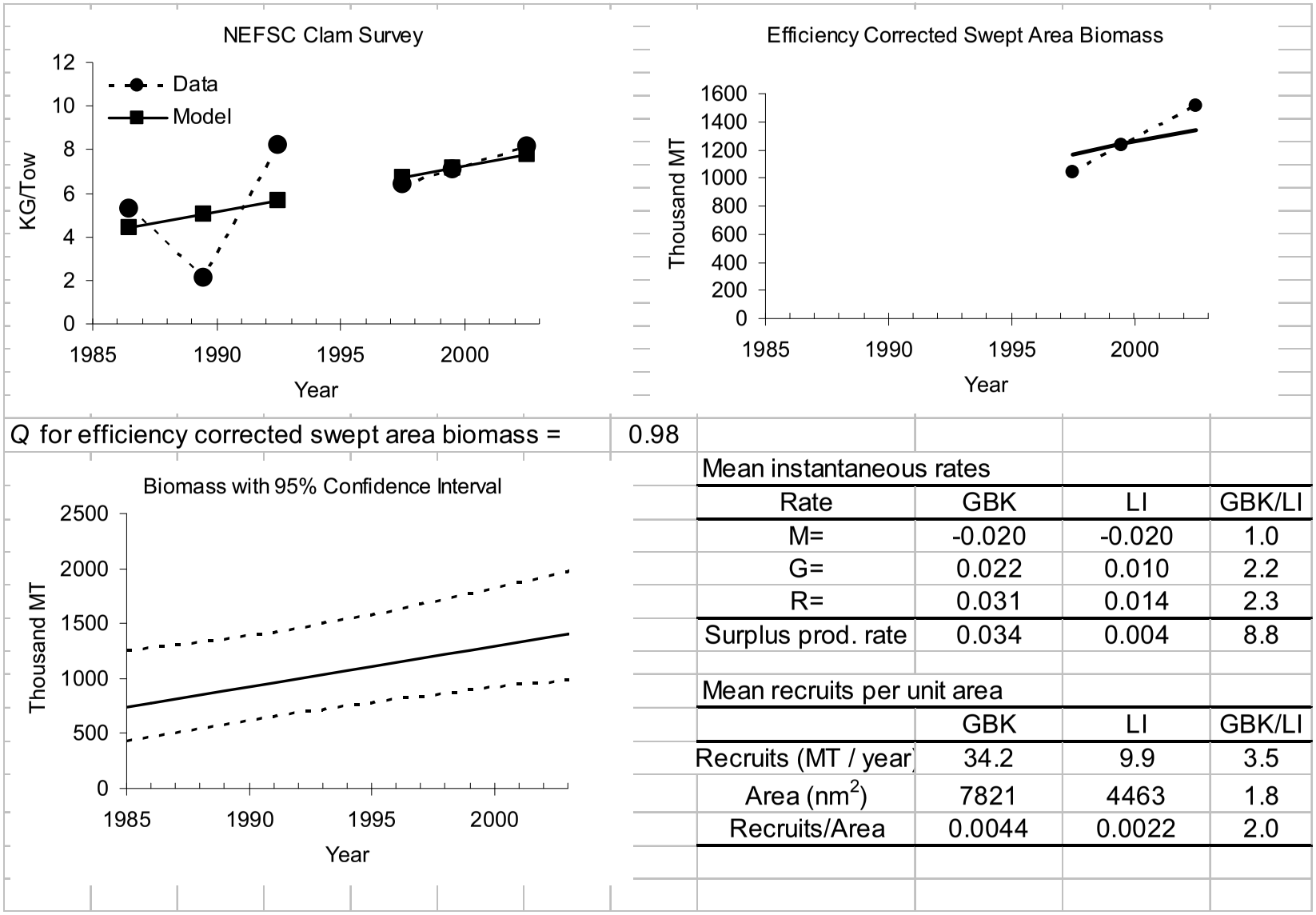

Mean instantaneous rates

Rate	GBK	LI	GBK/LI
M=	-0.020	-0.020	1.0
G=	0.022	0.010	2.2
R=	0.031	0.014	2.3
Surplus prod. rate	0.034	0.004	8.8

Mean recruits per unit area

	GBK	LI	GBK/LI
Recruits (MT / year)	34.2	9.9	3.5
Area (nm^2)	7821	4463	1.8
Recruits/Area	0.0044	0.0022	2.0

Figure A52. Results from a trial run of the KLAMZ model for ocean quahog in the GBK stock assessment region during 1986-2002 with all survey data in the model.

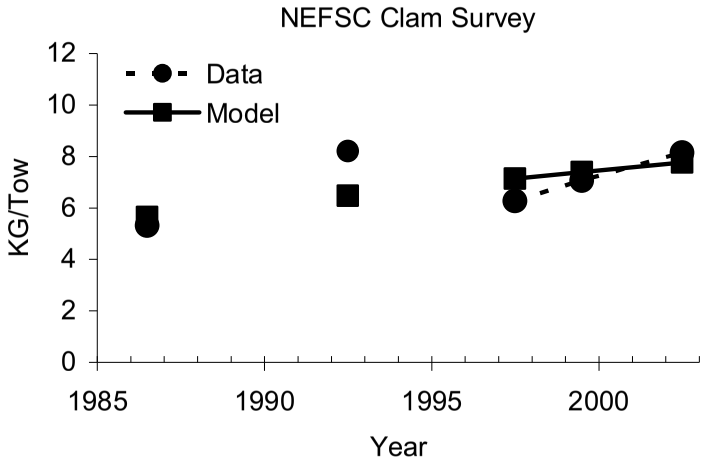

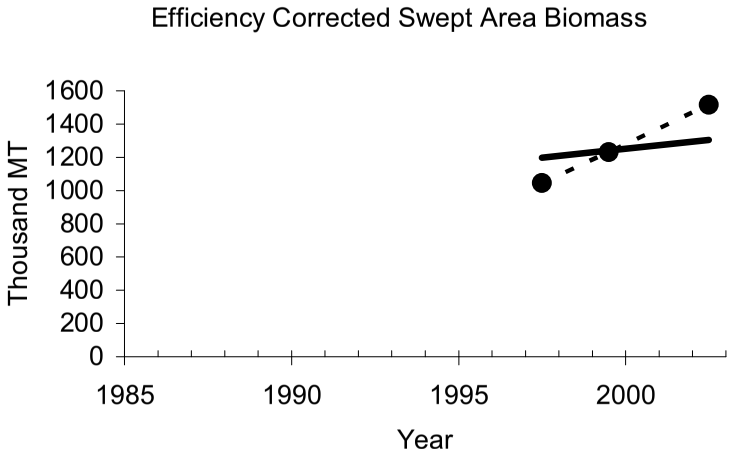

Q for efficiency corrected swept area biomass = 0.98

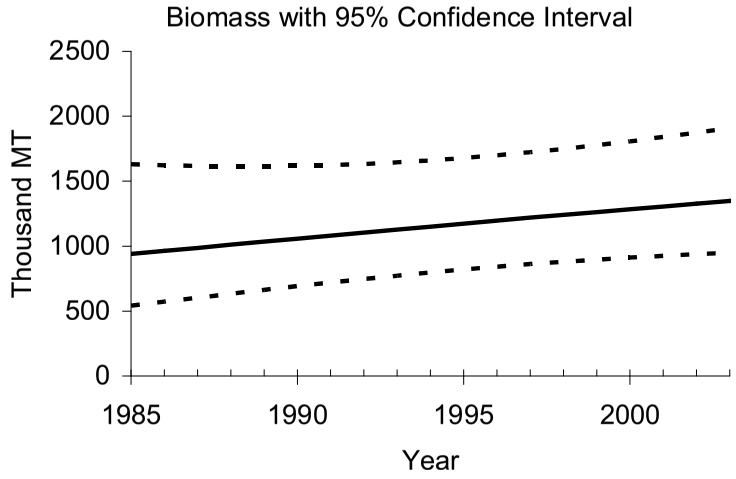

Mean instantaneous rates

Rate	GBK	LI	GBK/LI
M=	-0.020	-0.020	1.0
G=	0.017	0.010	1.7
R=	0.022	0.014	1.6
Surplus prod. rate	0.019	0.004	5.0

Mean recruits per unit area

	GBK	LI	GBK/LI
Recruits (MT / year)	25.4	9.9	2.6
Area (nm^2)	7821	4463	1.8
Recruits/Area	0.0033	0.0022	1.5

Figure A53. Results from a sensitivity run of the KLAMZ model for ocean quahog in the GBK stock assessment region with survey data for 1989 removed.

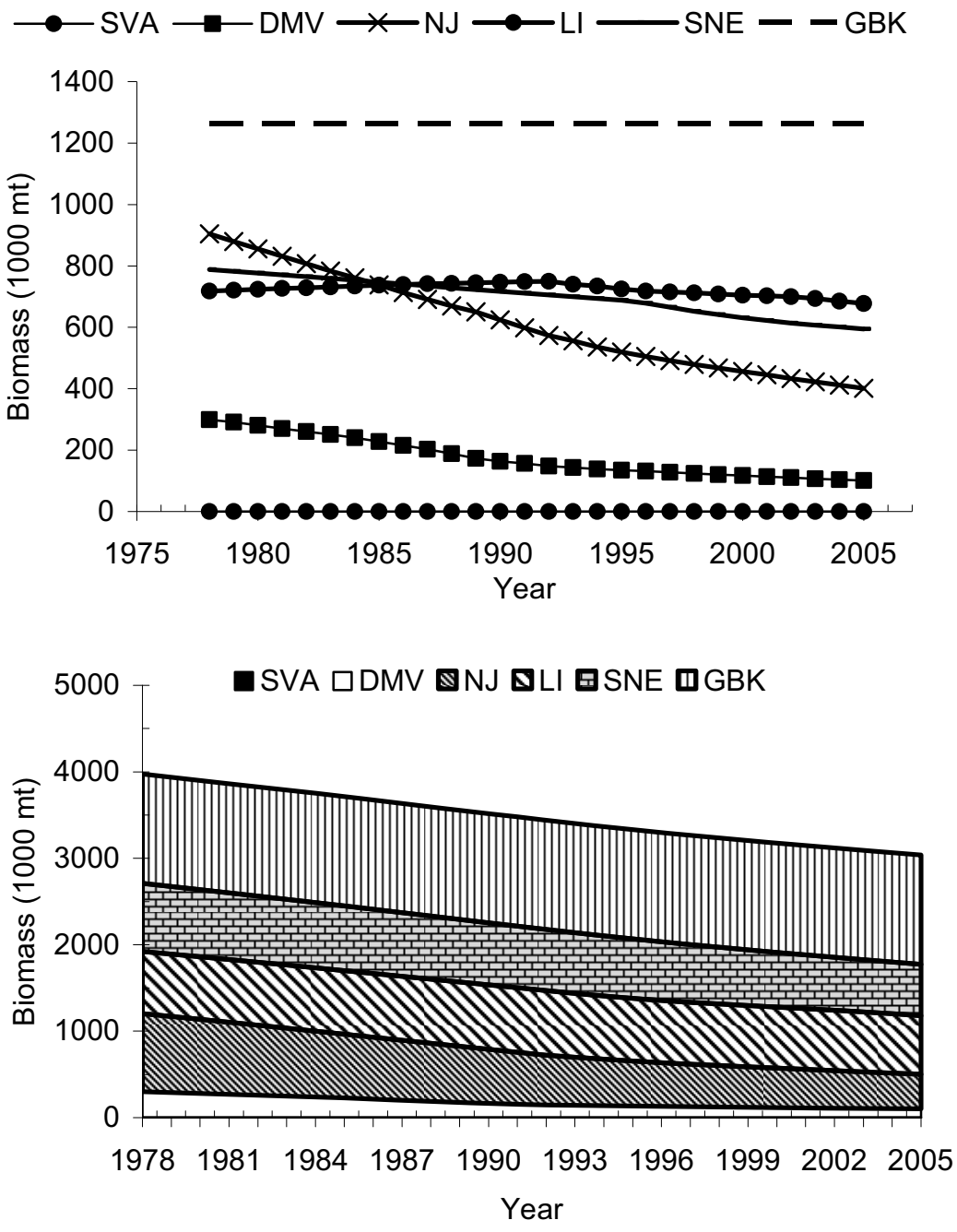

Figure A54. Best biomass estimates for ocean quahog in the US EEZ.

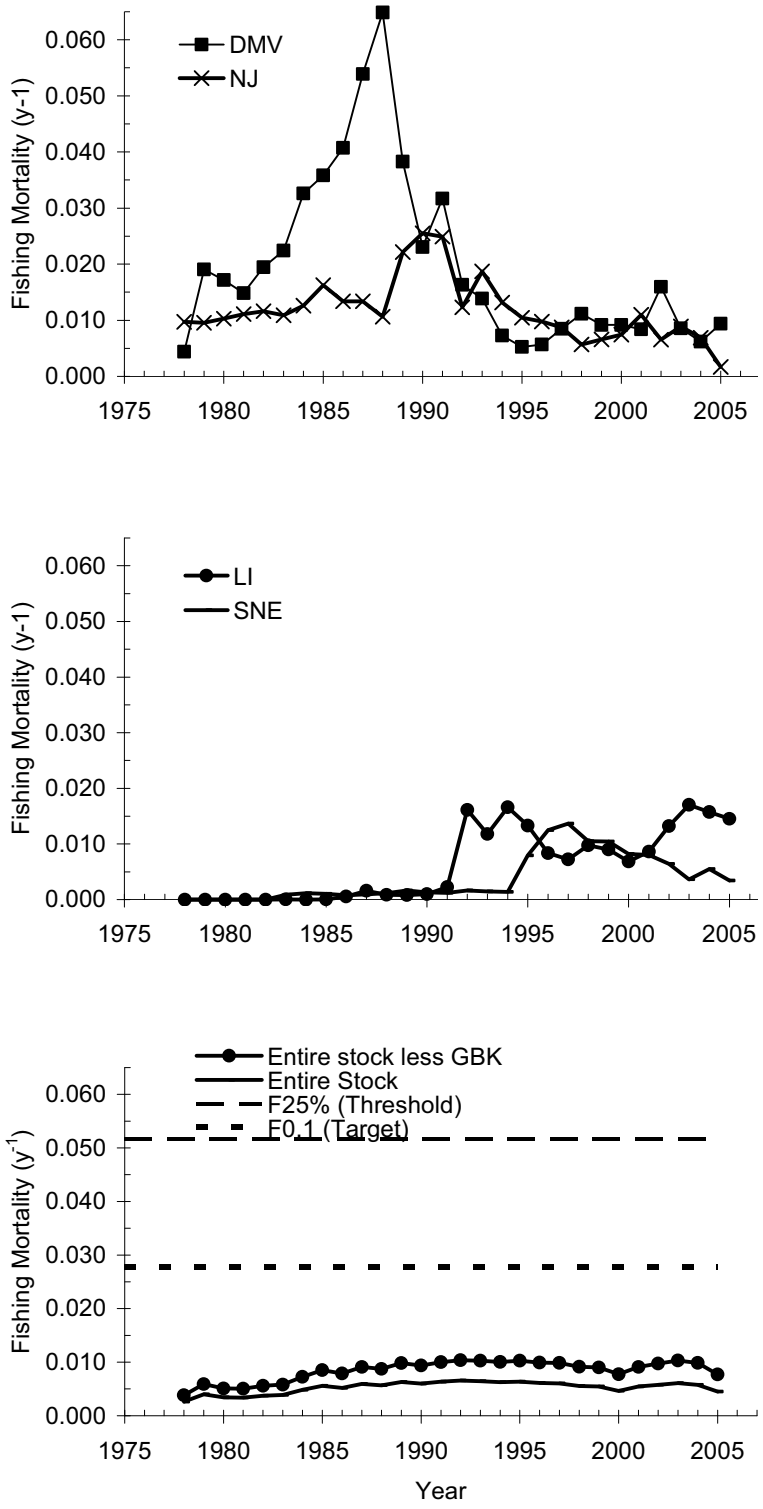

Figure A55. Best fishing mortality estimates for the ocean quahog stock in the US EEZ and the total stock less GBK.

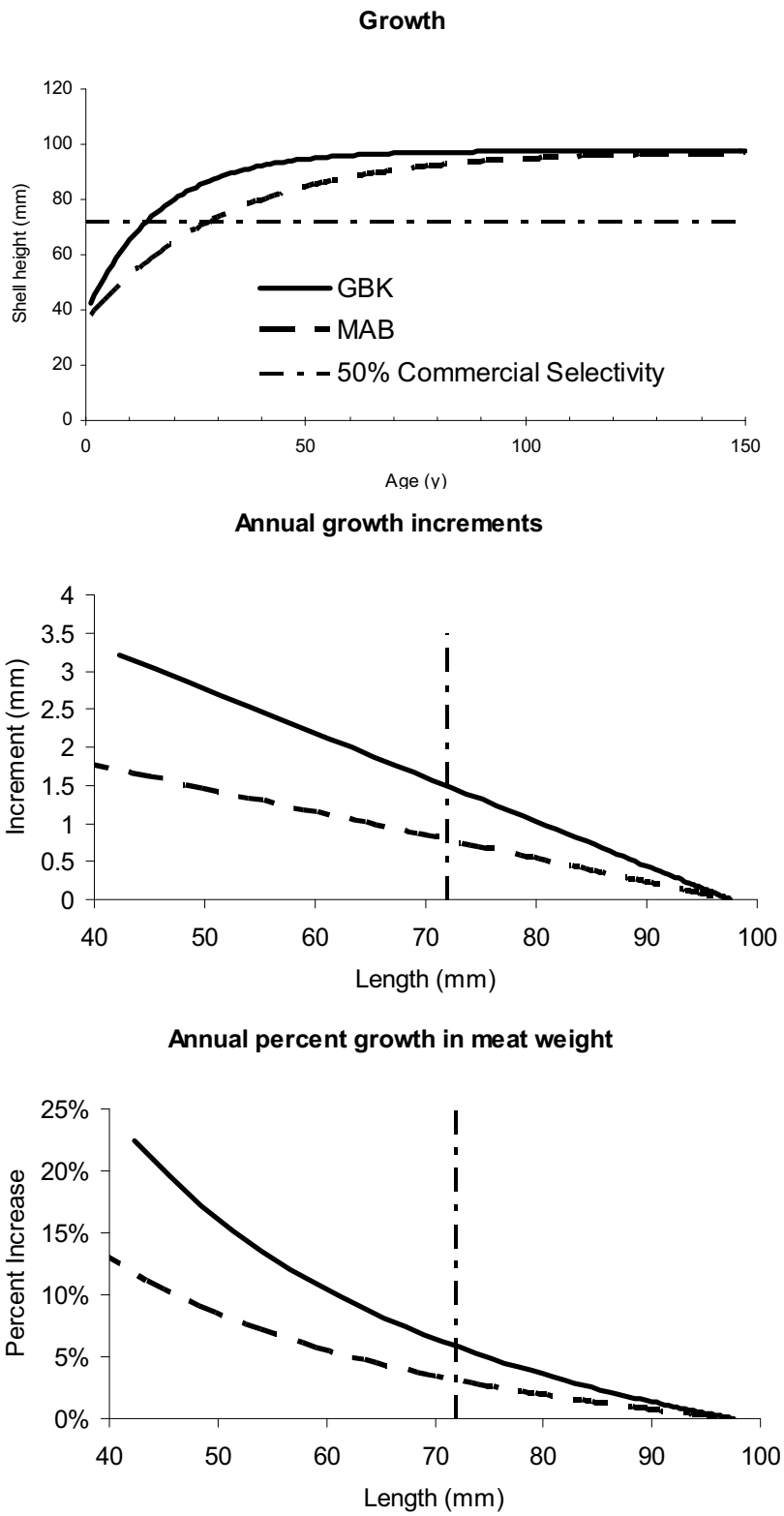

Figure A56. Growth, annual growth increments and percent annual change in meat weights for ocean quahog in GBK and in the Mid-Atlantic Bight (MAB) based on von Bertalanffy growth curves. The growth curve for GBK is from Lewis et al. (2001). The growth curve for MAB is used in this assessment for the fishable ocean quahog stock (which excludes GBK).

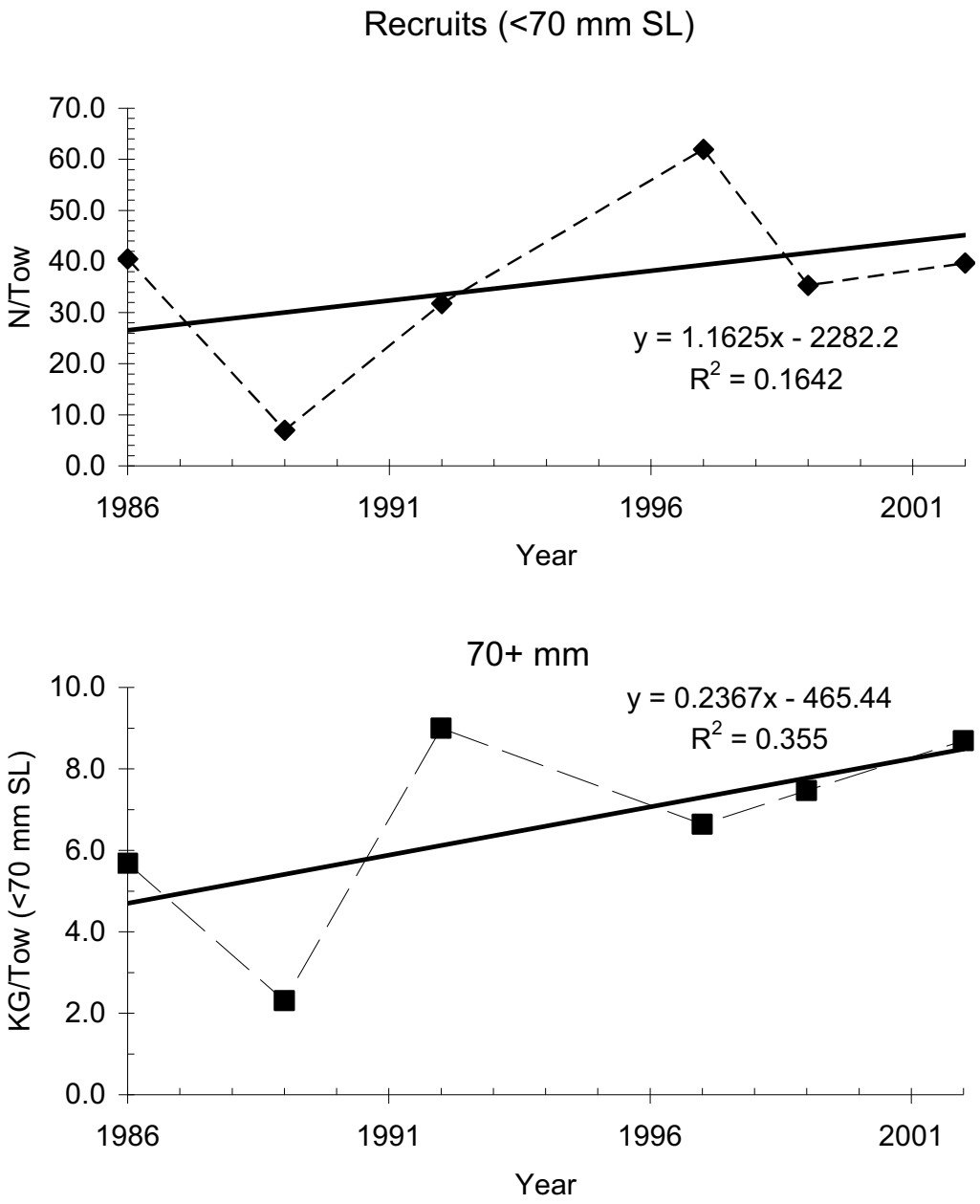

Figure A57. Trends in survey biomass (no correction for selectivity) for ocean quahog from NEFSC clam surveys during 1986-2002 (1994 omitted due to high pump voltage).

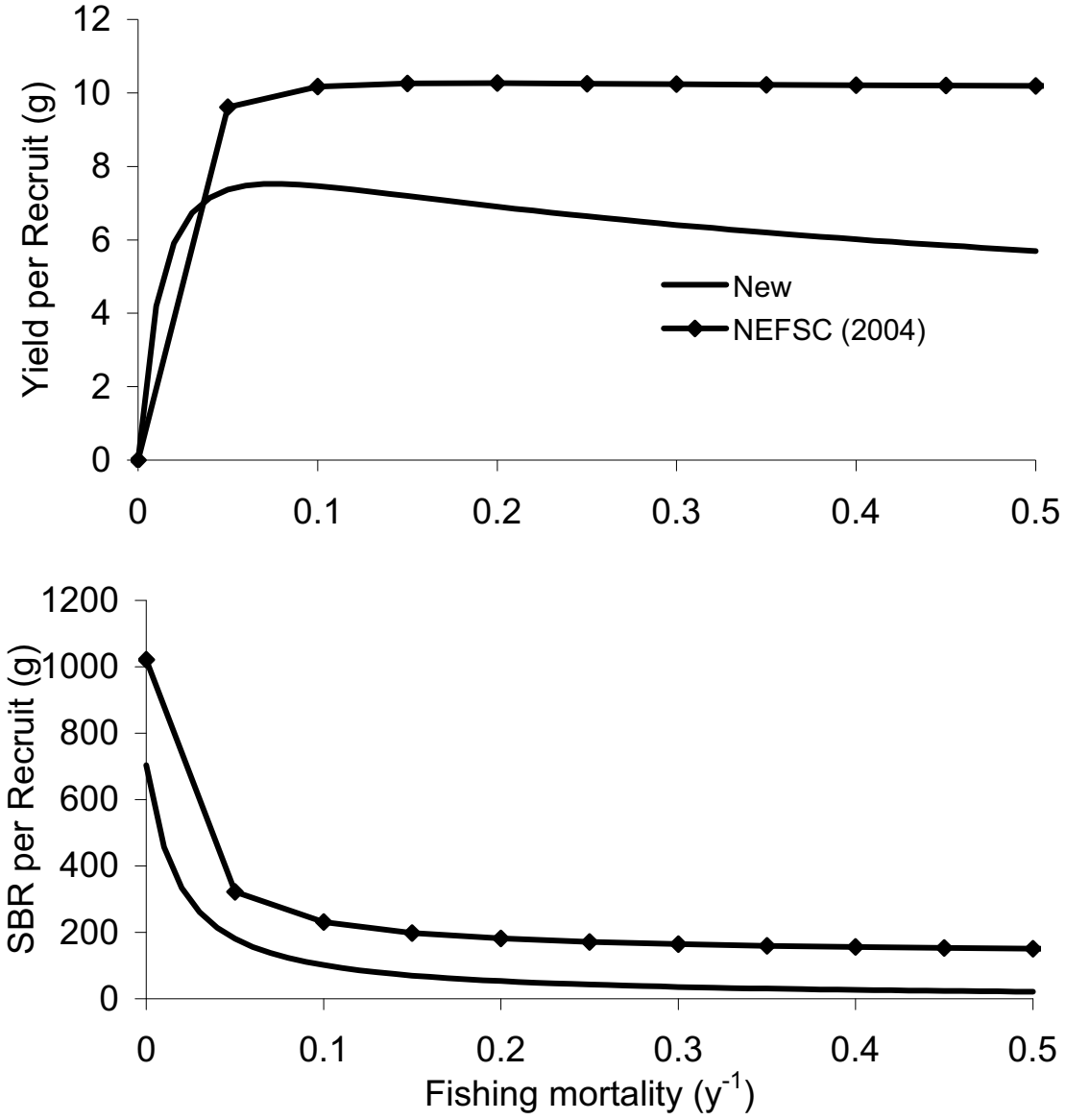

Figure A58. Per recruit model results from a new length based per recruit model and from NEFSC (2004).

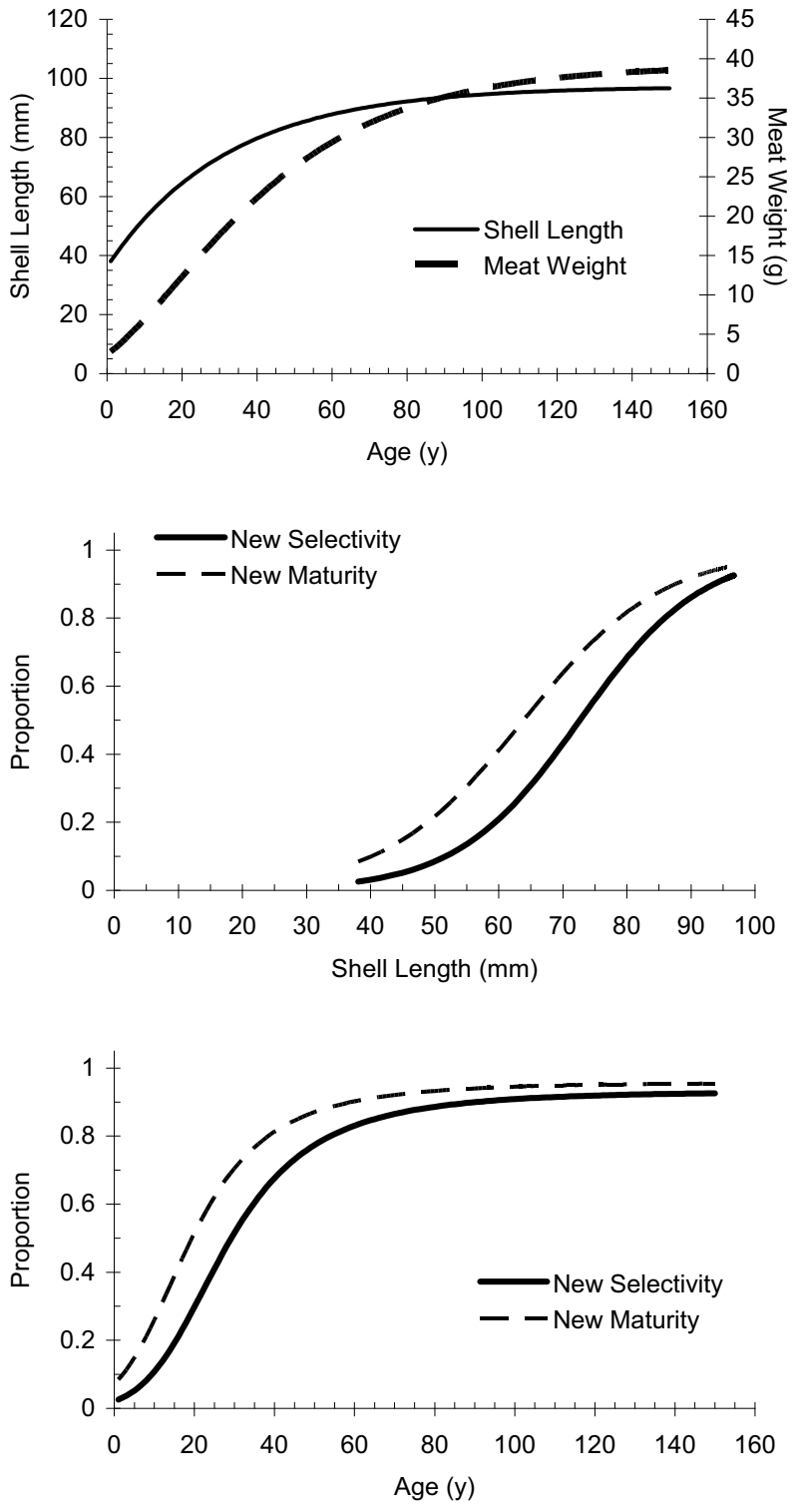

Figure A59. Growth, maturity and fishery selectivity curves used in length-based per recruit model used to calculate biological reference points for ocean quahog. Maturity and selectivity (originally functions of length, middle panel) were expressed as functions of age (bottom panel) by inverting the growth curve.

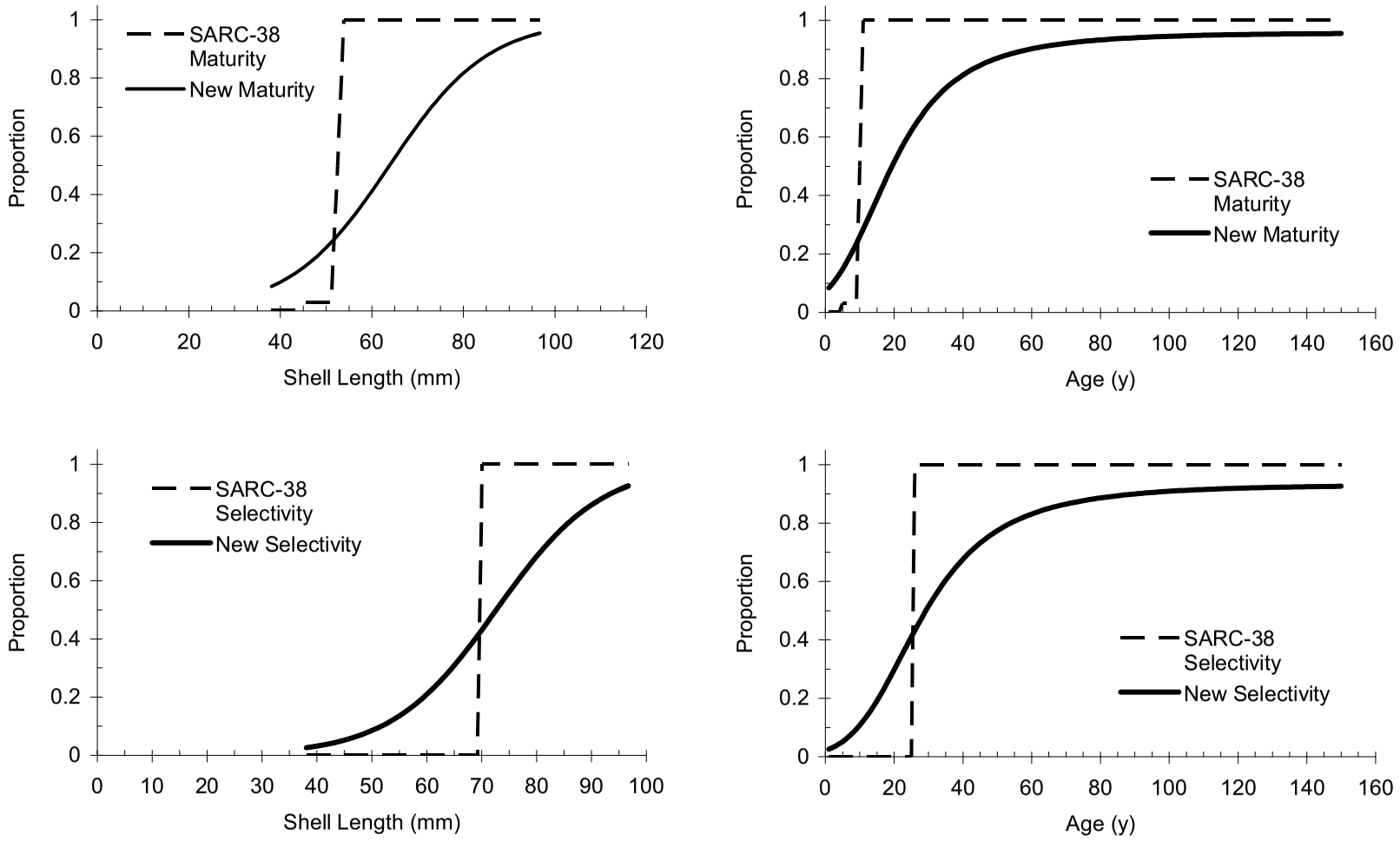

Figure A60. New and old (SARC-38 in NEFSC 2004) maturity and fishery selectivity curves used in per recruit models for ocean quahog.

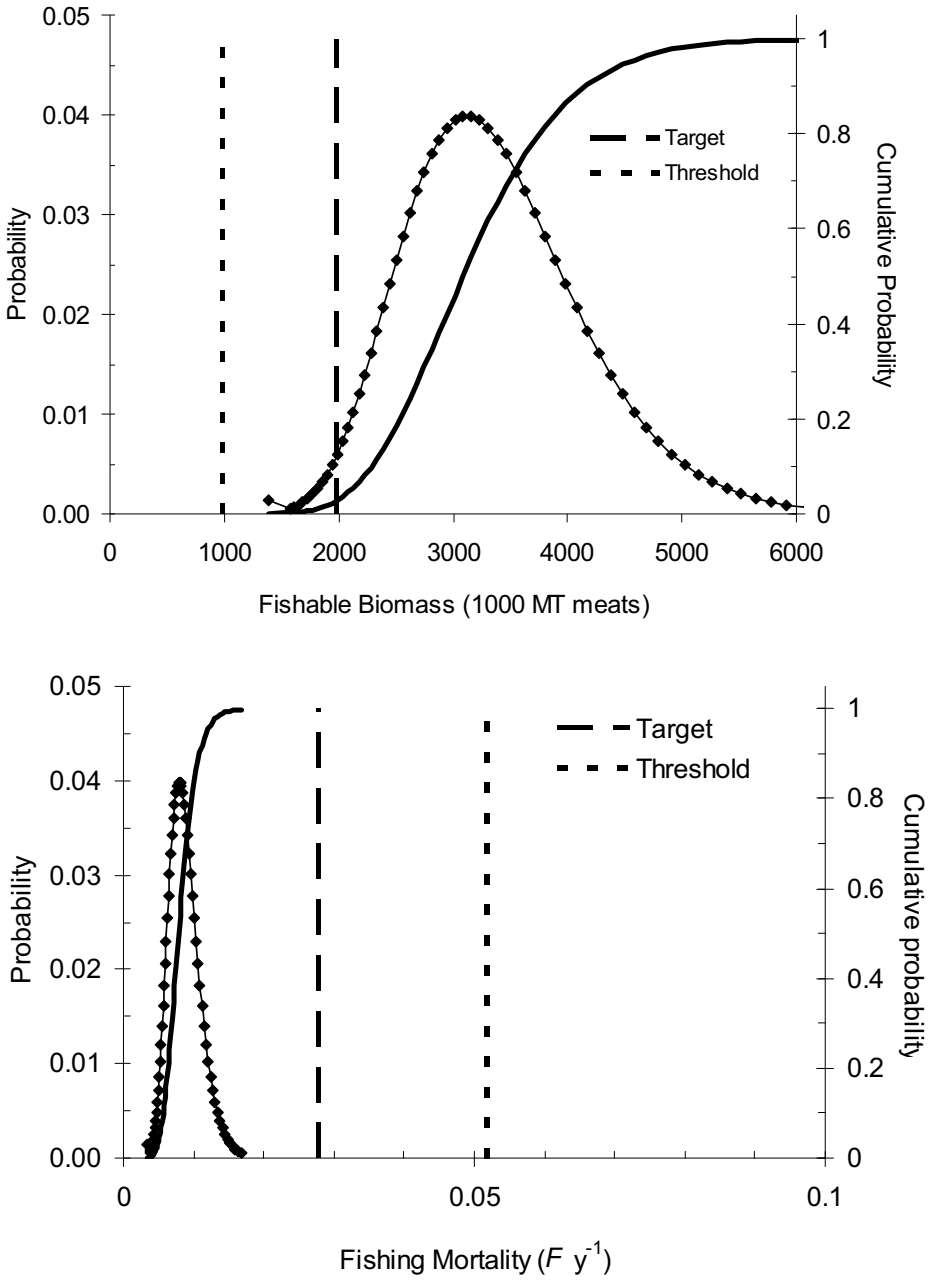

Figure A61. Best estimates of fishable ocean quahog biomass for the entire ocean quahog stock (top) and fishing mortality for the exploitable stock (excluding GBK) during 2005, with confidence intervals and reference points. The confidence intervals are approximate and based on the CV for the efficiency corrected swept-area biomass estimates for 2005.